Anaerobic Digestion Steady State model parameter estimation for determination of waste activated sludge characteristics.

By

J K du Toit
(DTTJOH023)

Dissertation presented for the Degree of
MASTERS OF SCIENCE in ENGINEERING
in the
Water Research Group (WRG)
Department of Civil Engineering

Supervisor: Dr. David S. Ikumi

(December 2020)

UNIVERSITY OF CAPE TOWN
IYUNIVESITHI YASEKAPA • UNIVERSITEIT VAN KAAPSTAD

Declaration

I know the meaning of plagiarism and declare that all the work in the document, save for that which is properly acknowledged, is my own. This thesis/dissertation has been submitted to the Turnitin module (or equivalent similarity and originality checking software) and I confirm that my supervisor has seen my report and any concerns revealed by such have been resolved with my supervisor.

Signed by candidate	24/06/2021
JK du toit	Date

Acknowledgements

First and foremost**, All thanks to The Almighty God,** for without your divine guidance I would never have had the opportunity to participate in this research. Without Your grace this dissertation would not have been possible.

George Ekama – Thank you for being such a professional. Providing guidance throughout the coursework as well as the dissertation. You truly are an exceptional human being, with your positivity and character, truly a lot can be learned.

David Ikumi – Thank you for your patience, understanding and guidance throughout this dissertation. No matter the situation, you were always calm and focused, assisting wherever you could with my dissertation. Without your guidance it would not have been possible to finish this dissertation. It was truly an honour working with you on this dissertation.

My parents – Thank you for all your love, support, patience, encouragement and understanding. It was a long and difficult road, but we made it!!

Njabulo Thela and Hector – Without whose guidance and assistance in the laboratory it would not have been possible to operate and test all the different components for this dissertation.

The rest of my friends – Thank you all for enduring my lack of attendance during 'social gatherings' and still being there whenever I needed the support. Thank you to Chris Gaszynski, Conre Rautenbach and Matthieu Quevauvilliers for keeping me company in the laboratory, the testing hours can be gruelling at times.

Abstract

Phosphorus (P) is an essential nutrient which supports growth and life. A need has developed to recycle P due it being a finite mined resource. At present, most P is lost due to runoff or wastewater (WW) effluent and ending up in rivers and oceans. In order to recycle P and other nutrients, Wastewater Treatment Plants (WWTPs) will need to be converted to Water and Resource Recovery Facilities (WRRFs). However, for WRRFs to be feasible, a better understanding of the current models predicting the fate of P and other material components in place are required.

The objective of this study is to utilise augmented batch tests to determine the characteristics of the Waste Activated Sludge (WAS) containing Polyphosphate Accumulating Organisms (PAOs) from a full-scale WWTP as input variables in the Steady State (SS) Anaerobic Digestion (AD) model to ensure accurate prediction of AD performance.

The experimental setup used in this research consisted of two completely mixed laboratory scale (20 litres volume, mesophilic 36℃) Anaerobic Digesters (ADrs). The ADrs were operated at SS for 15 day and 32-day Solid Retention Times (SRT) and were fed WAS from a full-scale treatment plant which consisted of a Membrane Bioreactor (MBR) Nitrification-Denitrification (ND) Biological Excess Phosphorus Removal (BEPR) Activated Sludge (AS) system.

Two different methods ((i) a novel approach by Maake & Ikumi, (2021) and (ii) the method used by Harding, (2009)) were compared in determining the saturation kinetic rates and the WAS characteristics as input variables for the SS AD models. It was determined that the novel approach by Maake & Ikumi, (2021) was very reliable in determining Chemical Oxygen Demand (COD) removal, Free and Saline Ammonia (FSA), system effluent pH and total alkalinity. With respect to the Ortho-Phosphates (OP), the parent system from where the WAS is sourced, had a long SRT. This resulted in a low predicted PAO count and Poly-Phosphate (PP) content, which resulted in low amounts of Organically bound Phosphate (OrgP) being released into the Anaerobic Digester Liquor (ADL), which equated to an underprediction of OP. Due to the low PP content found in the WAS fed to the ADrs, the ADL was not fully saturated, resulting in no struvite precipitation taking place. This was accurately modelled for both Maake & Ikumi, (2021) and Ikumi, Harding & Ekama, (2013) modelling scenarios.

List of Symbols and Abbreviations

A	Composition subscript for Nitrogen in organics empirical formulation (i.e., $C_XH_YO_ZN_AP_B$)
Ac^-	Acetic Acid
AD	Anaerobic Digestion
ADM-3P	Three Phase Anaerobic Digestion Model
ADL	Anaerobic Digester Liquor
ADr	Anaerobic Digester
ADrs	Anaerobic Digesters
Alk	Alkalinity
Alk H_3PO_4	Phosphate Alkalinity (as mg$CaCO_3$/l)
ANOs	Autotrophic Nitrifying Organisms
AS	Activated Sludge
ATP	Adenosine Tri-Phosphate
B	Composition subscript for Phosphorus in organics empirical formulation (i.e., $C_XH_YO_ZN_AP_B$)
b_{AD}	Acidogen Endogenous Respiration Rate (/d)
b_G	Specific Endogenous Mass Loss Rate of PAOs (0.04/d at 20℃)
b_H	Specific Endogenous Mass Loss Rate of OHOs (0.24/d at 20℃)
BEPR	Biological Excess Phosphorus Removal
BNR	Biological Nutrient Removal
BPO	Biodegradable Particulate Organics
BSO	Biodegradable Soluble Organics
C	Carbon
Ca	Calcium
$CaCO_3$	Calcium Carbonate
CH_4	Methane
CO_2	Carbon Dioxide
CSTRs	Continuously Stirred Tank Reactors
C_T	Total Carbon in Carbonate Weak acid/base sub-system
$C_XH_YO_ZN_AP_B$	Biomass Empirical Composition

d	day
℃	Degrees Celsius
DPAOs	Denitrifying Phosphate Accumulating Organisms
DWL	Dewatering Liquor
DWS	Department of Water & Sanitation
EBPR	Excess Biological Phosphorus Removal
EDC	Electron Donating Capacity
ER	Endogenous Residue
f	Value that relates the pH and equilibrium (pK_{p2}) in the AD Model
F	Filtered
FAS	Ferrous Ammonium Sulphate
FBSO	Fermentable Biodegradable Soluble Organics
f_C	Total Organic Carbon (TOC) to Mass (VSS or molar ratio) ratio
f_{cv}	COD to mass (VSS) ratio
f_{EG}	Endogenous residue Fraction of PAOs
f_{EH}	Endogenous residue Fraction of OHOs
f_{iPAO}	ISS Fraction of the PAOs (mgISS/mgPAOTSS)
f_{iOHO}	ISS Fraction of the OHOs (0.015 mgISS/mgOHO-VSS)
f_m, f_d and f_t	Activity Coefficient (mono-, di- and tri-valent) Ionic species
f_N	Nitrogen to mass (VSS) ratio
f_P	Phosphorus to mass (VSS) ratio
f_{pOHO}	Organic P content of OHOs (0.025 mgP/mgVSS)
FSA	Free and Saline Ammonia
FS_{ti}	Influent COD Flux
$f_{S'us}$	Fraction of Unbiodegradable Soluble COD
$f_{S'up}$	Fraction of Unbiodegradable Particulate COD
f_{xBGPP}	Intracellular PP content of PAOs (0.38 mgP/mgPAO-VSS)
f_{xBGP}	P fraction of PAOs (mgP/mgPAOVSS)
g	gram
GAOs	Glycogen Accumulating Organisms
GDA	Gallery Discreet Analyser

H	Hydrogen
H^+	Hydrogen ion (Proton)
H_2	Hydrogen gas (Hydrogen Molecule)
H_20	Water
HAc	Acetic Acid
$H_2CO_3^-$ Alk	Inorganic Carbon Alkalinity (as mg$CaCO_3$/l)
HCO_3^-	Bicarbonate
HPr	Propionic Acid
IC	Inorganic Carbon
ISS	Inorganic Suspended Solids
K	Potassium
K_a	Dissociation Constant for Weak acid/base
K_{c1}	Equilibrium Constant for H_2CO_3/HCO_3^- Weak acid/base sub-system
K_{c2}	Equilibrium Constant for HCO_3^-/CO_3^{2-} Weak acid/base sub-system
K_H	Henry's Law constant
k_h	Hydrolysis rate constant
k_M, K_S	Saturation kinetic rate constants
K_{sp}	Ionic Product
K_{spm}	Thermodynamic Solubility Product
l	Litre
LCFA	Long Chain Fatty Acids
MBR	Membrane Biological Reactor
Mg	Magnesium
mg	Milligram
MLE	Modified Ludzack-Ettinger
MLSS	Mixed Liquor Suspended Solids
MLVSS	Mixed Liquor Volatile Suspended Solids
N	Nitrogen

N_2	Nitrogen gas
NADH	Nicotinamide-adenine Nucleotide
ND	Nitrification-Denitrification
NH_4^+	Ammonium
NO_2^-	Nitrite (mgN/l)
$NO3^-$	Nitrate (mgN/l)
N_T	Total Nitrogen in Ammonia Weak acid/base sub-system
O	Oxygen
OHOs	Ordinary Heterotrophic Organisms
OP	Ortho-Phosphate
OUR	Oxygen Utilisation Rate
P	Phosphorus
PAOs	Phosphate Accumulating Organisms
p_{CO2}	Carbon Dioxide Partial Pressure
pH	Activity of Hydrogen ions
PHA	Poly- β -hydroxyalkanoates
PHB	Poly3-Hydroxybutyrates
pK_a	-Log10 of Dissociation Constant (K_a) in Acetate Weak acid sub-system
PMF	Proton Motive Force
PO	Particulate Organics
PP	Polyphosphate
PS	Primary Sludge
PSS	Primary Sewage Sludge
P_T	Total Phosphorus in Phosphate Weak acid/base sub-system
RAS	Return Activated Sludge
RBCOD	Readily Biodegradable Chemical Oxygen Demand (S'_{bsi})
r_h	Volumetric hydrolysis/acidogenesis rare (gCOD/(l.d))
r_{HYD}	Rate of hydrolysis
RPM	Revolutions Per Minute
SBCOD	Slowly Biodegradable Chemical Oxygen Demand (mgCOD/l)

SCFA	Short Chain Fatty Acids
SS	Steady State
SST	Secondary Settling Tank
S_{bp}	Residual Biodegradable Particulate COD (mgCOD/l)
S_t	Total Soluble Organic COD (mgCOD/l)
S_{ti}	Total Influent Soluble Organic COD (mgCOD/l)
SRT	Solid Retention Time
SU	Stellenbosch University
S_{usi}	Influent Soluble Unbiodegradable COD Concentration (mgCOD/l)
S_{use}	Effluent Soluble Unbiodegradable COD Concentration (mgCOD/l)
t	Time
TDS	Total Dissolved Solids
TCA	Tricarboxylic Acid
TKN	Total Kjeldahl Nitrogen (mgN/l)
TP	Total Phosphate (mgP/l)
TSS	Total Suspended Solids (mgTSS/l)
U	Unfiltered
UCT	University of Cape Town
UPO	Unbiodegradable Particulate Organics
USO	Unbiodegradable Soluble Organics
VFA	Volatile Fatty Acids
VSS	Volatile Suspended Solids (mgVSS/l)
WAS	Waste Activated Sludge
WRG	Water Research Group
WRRFs	Water and Resource Recovery Facilities
WWTPs	Wastewater Treatment Plants
WW	Wastewater
X	Composition subscript for Carbon in organics empirical formulation (i.e., $C_XH_YO_ZN_AP_B$)

X_{BG}	Active Biomass of the PAOs (mgVSS/l)
X_{BH}	Active Biomass of the OHOs (mgVSS/l)
X_{EG}	Endogenous Residue of the PAOs (mgERVSS/l)
X_{EH}	Endogenous Residue of the OHOs (mgERVSS/l)
X_I	Unbiodegradable Organics Concentration (mgUPOVSS/l)
X_{IO}	Inorganic Suspended Solids concentration (mgISS/l)
X_{IOH}	Inorganic Particulates (ISS) accumulated in AD system
X_{PP}	Inorganic PP formed as part of PAOs biomass
X_V	Volatile Suspended Solids Concentration (mgVSS/l)
Y	Composition subscript for Hydrogen in organics empirical formulation (i.e., $C_XH_YO_ZN_AP_B$)
Y_H, Y_G	OHO & PAO biomass yields respectively (Y_H, Y_G = 0.45)
Z	Composition subscript for Oxygen in organics empirical formulation (i.e., $C_XH_YO_ZN_AP_B$)
Z_{AD}	Acidogenic Biomass
Z_{AM}	Acetoclastic Methanogen biomass
Z_{HM}	Hydrogenotrophic Methanogen biomass

Table of Contents

List of Figures

List of Tables

Chapter 1 Introduction

The design and optimized operation of waste treatment systems has progressed over the past 15 years from the application of empirical techniques to utilization of complex mathematical models. The overarching goal of this project is the calibration of a mass balanced steady state Anaerobic Digestion (AD) model for AD systems fed Waste Activated Sludge (WAS) from Biological Nutrient Removal (BNR) Activated Sludge (AS) systems.

The research project was conducted in the Water Research Group (WRG) of the Civil Engineering Department at University of Cape Town (UCT) and supervised by Dr. D.S. Ikumi and Professor G.A. Ekama. This report will provide a detailed overview on the aspects that entail this research, including the findings from the experiments done.

1.1 Background

Phosphorus (P) is a chemical element found in all life forms. As an essential nutrient with which to support life, only a limited amount is found naturally in the environment, whereby large amounts are mined annually. This P is used in agriculture as fertilizer for crops to grow food. As the human population grows, it requires more food, and thus more P is required. However, much of the P, due to runoff or WW effluent, ends up in rivers, lakes and oceans causing eutrophication and thus being wasted. (Elser, 2012)

Eutrophication is the process where a water (H_2O) body receives an excessive amount of nutrients such as Nitrogen (N) and P which stimulates excessive plant and algae growth, thus causing in an imbalanced ecosystem. A large quantity of N and P is present in WW and should be removed to prevent eutrophication. Due to some autotrophic microorganisms that can fix nitrogen back into the aqueous phase from the atmosphere, P is usually the limiting component that could be removed from H_2O bodies to reduce eutrophication. Owing to the adverse effects of eutrophication, awareness around the world has grown in the need to control the P emissions from Water Resource Recovery Facilities (WRRFs).

In order to remove/recover nutrients (i.e., without the use of chemical dosing) such as N and P and to meet effluent requirements set out by the Department of Water & Sanitation (DWS) in the National Water Act 36 of 1998 (Department of Water and Sanitation, 1998), BNR-AS systems are required. However, due to strict effluent requirements and in some cases a lack of primary treatment, extended aeration is utilized resulting in the BNR systems (in South Africa and many developing countries) to be operated at high Solid Retention Times (SRT), resulting in the WAS characteristics to have a low biodegradable particulate fraction. This makes it unfavourable for AD (unless it is required for N and P removal/recovery), due to the low energy yield from the AD of WAS and the high N and P concentrations in the ADr Dewatering Liquor (DWL). (Ekama, 2017)

In order to better understand the removal/recovery of N and P in BNR-AS systems as well as the behaviour of the microorganisms governing these biological processes, Steady State (SS) models were derived to theoretically visualise these bioprocesses by means of mass balance, biochemical and physico-chemical processes, which ensured prediction of the variables dictating the performance of the BNR-AS systems.

Steady state models allow the sizing and optimisation (i.e., SRT, reactor volumes and recycle flow rates) of WRRF for known WW characteristics. After which, dynamic models allow for the simulation of WRRF and its operation to minimise a facility's energy consumption and cost while maximising the WRRF's nutrient recovery and improving the effluent quality.

1.2 Research Statement

For the transition of Wastewater Treatment Plants (WWTPs) to WRRFs to be feasible, a better understanding of the current models in place is required. These models act as tools to assist clients and investors in better management and long-term planning of WRRFs. Also, the development of appropriate testing procedures and instrumentation is integral to accurate application of these models towards design and operational procedures of future WRRFs.

1.3 Research Questions

How accurate do developed WRRF mathematical models track material components such as phosphorus? Are we confident in the predictive capabilities of these models, such that they can be utilised for tactical decision making in design and operation optimisation of WRRFs?

1.4 Research Objectives

The overarching objective of this study is the utilization of augmented batch tests and SS models to determine the comprehensive characteristics of WAS containing Phosphorus Accumulating Organisms (PAOs) as input to AD systems to ensure accurate prediction of AD performance.

This shall require:

1. the operation and testing of both a SS AD system and an Augmented Biomethane Potential (ABMP) test (ABMP operated and tested by Maake & Ikumi, (2021));
2. checking the results obtained against a SS AD model tailored to virtually replicate the experimental AD system.

1.5 Research Scope and Limitations

This project involves the utilization of data from ABMP reactors together with Parameter Estimation (PE) and SS AD models, to determine comprehensive characteristics of WAS from BNR. The data from ABMP tests were obtained from Maake & Ikumi (2021). The characterized WAS AD feed is from an UCT Membrane Bioreactor (MBR) AS system.

Only explicit SS models were applied to this study. This is to simplify the sludge characterization process presented by Gaszynski, (2020). The project does not include use of complex dynamic simulation models. Moreover, calibration procedures that are used when applying these complex dynamic models were not part of this thesis. The evaluation of the SS AD model results were carried by mass balance verification and comparison of the predicted data with measured experimental results from a SS laboratory scale AD system fed the UCT MBR WAS.

1.6 Thesis Layout

This report comprises of 7 chapters, which are briefly described below:

Chapter 2 – "Literature Review" consist of research done in the past about WAS fed Anaerobic Digesters (ADr) and the calibration of steady state AD models to monitor and predict the effluent quality of these systems. The behaviour and characteristics of the AD systems will also be discussed.

Chapter 3 – "Materials & Methods" will describe the materials used (i.e., feed characteristics, hardware) and how the tests were done in acquiring the required data. Any observations made on the AS and ADr systems that might have affected the experimental data,

Chapter 4 – "Experimental Results" will present the results obtained from the experiments. These results will be adequately analysed and discussed.

Chapter 5 – "Extended Steady State Anaerobic Digestion Model" will present the WAS characterisation and steady state AD model used to analyse the experimental results obtained from **Chapter 4**.

Chapter 6 – "Modelling Analysis and Discussion" will present the predicted results obtained from the steady state AD model in **Chapter 5** and compare the predicted results to those observed in **Chapter 4**.

Based on the results and analysis done, **Chapter 7** – "Conclusions & Recommendations", will provide conclusions and recommendations which will conclude the research.

Chapter 2 Literature Review

2.1 Introduction

The literature review identifies the research gap to be investigated in this project, through exploring the background knowledge on BNR AS systems and WAS fed ADrs. This includes a review of the behavioural patterns of microorganisms mediating the treatment processes and the physico-chemical processes governing the ADr, as well as the current state of the SS AD models.

The following headings will discuss all the relevant studies related to the project:

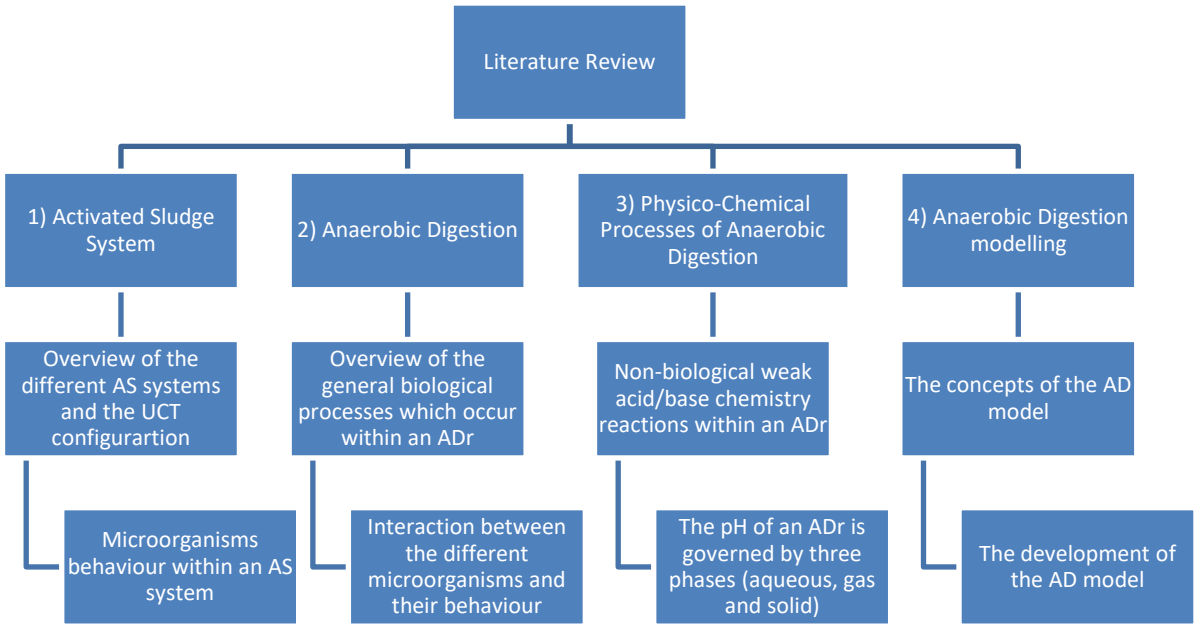

Figure 2-1:Literature Review layout

2.2 Activated Sludge System

Activated sludge systems are miniature ecosystems consisting of different kinds of microorganisms. Wastewater is retained in mixing tanks with microorganisms making up the activated sludge known as biomass. The combination of WW and biomass is known as mixed liquor. Once the WW has been sufficiently treated, it is passed onto clarifiers or through membranes to separate the biomass from the effluent. As in all AS systems, the biomass is returned (known as Return Activated Sludge (RAS)) to the start of the mixed tank to continue treating influent WW. To maintain a balance between the biomass and the WW, excess sludge is regularly wasted (wasted sludge known as WAS), maintaining a consistent SRT. The WAS requires further treatment either by anaerobic or aerobic digestion or other means prior to disposal or utilisation for agricultural purposes. (Ikumi *et al*., 2015)

AS systems contain a wide variety of microorganisms also known as a mixed culture. In order to simplify our bioprocess models, these microorganisms were lumped together as single entities according to general functionality in the AS system. The microorganism groups combined with "non- organism" components make up the AS Mixed Liquor Suspended Solids (MLSS) (Ikumi *et al*., 2015). AS MLSS can hence be fractionated as into the following:

- Ordinary Heterotrophic Organisms (OHO), which mediates the denitrification process (in the anoxic zone) and removal of organics.
- Autotrophic Nitrifying Organisms (ANO), mediating nitrification producing nitrates in the aerobic zone.
- Phosphorus Accumulating Organisms mediates phosphate and organics removal.
- The endogenous residue produced from the OHOs, ANOs and PAOs.
- "non-organism" material in the influent known as inert material, which stay conserved in the activated sludge process.

Although ANOs significantly impact the functioning of the AS system, they have a low yield value and contribute a relatively small population to the AS system biomass. Therefore, most microorganism groups in a BNR system are the OHOs and PAOs. However, according to Wentzel, *et al*., (1989), Wentzel, *et al*., (1989) and Wentzel *et al*., (1990), these two groups appear to operate independently of each other and only interact in the anaerobic zone. In this zone, the Rapidly Biodegradable Chemical Oxygen Demand (RBCOD) in the influent is converted into Short Chain Fatty Acids (SCFA) by the OHOs. The PAOs then in turn utilise the SCFA at a much faster rate than the conversion of the RBCOD, converting the SCFA to Poly3-Hydroxybutyrates (PHB; an internally stored high energy organic compound). The PAOs generate their energy for anaerobic metabolism from the breakdown of their internally stored Polyphosphate (PP) (Smolders *et al*., 1994). In the subsequent aerobic zone, the PAOs utilise their internally stored PHB for growth (which results in the uptake of phosphate that is accumulated in the new PAO biomass). In Nitrification-Denitrification (ND) Biological Excess Phosphate Removal (BEPR) AS systems, the described PAO metabolism provides them with a competitive advantage and allows them to coexist with OHOs, which can only utilise organics aerobically and anoxically (but not anaerobically) for their anabolic and catabolic activities. Since most configurations that promote BEPR (i.e., fostering the growth of PAO biomass) cater for the anaerobic zone as entry point of the influent WW, it is usually accepted that the PAOs (which can take up organics anaerobically) utilise all of the RBCOD while the OHOs only take up the Slowly Biodegradable COD (SBCOD), which requires slow conversion to RBCOD. (Wentzel *et al*., 1990)

Two other groups of microorganisms that might affect P removal is the Glycogen Accumulating Organisms (GAO) and the Denitrifying PAOs (DPAO). The GAOs compete directly with PAOs for the uptake of Volatile Fatty Acids (VFA) in the anaerobic zone with the disadvantage of not releasing any P. By utilising the glycogen stored within the GAOs as both an energy source and reducing agent, acetate uptake will occur (Filipe, Daigger & Grady Jr, C. P. L., 2001). The DPAOs removes P by using nitrates instead of oxygen as an electron acceptor in the uptake process of P in the anoxic zone. However, the DPAOs are only present within an anaerobic-anoxic cycle.

Different AS system configurations have been designed and used world-wide. Generally, the different AS configurations can be divided into ND systems and BEPR systems, both of which will be briefly discussed. The system used in this research is a ND-BEPR-AS system with an UCT configuration.

2.2.1 ND Systems

ND systems are used to remove N from the WW. This is desirable for it reduces the nutrient levels within the effluent, thus reducing the N levels within the receiving H_2O which in turn inhibits algae growth and reduces oxygen demand on the H_2O.

Through a biological process known as nitrification, Free and Saline Ammonia (FSA) is converted to Nitrite (NO_2^-) and then to Nitrate (NO_3^-), with the oxidation of FSA to NO_2^- being the rate limiting process. From this it is assumed that the conversion of NO_2^- to NO_3^- is a rapid conversion. A SRT of at

least 7 days is usually required to ensure that the nitrification process is effective. A sufficient supply of dissolved oxygen (4.57 mgO/mgN times the mass concentration of nitrate produced per day) is required by the nitrifiers for their growth. (Marais & Ekama, 1976)

Through a process known as denitrification, nitrates are converted to Nitrogen Gas (N_2) which escapes into the atmosphere and thus removed from the H_2O. Denitrification requires anoxic conditions in order to reduce nitrates to N_2 as well as an electron donor, usually obtained from organic matter. (Ikumi *et al*., 2015)

2.2.1.1 MLE Process

The Modified Ludzack-Ettinger (MLE) system is an example of a ND system. The system is divided into anoxic and aerobic zones as described in the ND systems. The influent and RAS (the s recycle) from the Secondary Settling Tank (SST) are mixed together in the anoxic zone in the first stage of the system. The influent WW serves as a carbon source in the anoxic zone, the RAS provides the biomass and the sludge recycle (the a recycle) from the aerobic zone provides the nitrates for the denitrification process. In the second stage (aerobic zone), nitrates are converted from FSA and organics are transformed to active biomass. (Henze *et al*., 2008)

2.2.2 Biological Excess Phosphorus Removal (BEPR) Systems

In a BEPR system, P is removed from the WW by transforming it from the aqueous phase to the solid phase. In biological phosphorus removal systems, PAOs take up phosphorus in aerobic conditions and are wasted from the system as excess sludge to maintain a consistent SRT. Alternating aerobic and anaerobic conditions are required in order to biologically remove phosphorus. (Ikumi *et al*., 2015)

Expanding the BEPR system to include nitrification-denitrification, a ND-BEPR system will then consist of an anoxic, aerobic, and anaerobic zone. ND-BEPR systems thus provide an environment which promotes the growth of mixed cultures (OHOs, ANOs and PAOs). In consideration of this, the yield for PAO biomass growth were found to be the same as that of OHOs (Y_G = 0.45), however, the endogenous respiration and fraction of endogenous residue to active biomass were found to be different with (b_G = 0.04/d) and ($f_{ep,G}$ = 0.25) respectively (Wentzel *et al*., 1990). The total mass of volatile solids (MX_v in mg) in the AS reactor is illustrated by **equation (2. 1)**:

$$MX_v = FS_{ti} * \left(\left(\left(1 - f_{S'up} - f_{S'us} - \frac{S'_{bsi}}{S_{ti}} \right) * \left(\frac{\left(1 + f_{ep,H} * b_H * SRT\right) * Y_H * SRT}{1 + b_H * SRT} \right) \right) + \left(\frac{S_{'bsi}}{S_{ti}} * \left(\frac{\left(1 + f_{ep,G} * b_G * SRT\right) * Y_G * SRT}{1 + b_G * SRT} \right) \right) + \left(\frac{f_{S'up} * SRT}{f_{cv}} \right) \right) \quad (2.\ 1)$$

Where:

- $f_{S'us}$ is the fraction of unbiodegradable soluble COD in the influent which can be measured as the filtered effluent soluble Chemical Oxygen Demand (COD) concentration ($S_{usi} = S_{use}$);

- $f_{S'up}$ is the fraction of unbiodegradable particulate COD in the influent;
- S_{ti} is the total soluble organic COD in the influent (mg COD/l);
- S'_{bsi} is the readily biodegradable COD (RBCOD) in the influent, which is then utilised and converted by the PAOs.
- Rs as SRT in days
- Endogenous residue of OHOs is (f_{EH} = 0.2);

2.2.2.1 UCT Configuration

A ND-BEPR-AS system with an UCT configuration was first developed in the early 1980's by Siebritz, Ekama & Marais, (1983) to avoid the recycle of nitrates to the anaerobic zone in an attempt to investigate the behaviour biological P removal. The UCT configuration (See **Figure 2-2**) entails an anaerobic, anoxic, and aerobic zone, which proved to be very effective in the removal of COD, N and P from WW. The reason for the effective P removal was due to the P being transformed from the dissolved liquid phase to the solid phase (Ikumi *et al*., 2015; Henze *et al*., 2008). **Figure 2-1** below illustrates a general UCT configuration.

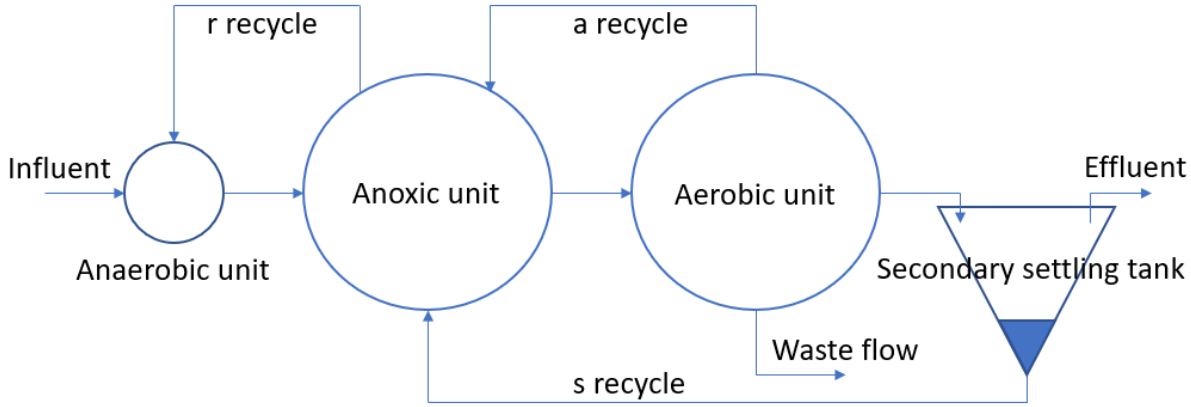

Figure 2-2: Process flow diagram for the UCT-NDBEPR-AS system

One of the benefits with the inclusion of the anoxic zone, is to promote denitrification which in turn protects the BEPR system from the negative effects of recycling nitrates to the anaerobic reactor. By regulating the a-recycle, the nitrate load into the anoxic zone can be controlled, thus achieving the denitrification potential which in turn minimises the nitrates entering the anaerobic reactor via the r-recycle.

2.2.3 WAS Fractionation and Elemental Compositions of Organics

In order to track the elemental material components such as P and N from the parent system (ND-BEPR AS system) to the ADr and determining their fate, the WAS output must be transformed to an appropriate input form required for the SS AD model (ADM-3P), linking the BEPR WAS to ADr.

An AS SS model describing the behaviour of a mixed cultured (OHOs and PAOs) was developed by Wentzel *et al*., (1990) and then extended by Harding, (2009) to determine the elemental composition of NDBEPR WAS which includes the elements Carbon (C), Hydrogen (H), Oxygen (O), N and P in the form $C_XH_YO_ZN_AP_B$ with the various molar units X, Y, Z, A and B. In order to characterise the WAS and obtain the elemental composition, Harding, (2009) had three experimental setups; (1) MLE AS system treating settled WW, (2) MLE AS system treating raw WW and (3) UCT AS system treating

settled WW. All three systems were operated at a low SRT of 10 days and temperature of 20°C. (Ikumi *et al*., 2015; Harding, 2009)

Fractionation:

Due to the much greater P and metals (i.e., Calcium (Ca), Magnesium (Mg), Potassium (K)) content in the NDBEPR WAS as opposed to that found in MLE WAS, the fractionation procedure for WAS by Sötemann, Ristow *et al*., (2005) was extended to integrate this aspect into the Biodegradable Particulate Organics (BPO) and Unbiodegradable Particulate Organics (UPO) components of the NDBEPR WAS. The first step of a 2-step process was to fractionate the NDBEPR WAS Particulate Organics (PO) Volatile Suspended Solids (VSS) into its components (active OHOs & PAOs, endogenous OHOs and PAOs, inert organic masses from the influent) and then determining the P content of PAOs. The second step used the VSS fractionation to determine the BPO and UPO components of the WAS. (Harding, 2009)

Elemental Composition of Organics:

Once the concentration for PO, BPO and UPO of VSS were known, they were transformed into their respective elemental compositions using the mass ratios (i.e., COD/VSS (f_{cv}), N/VSS (f_N) and P/VSS (f_P)) measured on the PO VSS WAS. The following equations describe the procedure to calculate the mass fractions (Ekama, 2009):

$$f_{cv} = 8\left(\frac{4}{12}f_C + f_H - \frac{2}{16}f_O - \frac{3}{14}f_N + \frac{5}{31}f_P - f_{charge}\right) \quad (2.2)$$

Where:

- f_C refer to TOC/VSS;
- f_O and f_H are usually not measured so will have to be transformed in terms of measured ratios;

$$f_O = \frac{16}{18}\left(1 - \frac{1}{8}f_{cv} - \frac{8}{12}f_C - \frac{17}{14}f_N - \frac{26}{31}f_P\right) \quad (2.3)$$

$$f_H = \frac{2}{18}\left(1 + f_{cv} - \frac{44}{12}f_C + \frac{10}{14}f_N - \frac{71}{31}f_P\right) \quad (2.4)$$

Being mass ratios, the sum of all the ratios should be equal to 1 ($f_C + f_N + f_O + f_H + f_P = 1$). Using the mass ratios, the general molar elemental composition $C_XH_YO_ZN_AP_B$ for any of the VSS components for WAS can be obtained. The constituents X, A, B and Z can be calculated as follow:

$$X = \frac{f_C}{12}\left(\frac{Y + 16Z}{1 - f_C - f_N - f_P}\right) \quad (2.5)$$

$$A = \frac{f_N}{14}\left(\frac{Y + 16Z}{1 - f_C - f_N - f_P}\right) \quad (2.6)$$

$$B = \frac{f_P}{31}\left(\frac{Y + 16Z}{1 - f_C - f_N - f_P}\right) \quad (2.7)$$

$$Z = \frac{Y}{2}\left(\frac{1 - \frac{1}{8}f_{cv} - \frac{8}{12}f_C - \frac{17}{14}f_N - \frac{26}{31}f_P}{1 + f_{cv} - \frac{44}{12}f_c + \frac{10}{14}f_N - \frac{71}{31}f_P}\right) \quad (2.8)$$

For the final step, the polyphosphate component of the PAOs needs to be integrated with respect to the PAOs (q_{PAO}) in the format of $C_XH_YO_ZN_AP_B.q_{PAO}[MePO_3]$. After which it is then incorporated with respect to the biodegradable PO (q_{BPO}) and PO or VSS (q_{PO}) (Harding, 2009). By selecting the molar unit of Y to be 7, the molar units of X, A, B and Z yield values with respect to H_7, yielding the organic components of the NDBEPR WAS expressed in their elemental compositions.

2.2.4 Biodegradability of Organics

Biodegradability defines the extent to the operating success of a WRRF, for if the $f_{S'up}$ of the influent into a dynamic treatment plant is high, the efficiency will be poor for there is less feed for the microorganisms, thus smaller microorganism populations which would result in slow kinetic rates. There are two unbiodegradable organics found within an AS system; the unbiodegradable organics in the influent and the unbiodegradable organics produced from by the biomass called Endogenous Residue (ER). Experiments run on short SRT BEPR AS systems as parent systems provided the WAS which was fed to ADr's with SRTs ranging from 10-60 days determined that the material that is unbiodegradable in the AS system (i.e., influent unbiodegradable material and ER) is not further degraded in ADr's. (Ikumi *et al*., 2015)

The $f_{S'up}$ is determined by finding the value at which it matches the calculated mass of VSS (MXv, gVSS) or to the flux of oxygen utilised (gO/d) in the BEPR AS system measured. Therefore, by making $f_{S'up}$ the subject of the equation used to calculate MXv (OHOs and PAOs) from the measured influent COD flux (FSti) and SRT as follow:

$$f_{S'up} = \frac{\frac{MXv}{FSti} - \left[\left(1 - f_{S'us} - \frac{S'_{bsi}}{S_{ti}}\right).\left(\frac{Y_H.SRT}{1+(b_H.SRT)}.(1 + f_{EH}.b_H.SRT)\right)\right] - \left(\frac{S'_{bsi}}{S_{ti}}\right).\left(\frac{Y_G.SRT}{1+(b_G.SRT)}.(1 + f_{EG}.b_G.SRT)\right)}{\left[\frac{SRT}{f_{cv}} - \left(\frac{Y_H.SRT}{1+(b_H.SRT)} * (1 + f_{EH}.b_H.SRT)\right)\right]}$$

(2.10)

Where:

- S'_{bsi} is the readily biodegradable COD obtained by the PAOs for their growth.

As mentioned in **Section 2.2.2**, for OHOs and PAOs, the endogenous residue were determined as 0.2 and 0.25 respectively, with the death regeneration model predicting an unbiodegradable fraction of 0.08 which was accepted for both OHOs and PAOs. (Ikumi *et al*., 2015; Wentzel *et al*., 1990)

In summary the concentration of unbiodegradable COD in WAS ($S_{up\ WAS}$) can be calculated as follow:

$$S_{up-WAS} = \frac{F_{sti}.f_{S'upi}.SRT}{V_{AS}} + \left((X_{BH}.f_{EH}.b_H.SRT) + (X_{BG}.f_{EG}.b_G.SRT) + \left(f'_{EH}.X_{BH}.+f'_{EG}.X_{BG}\right)\right).f_{cv} \quad (2.\ 11)$$

Where X_{BH} and X_{BG} are the OHO and PAO biomass concentrations respectively which can be calculated as follow:

$$X_{BH} = \frac{\left(\frac{Y_H.Q_i.\left[\left(S_{ti}.\left(1-f_{S'us}-f_{S'up}\right)\right)-S_{bPAO}\right].SRT}{1+(SRT.b_H)}\right)}{V_{AS}} \quad (2.\ 12$$

$$X_{BG} = \frac{\left(\frac{Y_G.Q_i.S'_{bPAO}.SRT}{1+(SRT.b_G)}\right)}{V_{AS}} \quad (2.\ 13)$$

Where:

- S_{bPAO} is the influent biodegradable COD obtained by the PAOs;
- V_{AS} is the equivalent volume of the AS systems at the aerobic reactor VSS concentration at which the WAS is wasted from;

With **Section 2.2.3** describing both the procedure to characterise BEPR WAS and obtaining the CHONP element mass balance of the PO, in combination with determining the biomass concentrations and the biodegradability of the WAS, tracking, and determining the fate of the material components through a dynamic plant, linking it to a lab scale steady state ADr and predicting the effluent quality of an ADr is now possible.

2.2.5 Phosphate Accumulating Organisms

The microorganism group responsible for P removal from WW is known as PAOs. They require successive anaerobic-aerobic conditions for growth and play a significant role in nutrient removal systems and thus will be briefly discussed in the Activated Sludge System section. In an anaerobic environment, they can take up VFAs and convert them to intracellular Poly-β-hydroxyalkanoates (PHA) (Wentzel *et al*., 1990). The energy and reducing power required for the uptake of VFAs and its conversion to PHAs are obtained from the hydrolysis of stored PP and glycogen (Oehmen, 2004). In the subsequent aerobic environment, the stored PHAs are oxidised to gain energy for growth, glycogen replenishment and P uptake. P removal is achieved with the PP rich sludge wasted from the aerobic zone.

PAOs, like all other microorganisms, only act according to the capabilities afforded to them by the surrounding environment. With research done by Wentzel *et al*., (1990); Mino *et al*., (1987) and more, it is shown that PAOs in the anaerobic zone of the AS system are capable of taking up VFAs and releasing PP. Thus, it would be expected that PAOs in an ADr with VFAs present would utilise their PP reserves as they would in the anaerobic zone of an AS system with storage of PHAs (Ikumi *et al*., 2016). However, due to no alternating aerobic zone, all the PAO stored products will eventually get released. Although it will not be investigated in this project, a question that can be asked is whether the metabolic pathways developed for PAOs in an AS system with alternating anaerobic and aerobic zones still be able to accurately describe and predict the products and pH of an ADr?

2.2.5.1 Polyphosphate Composition and Structure

As mentioned in **Section 2.2.5**, P is removed from WW by waste sludge containing PAOs saturated with PP. Understanding the formation and structure of PP will provide insight into the biochemical metabolic pathways of PAOs and the physico-chemical process of ADrs.

The inorganic PP has a linear structure of polymers consisting of Ortho-Phosphate (OP) with chain lengths of a few monomers to several hundred. The OP components are linked with energy rich phosphoanhydride bonds with each OP monomer component within the chain carrying a negative charge. (Harding, 2009)

Figure 2-3: Polyphosphate linear Structure (Kornberg, et al., 1999)

In combination with P release and uptake, metal cations are also released and taken up, respectively. The function of these metal cations are to neutralize the charges of the P polymer within the PAOs which reduces the activity of the PP. The metal cations involved in this activity are K, Ca and Mg and form a complex formulation of $Mg_cK_dCa_ePO_3$.

The degradation of the PP in an ADr is referred to as hydrolysis of PP which provides energy to PAOs for the uptake of VFAs. This hydrolysis of PP produces Adenosine Tri-Phosphate (ATP) when it is assumed that no energy is produced. An equation used by Smolders, Van Loosdrecht, M. C. M. & Heijnen, (1995) illustrates this process:

$$[MePO_3]_n + xH_2O \leftrightarrow aATP + bH_2PO_4^- + cMe^+ \qquad (2.14)$$

The elemental composition of the PP relates to the molar ratio P: Mg: K: Ca of which was found to be on average 1: 0.275: 0.295: 0.05, respectively. (Harding, 2009)

2.2.5.2 PAO Inorganic Suspended Solids (ISS) Content

An ISS model for AS systems was developed by Ekama & Wentzel, (2004) due to ISS having a major influence on units such as secondary settling tanks and ADrs. This model assumed that the influent organic material's ISS content is negligible.

It was noted that the longer the SRT, the longer the biomass (OHOs and PAOs) endogenous processes have continued, which resulted in an increased return of dissolved inorganic solids back into the aqueous phase. This means that the contributions from the fixed ISS flux by the OHOs and PAOs are different depending on their active fractions of the VSS. (Ekama & Wentzel, 2004)

In the model, OHOs were assigned an ISS content of 0.15 mgISS/mgOHO-VSS (known as f_{iOHO}). It was found that the difference between the influent ISS and measured ISS at different stages in a WRRF would be much greater for BEPR systems. This is due to the PAOs taking up inorganic PP in aerobic environments. This inorganic PP increases the ISS content of the PAOs up to 6 times higher than that of OHOs (Ekama & Wentzel, 2004). A linear relationship was determined between the P and ISS content of PAOs:

$$f_{iPAO} = f_{iOHO} + 3.286 * \left(f_{xBGP} - f_{p\,OHO}\right) \qquad (2.\ 15)$$

Where:

- f_{iPAO} in mgP/mgISS;
- 3.286 is the ISS content of intracellular PP as P which precipitates in the drying step of the TSS-VSS test;
- f_{pOHO} in mgP/mgVSS (general Organic P of 0.025 mgP/mgVSS) (Wentzel *et al*., 1989).
- f_{xBGP} in mgP/mgPAO-VSS (intracellular PP content of 0.38 mgP/mgPAO-VSS).
- F_{iOHO} is the ISS Fraction of the OHOs (0.015 mgISS/mgOHO-VSS).

The reason for the higher ISS of PAOs as compared to OHOs is due to the PP content within the PAOs. The PP, as mentioned in **Section 2.2.5.1**, consists of K, Ca, and Mg, which are all inorganic material contributing to the ISS content.

2.2.5.3 Hypothesized PAO behaviour in an ADr

In an anaerobic environment of an activated sludge system, PAOs releases PP in conjunction with the production of protons which produces a Proton Motive Force (PMF) that energises the uptake of acetate and reduces it to PHAs. The reducing power required for the synthesis of the PHAs are theorised to either come from the degradation of glycogen (Mino *et al*., 1987), from Nicotinamide-adenine Nucleotide (NADH) formed by oxidation of acetate to Carbon Dioxide (CO_2) via the Tricarboxylic Acid (TCA) cycle (Wentzel *et al*., 1986; Comeau *et al*., 1986) or a combination of glycolysis and the TCA cycle (Hesselmann *et al*., 1999; Pereira *et al*., 1996; Smolders, Van Loosdrecht, M. C. M. & Heijnen, 1995). However, is it possible that PAOs behave the same way in AD environments? This research question has been posed by Ikumi & Ekama, (2019). Moreover, do parent AS systems that treat the WAS at long solid retention times have enough active PAO biomass (with PP) to cause significant changes in the system behaviour? These are questions that are not addressed in this project, however, needs to be investigated further.

After PAOs release P and take up acetate to form PHAs, an electron acceptor (i.e., oxygen) is required to utilise the PHAs for growth and maintenance, however, oxygen is not available in an AD system. This results in the continuous AD release of stored PP and PHAs. It was noted by Harding, (2009) that

PAOs releases practically all the stored PP in 5-8 days. It is uncertain if the P release rate is faster than the PAOs death rate in an ADr however, it is significantly faster than AS biomass hydrolysis rate in an ADr. (Ikumi & Ekama, 2019)

The flow diagram of PP illustrated in **Figure 2-4** provides a tracking record in the aerobic and anaerobic environments. From the schematic representation, the aerobic PHA utilisation and anaerobic PP release can be observed for an AS-ADr linked WRRF.

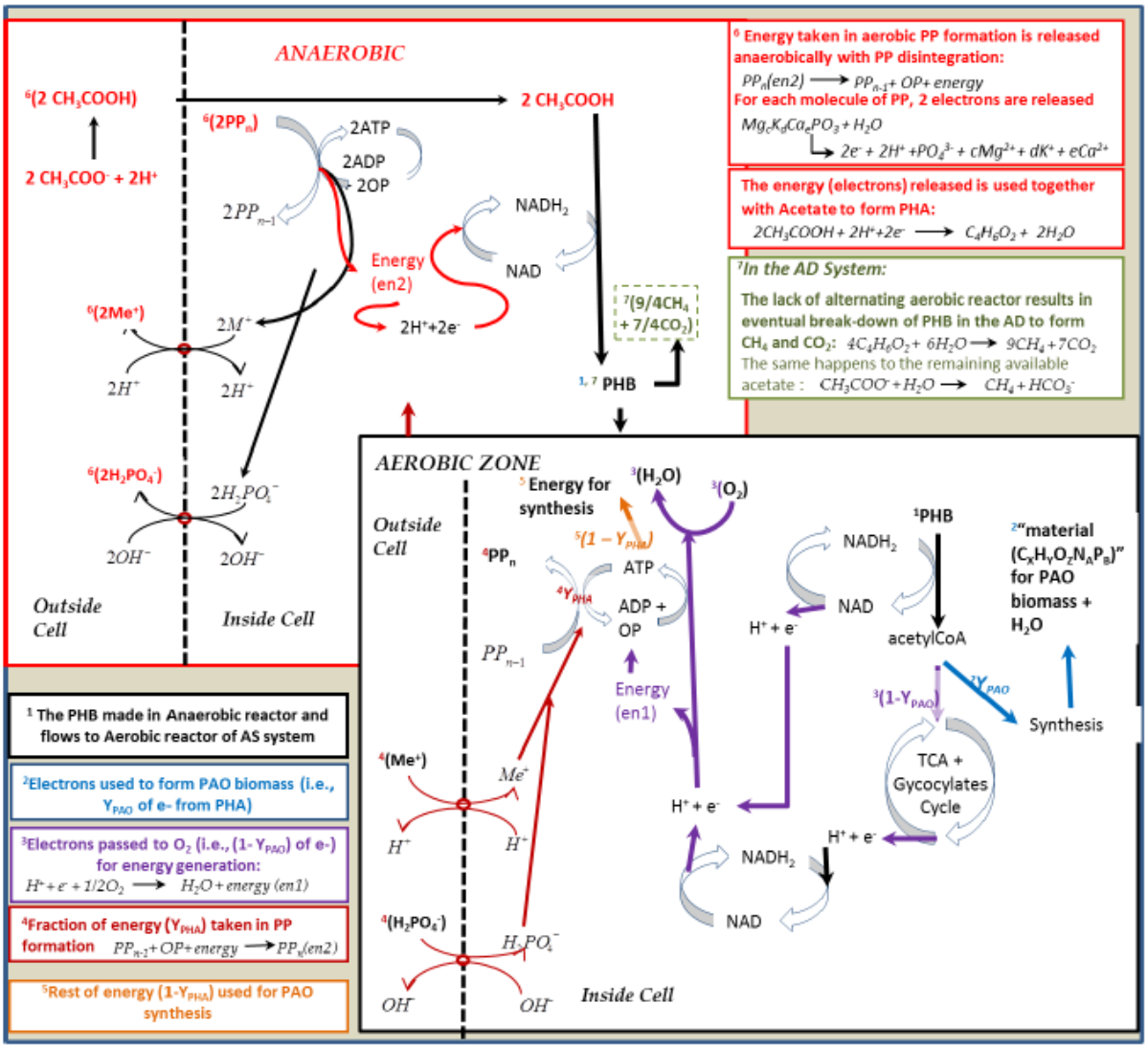

Figure 2-4: Flow diagram tracking PP in an aerobic and anaerobic environment (Ikumi & Ekama, 2019)

2.3 Anaerobic Digestion

Anaerobic digestion is a biological sludge treating process in the absence of terminal electron acceptors such as oxygen, nitrates, and sulphates. The main aim of AD is to stabilise the sludge (i.e., for municipal waste this refers to Primary Sludge (PS) or WAS). A WRRF for these sludges carry with them health risks such as a high pathogen content and have a big environmental impact. By reducing the sludge mass through the production of gaseous products like Methane (CH_4) and CO_2 the solid waste burden to landfill sites are reduced. (Harding, 2009)

In an ADr treating municipal sludges, methane usually constitutes approximately 65 to 75% of the gas produced, with 25 to 40% constituted to CO_2 and 1 to 5% to N, H, and hydrogen sulphide. Methane is

a biogas which can be used for electricity generation reducing the electricity load of the WRRF. (Ikumi *et al*., 2015)

2.3.1 Anaerobic Digestion Biological Processes

According to Batstone *et al*., (2002), the biological processes are catalysed by intra or extracellular enzymes which act on biological organic substrate. Dead biomass (OHOs and PAOs) are disintegrated into particulate constituents, which are further hydrolysed into soluble monomers by extracellular enzymes. Biomass growth and subsequent decay are due to the degradation of soluble material by intracellular enzymes. These processes are governed by four organism groups in the ADr (Harding, 2009; Batstone *et al*., 2002):

- Acidogens: These organisms convert complex organics into SCFA, CO_2 and Hydrogen Gas (H_2).
- Acetogens: Converts propionic and higher SCFA (two or more carbon atoms) to acetic acid.
- Acetoclastic methanogens: Are responsible in mediating the conversion process of acetic acid to CO_2 and CH_4.
- Hydrogenotrophic methanogens: Converts H_2 to CH_4 using CO_2 as an electron acceptor.

The four major groups mentioned and the reactions they mediate are as illustrated in **Figure 2-5**. It is important to note that due to the slow growth rate of some of these microorganisms, it may take a considerable time for an ADr to reach steady state. If not all the organism groups reached steady state, it may lead to a misinterpretation of results.

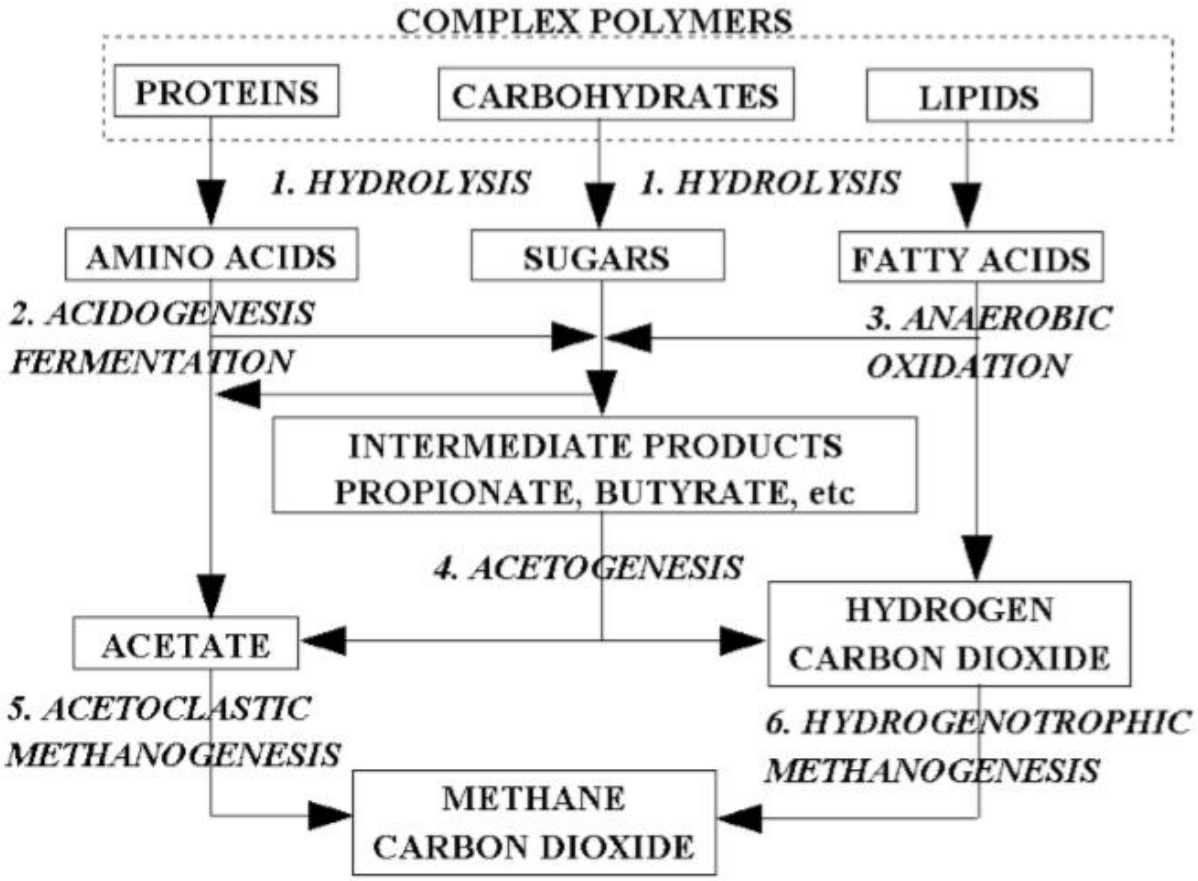

Figure 2-5: A simplified depiction of the AD process (Ikumi et al., 2015)

2.3.1.1 Hydrolysis (Step 1)

For microorganisms to utilise complex organic material (carbohydrates, lipids, proteins), the material first needs to be broken down to soluble compounds (polymers and monomers) in a process known as hydrolysis. This process is carried out extra cellularly by the acidogens, allowing small enough products (amino acids, sugars, alcohol, and fatty acids) to transport across the cell membrane of the acidogenic microorganisms. (Van Rensburg, 2001)

The hydrolysis process is however the slowest process step thus it is the rate limiting step. Due to this reason, the kinetic rates that describe the hydrolysis govern the overall rate of WAS digestion.

2.3.1.2 Fermentation/Acidogenesis (Step 2)

Fermentation or acidogenesis is the process by which the end products from hydrolysis are intracellularly converted to SCFA such as Acetic (HAc), Propionic (HPr) and Butyric Acid, CO_2, and H_2. The type of substrate and the hydrogen partial pressure governs the biochemical pathways for fermentation as well as the type of SCFA produced.

Acidogens are generally faster growing and more resistant to inhibition as compared to the other ADr microorganisms and thus is sometimes omitted from the model development for it will not limit the overall process and thus have a small influence on the system. (Van Rensburg, 2001)

Anaerobic oxidation (step 3) is the process by which Long Chain Fatty Acids (LCFA) are oxidised to HAc, HPr and H. It is a process that roughly follow the same kinetics and reaction schemes as the acidogenesis.

2.3.1.3 Acetogenesis (Step 4)

Acetogenesis is the intermediate step between acidogenesis and methanogenesis. The reason being that SCFA with more than 2 carbon atoms such as HPr and butyric acid cannot be fermented directly to CH_4. Hydrogen-producing acetogenic bacteria are however capable of converting these SCFA to HAc, CO_2 and H_2, provided the hydrogen partial pressure is low. (Van Rensburg, 2001)

For a successful degradation of the intermediate products an efficient removal of H_2 is therefore very important.

2.3.1.4 Methanogenesis (Step 5 & 6)

The acetoclastic methanogens produce CO_2 and CH_4 from HAc in a process known as acetoclastic methanogenesis. They are however very sensitive to pH with an optimum pH of 7.4 to 7.8 and are inactive with a pH below 6.7. (Van Rensburg, 2001)

Hydrogenotrophic methanogens utilise H as a sole energy source with CO_2 used as a C source to produce CH_4 and H_2O.

2.3.2 PAOs in Anaerobic Conditions

Due to the impact PAOs have on BNR systems and their effluent quality, it is important to understand the role and effect PAOs have on the AD SS model. In this section, the effects of PP release, VFA uptake, PAO death and the degradation of PAOs are briefly explained.

Energy Generated from PP Degradation:

For PAOs to take up acetate and reduce it to PHA energy is required. With the use of enzymes, PP is degraded via hydrolysis in the presence of ADP, thus releasing P and producing ATP. The hydrolysis of PP release metal ions Mg, Ca, and K into the aqueous phase as well as $H_2PO_4^-$ as shown in the overall stoichiometry **equation (2. 16)**. (Ikumi & Ekama, 2019)

$$Mg_cK_dCa_ePO_3 + H_2O \rightarrow H_2PO_4^- + cMg^{2+} + dK^+ + eCa^{2+} \quad (2.16)$$

Anaerobic Uptake of Acetate:

As per the Comeau/Wentzel model, the first step for PAOs in acetate uptake is the passive diffusion of acetate across the membrane wall into the PAO (Ikumi & Ekama, 2019; Comeau *et al*., 1987; Wentzel *et al*., 1986). Once taken up, acetate is converted to Acetyl-CoA, and then further reduced to PHA with the use of $NADH_2$ (formed when NAD^+ take up the 2 protons and electrons from PP hydrolysis).

By analysing the stoichiometry, it was observed that more glycogen is utilised in PHA formation than is manufactured in the aerobic zone of an alternating aerobic/anaerobic AS system. It can be theorised that glycogen is generated anaerobically intracellularly by the PAOs with energy provided by the PP degradation. The glycogen is then utilised in the formation of PHAs as illustrated in **equation (2. 17)**.

$$\begin{aligned} Y_{PP}Mg_cK_dCa_ePO_3 + CH_3COO^- + Y_{gl}C_4H_7O_{3.5} \\ \rightarrow \left(\frac{7Y_{gl}}{18} - Y_{PP} + \frac{4}{9}\right)H_2O + \left(\frac{4Y_{gl}}{9} + \frac{2}{9}\right)CO_3{}^{2-} \\ + \left(\frac{8Y_{gl}}{9} + 2Y_{PP} - \frac{5}{9}\right)H^+ + Y_{PP}cMg^{2+} + Y_{PP}dK^+ + Y_{PP}eCa^{2+} \\ + \left(\frac{8Y_{gl}}{9} + \frac{4}{9}\right)C_4H_6O_2 + Y_{PP}PO_4{}^{3-} \end{aligned} \quad (2.17)$$

Where Y_{gl} is the mols of glycogen used per mol of PHA formed and $C_4H_6O_{3.5}$ is the glycogen composition. The energy is modelled to be all from glycolysis. (Ikumi & Ekama, 2019)

PAO Degradation within an ADr:

In an ADr, PAOs will no longer enter an AS system with an aerobic zone where an electron acceptor such as oxygen is available for growth and maintenance. Overtime, the PAOs are hydrolysed and used as a substrate by the ADr biomass. All the stored components within the PAOs (i.e., PHAs, PP and glycogen) eventually also gets broken down as the PAOs are hydrolysed. With the digestion of PHAs, carbon dioxide, protons and electrons are released into the ADr aqueous solution as illustrated in **equation (2. 18)** (Ikumi & Ekama, 2019). The products of this breakdown of PHAs contribute towards ADr biomass growth and methane generation.

$$C_4H_6O_2 + 6H_2O \rightarrow 4CO_2 + 18H^+ + 18e^- \quad (2.18)$$

The remaining PP not released initially with acetate uptake and reduction to PHAs eventually gets hydrolysed since the dead PAOs can no longer hold onto the PP. The PP release with the death of PAOs in an ADr was observed to be a slow process, however there is a chance that this remaining PP is degraded faster as in the anaerobic zone of an AS system (Ikumi & Ekama, 2019). A stoichiometry equation is provided by Harding, (2009) to show this process.

$$Mg_cK_dCa_ePO_3 + fH_2O + (1-f_c)HCO_3^- \rightarrow (1-f_c)CO_2 + f_pH_2PO_4^- + (1-f_p)HPO_4^{2-} + cMg^{2+} + dK^+ + eCa^{2+} \quad (2.\ 19)$$

Where the f value fractionates the phosphate species to HPO_4^{2-} and $H_2PO_4^-$ according to pH which is at about 7 normally for an ADr (Harding, 2009). This final degradation of PP releases additional $H_2PO_4^-$ into the aqueous solution, increasing the overall alkalinity.

Effect of PAO Death on an ADr:

With the eventual PAO death in an ADr, all the components stored within the PAOs are released and degraded by the ADr biomass, causing a change in the acid/base chemistry of the 3-phase ADr system. As shown in **equation (2. 20)**, the PP released from the death of PAOs is released as $H_2PO_4^-$ and HPO_4^2, keeping the H_3PO_4 alkalinity in the aqueous phase constant. The release of a proton from $H_2PO_4^-$ results in the formation of HPO_4^{2-} which increases the Partial Pressure (p_{CO2}) of the system and lowers the pH. The released proton is added to HCO_3^- producing H_2CO_3 (dissolved CO_2). Once the Henry's equilibrium constant is exceeded, the H_2CO_3 escape the aqueous phase and is released as CO_2 into the atmosphere. (Ikumi & Ekama, 2019)

$$H_2PO_4^- + HCO_3^- \rightarrow HPO_4^{2-} + H_2O + CO_2 \quad (2.\ 20)$$

Organic P released from the hydrolysed dead PAOs are released as H_3PO_4. This is a reference species for the phosphate weak acid/base chemistry in the aqueous phase, unlike $H_2PO_4^-$ and HPO_4^{2-}, thus does not cause a change in the H_3PO_4 alkalinity. However, with an ADr pH of about 7, the $H_3PO_4^-$ species lose 1 or 2 H^{2+} protons to become $H_2PO_4^-$ and HPO_4^{2-}. With an increased release of ammonia (NH_4^+) and the rapid degradation of PP releasing high concentrations of P, Mg, Ca and K in the AD liquor, struvite precipitation will occur. A decrease in total alkalinity as phosphate is taken up in struvite precipitation, increases pCO_2 and decreases the ADr pH. **Equation (2. 21)** provides a representation of the struvite precipitation. (Ikumi & Ekama, 2019)

$$Mg^{2+} + NH_4^+ + PO_4^{3-} \rightarrow MgNH_4PO_4 \quad (2.\ 21)$$

It has been noted by Ikumi & Ekama, (2019) that for AD WAS treatment, pH is currently underpredicted, impacting precipitation potential predictions, hence, resulting in inaccurate ADr aqueous phase effluent predictions. Creating a definite model for predicting pH for a mixed WAS fed ADr will result in better resource management and the possibility to take full advantage of the ADr benefits such as the production of fertiliser and biogas. Predicting accurate ionic strength and fractionation of particulate P (concentrations of organic P, PP and P bound struvite) will be useful in creating the above-mentioned definite model.

2.3.3 Review to Anaerobic Digestion

A brief overview was provided about the microorganisms in the ADr and their influence on the system. For a WAS fed mixed culture ADr, steady state is achieved with equilibrium found between the above-mentioned microorganisms and PAOs.

The existence of PAOs in AD also influence the system pH because they take up acetate while releasing metal ions and phosphate. If the conditions are met, the metal ions will precipitate within the ADr, decreasing the pH. The exact process and reasoning for this is explained in **Section 2.4**. The PAOs

might also compete with the acetoclastic and hydrogenotrophic bacteria for the SCFA, however to what extent still needs to be thoroughly investigated. It is generally accepted however that the PAOs utilises all the RBCOD while the OHOs only utilises the SBCOD as mentioned in **Section 2.2**.

2.4 Physico-Chemical Processes of Anaerobic Digestion

In an ADr there are two types of processes, biological processes and non-biological processes that exclude enzyme activities and are called physico-chemical processes (Harding, 2009). According to Batstone *et al*., (2002), physico-chemical processes are divided into the three types as follows:

- Single phase aqueous weak acid/base chemistry
- Two phase aqueous-gas weak acid/base chemistry (e.g., escape of gas such as CH_4 and CO_2)
- Three phase aqueous-gas-solid weak acid/base chemistry (precipitation/solubilisation processes)

In the ADr, the process of digestion results in different chemical species and ionic speciation with different molar concentrations within the ADr liquor (Ikumi *et al*., 2015). A typical methanogenic ADr includes phosphate, carbonate, ammonia, acetate, and water weak acid/base subsystems.

The ionic speciation within an ADr refers to the distributions of the total concentrations between the ionic species. There are many different ionic species in an ADr liquor, however, the ionic species that have a significant role in modelling of a P rich ADr are the H^+, Ca, Mg, K, NH_4^+, PO_4^{3-} and CO_3^{2-}. (Brouckaert, Ikumi & Ekama, 2010)

2.4.1 Single Phase Aqueous weak acid/base chemistry

The substrate in an ADr directly affects the aqueous concentration of the digestion product, with the species produced being a function of the concentration and composition of the substrate. The pH of the ADr is entirely dependent on the composition of the influent organics and inorganics. (Harding, 2009)

Table 2-1: Weak acid Dissociation Constants and Struvite Solubility Product and their Temperature Dependency. pK = (A/T) - B + C.T. where T is in Kelvin (Loewenthal, Kornmüller & Van Heerden, 1994)

		pK 25 C	A	B	C
Water	pK_W	14.000			
Carbonate	pK_{c1}	6.352	3404.7	14.8435	0.03279
	pK_{c2}	10.329	2902.4	6.4980	0.02379
Henry's constant	pK_H	1.47	-1760.0	-9.619	-0.00753
Phosphate	pK_{p1}	2.148	799.3	4.5535	0.01349
	pK_{p2}	7.198	1979.5	5.3541	0.01984
	pK_{p3}	12.023		not given	
Acetate	pK_a	4.756	1170.5	3.165	0.0134
Ammonium	pK_n	9.245	2835.8	0.6322	0.00123
Struvite solubility product	pK_{spm}	12.60			

No matter how insignificant the impact of a sub-system, it still has an effect on the pH of an ADr and thus the set of aqueous phase equilibrium and mass balance equations of the sub-systems are described in **Section 2.4.1.1**.

2.4.1.1 Aqueous Phase Equilibrium Equations

- Carbonate sub-system (C_T):

$$K'_{C1} = \frac{(H^+)[HCO_3^-]}{[H_2CO_3]} \quad (2.\ 22)$$

$$K'_{C2} = \frac{(H^+)[CO_3^{2-}]}{[HCO_3^-]} \quad (2.\ 23)$$

- Ammonia sub-system:

$$K'_N = \frac{(H^+)[NH_3]}{[NH_4^+]} \quad (2.\ 24)$$

- Phosphate sub-system:

$$K'_{P1} = \frac{(H^+)[H_2PO_4^-]}{[H_3PO_4]} \quad (2.\ 25)$$

$$K'_{P2} = \frac{(H^+)[HPO_4^{2-}]}{[H_2PO_4^-]} \quad (2.\ 26)$$

$$K'_{P3} = \frac{(H^+)[PO_4^{3-}]}{[HPO_4^{2-}]} \quad (2.\ 27)$$

- Acetate sub-system (assumed to represent the SCFA):

$$K'_{A1} = \frac{(H^+)[Ac^-]}{[HAc]} \quad (2.\ 28)$$

- Water sub-system:

$$K'_W = (H^+)[OH^-] \quad (2.\ 29)$$

Where (H^+) is the hydrogen ion activity and [] the species molar concentrations.

2.4.1.2 Mass Balance Equations

For characterisation of the system to be done, the total species of all the various sub-species need to be known (Loewenthal, Marais & Ekama, 1989). The following equations define the total species concentrations of the weak acid/base systems:

$$C_T = [H_2CO_3] + [HCO_3^-] + [CO_3^{2-}] \quad (2.\ 30)$$

$$P_T = [H_3PO_4] + [H_2PO_4^-] + [HPO_4^{2-}] + [PO_4^{3-}] \quad (2.\ 31)$$

$$N_T = [NH_4^+] + [NH_3] \quad (2.\ 32)$$

$$A_T = [HAc] + [Ac^-] \quad (2.\ 33)$$

It was accepted by Sötemann, Van Rensburg *et al*., (2005) that the pH of an ADr system treating PS or nitrifying and denitrifying WAS is primarily affected by the inorganic carbon system. This is due to the inorganic carbon system having a much higher concentration compared to any other weak acid/base species present. For a pH between 6.5 - 7.5, Bicarbonate (HCO_3^-) species (as dissolved CO_2) is the main inorganic carbon system present in the ADr liquor, which is generated by the N and VFA content of the WAS. These processes are described as follow (Harding, 2009):

- The products of anaerobic digestion, NH_3 and dissolved CO_2 (H_2CO_3), produce Ammonium (NH_4^+) and HCO_3^- which are both products of physico-chemical processes according to $NH_3 + H_2CO_3^* \Rightarrow NH_4^+ + HCO_3^-$ (Sötemann *et al*., 2005).
- The reaction between dissociated Acetic Acid (Ac^-) and the dissolved CO_2 form HAc and HCO_3- due to the acetoclastic methanogens utilising the associated form of acetic acid.

The measured influent characteristics are required in order to predict the aqueous concentrations of the weak acid/base species in the final ADr products (HCO_3^-, $H_2PO_4^-$, HPO_4^{2-}, NH_4^+ and Ac^-) which in turn can be used to determine the ADr pH. (Ikumi *et al*., 2015)

Due to high concentrations of P in a WAS fed ADr, it is necessary to include the P_T system for it influences the pH of the ADr. It is noted that $[H_3PO_4]$ and $[PO_4^{-3}]$ is considered zero in the pH range between 5 - 9, resulting in P_T being equal to $[H_2PO_4^-] + [HPO_4^{-2}]$. From **equations (2. 25)** to **(2. 27)**, the *f* value fractionates the P_T species for the calculation of pH. **Equation (2. 34)** to **(2. 36)** illustrates the relationship of the *f* value with P_T species $H_2PO_4^-$ and HPO_4^{-2}.

$$[H_2PO_4^-] = fP_t = f\left[B + q - pE\frac{\gamma_S}{\gamma_B}\right] \quad (2.\ 34)$$

$$[H_2PO_4^-] = \frac{P_t}{1 + 10^{pH-Kp2}} \quad (2.\ 35)$$

$$f = \frac{1}{1 + 10^{pH-pKp2}} \quad (2.\ 36)$$

By using the proton accepting/donating capacity parameters relative to a reference species for a specific weak acid/base subsystem, Loewenthal *et al*., (1991) was able to deal with problems such as chemical changes which made it difficult to determine the change of state. **Equations (2. 37)** to **(2. 41)** describe the total alkalinity, where the proton balance is based on the weak acid reference species in its most protonated form.

- Inorganic carbon:

$$H_2CO_3 * Alk = [HCO_3^-] + 2[CO_3^{2-}] + [OH^-] + [H^+] \quad (2.\ 37)$$

- Phosphate:

$$Alk.H_3PO_4 = [H_2PO_4^-] + 2[HPO_4^{2-}] + 3[PO_4^{3-}] \quad (2.\ 38)$$

- Ammonia:

$$Alk.NH_4^+ = [NH_3] \quad (2.\ 39)$$

- Acetate:

$$Alk.HAc = [Ac^-] \quad (2.\ 40)$$

With a mixture of inorganic carbon, phosphate, ammonia and acetate weak acid/base subsystems in an AD system, **equation (2. 41)** could be formulated.

$$Total\ Alk = H_2CO_3 * Alk + Alk.H_3PO_4 + Alk.NH_4{}^+ + Alk.HAc$$
$$Total\ Alk = [HCO_3{}^-] + 2[CO_3{}^{2-}] + [H_2PO_4{}^-] + 2[HPO_4{}^{2-}] + 3[PO_4{}^{3-}] + [NH_3] + [Ac^-] + [OH^-] - [H^+] \quad (2.\ 41)$$

2.4.2 Two-Phase Aqueous-Gas Weak/Acid Base Chemistry

The liquid-gas transfer equilibrium in an ADr is dependent on the partial pressure of the gas phase. The relationship between the liquid and gas phases can be described be applying Henry's law as illustrated in **equation (2. 43)** (Harding, 2009). Due to the solubility of CH_4 being so low, it can be assumed to be insoluble, however CO_2 is considerably soluble and forms both the gaseous CO_2 and dissolved species (aqueous $H_2CO_3{}^*$).

Due to the CO_2 and CH_4 being the major components of biogas in an ADr, the pCO_2 can be determined from the following equation:

$$p_{CO2} = \frac{[CO_2]_g}{([CO_2]_g + [CH_4]_g)} \quad (2.\ 42)$$

Where:

- $[CO_2]$ and $[CH_4]$ are in their molar concentrations.

It is possible to calculate the pH of the ADr by knowing the pCO_2 and HCO_3^- concentrations generated. For the inorganic carbon system at equilibrium, the H_2CO_3 species exists both in gaseous CO_2 and aqueous (H_2CO_3*) phase. In steady state, the dissolved CO_2 species concentration in the aqueous phase is in equilibrium with the partial pressure (pCO_2) in the AD headspace (Ikumi *et al*., 2015). Using Henry's law expression, the $[H_2CO_3{}^*]$ concentration can be calculated as follow (Loewenthal, Kornmüller & Van Heerden, 1994):

$$[H_2CO_3{}^*] = K'_{HCO2} * p_{CO_2} \quad (2.\ 43)$$

Where:

- K'_{HCO2} is Henry's law constant; At 37°C is 1.59;
- $[H_2CO_3{}^*]$ is the dissolved CO_2 concentration in mol/litre;

2.4.3 Three-Phase Aqueous-Gas-Solid Weak/Acid Base Chemistry

Under favourable conditions, soluble species such as Mg, Ca, PO_4^{3-}, NH_4^+ and CO_3^{2-} are likely to precipitate into various mineral forms. Mineral precipitates likely to form in an ADr are struvite ($MgNH_4PO_4.6H_2O$), K-struvite ($MgKPO_4.6H_2O$), Newberyite ($MgHPO_4.3H_2O$), Amorphous Calcium

Phosphate ($Ca_3(PO_4)_2$), Magnesium Carbonate ($MgCO_3$) and Calcium Carbonate ($CaCO_3$). (Musvoto, Wentzel & Ekama, 2000)

2.4.3.1 Struvite

The most likely mineral to precipitate in a WAS fed ADr is struvite. Precipitation will occur when the thermodynamic solubility product of the struvite in the aqueous phase is exceeded by the ionic product of the molar activities of Mg, PO_4^{3-} and NH_4^+ in the solution, as illustrated in **equation (2. 44)**. (Loewenthal, Kornmüller & Van Heerden, 1994)

$$[Mg^{2+}] \cdot [NH_4^+] \cdot [PO_4^{3-}] = \frac{K_{spm}}{f_d f_m f_t} = K'_{spm} \qquad (2.\ 44)$$

Where:

- $K_{spm\_struv} = 12.6$
- f_m, f_d and f_t = activity coefficients of mono-, di- and tri-valent ionic species

Loewenthal *et al*., (1991) describes how the activity coefficients of the respective ionic species can be determined and is based on a modification of the Debye-Huckel theory, which describes the activity of ions in low salinity water (Butler, 1964).

Due to precipitation of R mol/l $MgNH_4PO_4$, the R mol/l of Mg, NH_4^+ and PO_4^{3-} species are used and removed from the aqueous phase (Ikumi *et al*., 2015). The final concentrations of the species would thus differ from the initial stoichiometry predicted concentrations:

For magnesium:

$$[Mg^{2+}]_{final} \approx [Mg^{2+}]_{initial} - R \qquad (2.\ 45)$$

For NH_4^+ (N_T is mainly NH_4^+, R mol/l of NH_4^+ used for struvite precipitation):

$$[NH_4]_{final} \approx [NH_4]_{initial} - R \qquad (2.\ 46)$$

A result in the net decrease of P_T by R mol/l and total alkalinity of 3R mol/l due to precipitation of P_T occurring, with the least protonated species of the P system most likely to be used first. This change in total alkalinity is due to $[PO_4^{3-}]$ being in struvite and is $3H^+$ away from the H_3PO_4 reference species (Loewenthal, Kornmüller & Van Heerden, 1994). **Equation (2. 47)** thus illustrates that if the molar products of Mg_T, N_T and PO_{4T} are above the solubility product, struvite precipitation will occur.

$$([Mg_T] - [R]) \cdot ([N_T] - [R]) \cdot ([P_T] - [R]) = Ksp_{Struvite} \qquad (2.\ 47)$$

After the molar concentration of struvite, final P_T, final N_T and final Mg_T aqueous concentrations are calculated via deducting R mol/l from their respective initial stoichiometry predicted molar concentrations. Determining the relevant HPO_4 and H_2PO_4 species concentrations in the ADr by speciation, where R mol/l of P_T are used in the struvite formation.

$$[H_2PO_4]_{final} = [H_2PO_4]_{initial} - (f \cdot R) \qquad (2.\ 48)$$

$$[HPO_4^-]_{final} = [HPO_4^-]_{initial} - ((1 - f) \cdot R) \qquad (2.\ 49)$$

Struvite precipitation incites a change in the gaseous CO_2 concentration (carbon dioxide partial pressure: pCO_2). As struvite precipitation occurs, H^+ ions are released from the phosphate species. These ions are taken up by HCO_3^- and forms dissolved CO_2 (H_2CO_3). According to Henry's law, some of the H_2CO_3 is converted to CO_2 (gas) and released as head space to maintain aqueous-gas phase equilibrium, increasing the pCO_2. As H^+ is released, the H_2CO_3/HCO_3^- ratio increases thus decreasing the digester pH. It has been observed that struvite precipitates only above a digester pH of 6.9, which is in a pH range for stable digester operations. (Ikumi *et al*., 2015)

Equation (2. 50) illustrates struvite precipitation in a digester.

$$RMg^{2+} + RNH_4{}^{+} + 6RH_2O + \big((1-f)\cdot R\big)HPO_4{}^{-} + \big((1+f)\cdot R\big)HCO_3{}^{-} + (f\cdot R)H_2PO_4 \rightarrow RMgNH_4PO_4\cdot 6H_2O + \big((1+f)\cdot R\big)H_2CO_3 \quad (2.\ 50)$$

The ADr pH changes as precipitation occurs, thus the f value that fractionates the P species also changes (Harding, 2009). Accepting that the mineral which precipitated is struvite, and then the effect on the ADr behaviour is illustrated in **equation (2. 51)** below.

$$Mg_cK_dCa_ePO_3 + RNH_4{}^{+} + \big(f + R\cdot(5-f)\big)H_20 + \big((1-f) + R\cdot(1+)\big)HCO_3{}^{-} \rightarrow \big((1-f) + R\cdot(1+f)\big)CO_2 + f\cdot(1-R)H_2PO_4{}^{-} + (1-f)\cdot(1-R)HPO_4{}^{2-} + (c-R)Mg^{2+} + dK^{+} + eCa^{2+} + RMgNH_4PO_4\cdot 6H_2O \quad (2.\ 51)$$

Struvite precipitation is limited by the availability of Mg found in PP which means that **equation (2. 51**) is rather an extension of PP hydrolysis rather than of biomass products utilisation part of the stoichiometry. Due to the gaseous CO_2 terms which differ with and without struvite precipitation, and the CH_4 terms remains unchanged (not included in PP release or struvite precipitation stoichiometry), pCO_2 thus changes when struvite precipitation occurs. (Ikumi *et al*., 2015)

2.5 Anaerobic Digestion Modelling

In this section, the theory and concepts behind anaerobic digestion modelling will be reviewed so as to create a brief background leading up to **Section 5**, where the extended anaerobic digestion model (Ikumi *et al*., 2015; Harding, 2009) used in this project will be discussed.

One of the key benefits of AD is the significant reduction in pathogen content within PS and WAS. The sludge mass from these sludges are reduced in AD, thus reducing the solid waste dumped on landfill sites. Another benefit is that AD produces biogas via the production of CH_4, and can thus be used to generate energy, reducing the required energy from fossil fuels.

2.5.1 Rate-Limiting Concepts

Concepts behind anaerobic digestion are used to derive mathematical models to try and explain how processes like biological fermentation work and to define the main performance characteristics of the process (McCarty & Mosey, 1991). The two concepts that have the most significant impact on the modelling of AD is the hydrolysis of complex organics where first-order rate equations are commonly used, and methanogenesis of acetate where Monod kinetics are used to describe the processes.

Methanogenesis as Rate-Limiting:

Methanogenesis can be considered as the rate-limiting reaction due to the bacteria which ferment acetate to biogas (CH_4), which has a slow growth rate. The kinetics of their growth rate often dominate the overall rate of the reaction. On average, about 70% of all the methane produced come from the following reaction:

$$CH_3COOH = CH_4 + CO_2 \quad (2.52)$$

This equation is assumed to be the last reaction in the AD process and the most important. The Monod kinetics were derived with a concept where a single strain of bacteria growing on a single rate-limiting substrate, which then relates the rate of uptake of the substrate to its concentration in the growth medium. It further assumes that all the other nutrients and substrates present are in excess, and that the fermentation reaction do not accumulate sufficiently to inhibit the process.

$$\frac{dX}{dt} = \frac{Y\ x\ dS}{dt} = \frac{k\ x\ X\ x\ S}{(K+S)} \quad (2.53)$$

Where:

- Y is the yield coefficient;
- dS/dt is the rate of uptake of the substrate;
- k is the rate constant;
- S is the concentration of the substrate;
- X is the concentration of the bacteria;
- K is the saturation constant.

Hydrolysis as Rate-Limiting:

With hydrolysis of complex organics, acetate fermentation is not always rate-limiting, as compared to methanogenesis. Usually, the organics are measured and illustrated either in COD or as volatile solids. However, due to the different forms and mixtures a complex substrate may have, it is difficult to use a single equation to describe the overall rate of hydrolysis. The first-order rate equations are provided below:

$$\frac{dS}{dt} = k_h\ x\ S \quad (2.54)$$

$$S = S_o\ x\ e^{-k_h\ x\ t} \quad (2.55)$$

Where:

- S_o is the initial concentration of substrate;
- S is the concentration of remaining substrate;
- t is time;
- k_h is the hydrolysis rate constant.

It was discovered that with digestion of activated sludge and with methane fermentation of biomass (i.e., wheat straw and corn stover), that hydrolysis was the rate-limiting step. (McCarty & Mosey, 1991)

2.5.2 Model Development

A two-phase (aqueous-gas) steady state model for AD was developed by Sötemann *et al*., (2005). This model was developed to describe the AD of PS and ND WAS, which included the C, H, O and N (CHON) and COD mass balance for substrate to AD end products. The model comprise of three parts:

- Determining the biodegradable COD concentration hydrolysed based on hydrolysis kinetics;
- Reaction stoichiometry which converts the biodegradable COD to AD end products such as NH_4^+, biomass ($C_5H_7O_2N$), HCO_3^- and gaseous CO_2 and CH_4, which set the partial pressure of CO_2 (pCO_2);
- An inorganic weak/acid base chemistry part from which the pH of the ADr can be determined as described in **Chapter 2**.

To determine the COD based hydrolysis kinetics, Sötemann *et al*., (2005) considered four different rate equations to describe the kinetic rate of hydrolysis. These rates are as follow:

- First order kinetic rate with respect to the residual biodegradable particulate organics COD concentration (S_{bp}): $r_h = S_{bp} \times K_{H;}$
- First order kinetic rate with respect to the residual biodegradable particulate organics COD concentration (S_{bp}) and the Acidogens concentration (Z_{AD}): $r_h = K_h \times S_{bp} \times Z_{AD}$;
- Monod kinetics: $r_h = K_m \times S_{bp} / (K_S + S_{bp}) Z_{AD}$;
- Saturation kinetics: $rh = K_M (S_{bp}/Z_{AD}) / [K_S + (S_{bp}/Z_{AD})] Z_{AD}$;

Where:

- r_h = volumetric hydrolysis/acidogenesis rate (gCOD/ (l.d))

The different rate equations to utilise the BPO (S_{bp}) were used to derive the COD based kinetic model for AD where the model relates the Z_{AD} and the S_{bp} to the SRT of the ADr (Harding, 2009). However, data from literature (i.e., PS mixture data and "pure" PS data) was used to validate this AD model.

Further research was done to expand the SS AD model to a three-phase (aqueous-gas-solids) SS model. To achieve this, Harding, (2009) coupled a ND-BEPR AS system to an anaerobic digester. In doing this, the model could be extended to describe the digestion of WAS from a ND-BEPR AS system. In the extension of Sötemann *et al*., (2005)'s model, components such as phosphorus (P) (i.e., biomass P and PP) and counter-ion metal components (i.e., Mg, Ca, and K) contained in the WAS was then included in the SS AD model. The weak/acid base chemistry for the SS AD model was also extended and is discussed in **Section 2.4**.

The complexities in extending the SS AD model and including P in the mass balanced stoichiometry centred around (1) the different rates PP and organically bound are released into the ADr liquor, (2) the effect of the 2nd dissociation constant of the OP weak acid/base system and (3) the precipitation of metal phosphates such as struvite due to the above-mentioned metals that are released into the ADr liquor. (Harding, Ikumi & Ekama, 2011)

Research was done by Ikumi & Ekama, (2019) in order to develop the inclusion of PP release mass balanced stoichiometries that occur with AD of P rich WAS into the extended SS AD model. The steps in developing the stoichiometry essentially include (1) the release of PP with the formation PHB, (2) the release of PP with the death of PAO biomass and (3) the degradation of the PHB formed due to the lack of an oxygen in an ADr. It was noted in the study that more accurate predictions for pH and the AD end products were obtained with acetate uptake for PHB formation than when modelling the AD PP release to occur with PAO death and hydrolysis. The new extended model will be discussed in

Chapter 5 for this model will be validated against WAS produced from a full-scale plant and fed to lab-scale ADrs as described in **Chapter 1**, **2** and **3**.

2.6 Closure

This chapter presented and reviewed different sources that did research on the different systems (AS systems and ADr's) and microorganisms (OHOs and PAOs) pertaining to the research project. Mathematical models for AS, BEPR WRRFs and ADrs are based on the behavioural patterns of the microorganisms governing the treatment processes. It is assumed that these microorganisms are incapable of thinking or planning and only act according to the environmental capabilities afforded to them (Ikumi & Ekama, 2019). The extended model AD by Harding, (2009) will be used to track the material components from the full-scale plant AS system to the ADr and predict the fate of the components in the effluent.

Background literature on the characterisation of NDBEPR WAS is presented in **Section 2.2.3**. To support the characterisation procedure for NDBEPR WAS, the AS system producing the WAS is briefly reviewed in **Section 2.2.2**. To feed the WAS to the AD system, characterisation of the WAS is required after which the outputs from the AS models are transformed into a format ready for the AD model. This will make modelling of the material components and predicting their fates through the AS and AD systems possible.

As WAS is fed to an ADr, P is released from PAOs with high concentrations of metals, resulting in a change in the weak acid/base chemistry of the ADr liquor. Modelling the ionic speciation and re-speciation within the ADr liquor will result in proper management of WRRFs, ensuring a higher efficiency of recycling of fertiliser (struvite) and biogas (CH_4) making the WRRFs self-sufficient, economical, and green. **Section 2.3** reviewed literature about AD and the different microorganisms with their behavioural tendencies which populate the sludge. The composition of PP and its constituents are and their impact on AD systems are also reviewed in **section 2.2.5.1**. PAOs have been theorised to have 1 or more metabolic pathways and thus are also briefly mentioned. However, ongoing research on which metabolic pathways PAOs utilise under which conditions are still ongoing and will not be included in the scope of this project.

Section 2.4 presents background literature on the physico-chemical processes associated with the AD of ND-BEPR WAS. **Section 2.4.1** and **Section 2.4.2** reviewed literature on the gas and gas-aqueous phase processes in AD, respectively. **Section 2.4.3** reviewed the interaction between all three phases (gas-aqueous-solid) and the likely effect precipitation of struvite has on ADr's.

With the development of a SS AD model, which has been extended numerous times to include the digestion of WAS from a ND-BEPR AS system, it is now possible to accurately predict ADr pH and AD end products. However, this extended model has only been validated with experimental and literature data. To what extent can this SS model predict the end products of an ADr fed with WAS from a full-scale plant?

Chapter 3 Materials & Methods

3.1 Introduction

The project objectives, provided in **Chapter 1**, require generation of experimental data that allows for: (1) the determination of influent characteristics as input data in the extended AD model, (2) as well as ADr data; of WAS from excess BNR AS systems. For this data generation process, two laboratory scale AD systems (experiment 1) (detailed in **Section 3.1.2**) have been set up for steady state operation at different SRTs (15d and 32d). A parallel study was also done to obtain the saturation kinetic rates and the unbiodegradable particulate fraction of the feed (experiment 2) (Maake & Ikumi, 2021). This study involved the use of ABMP. The feed for both these AD systems and the parallel study was sourced from a full-scale ND BEPR AS system with a UCT Membrane (MBR) configuration from Zandvliet WWTP, in Cape Town, South Africa (will be referred to as the parent system) (see **Section 3.1.1** for details).

The general experiment layout is as shown in **Figure 3-1**.

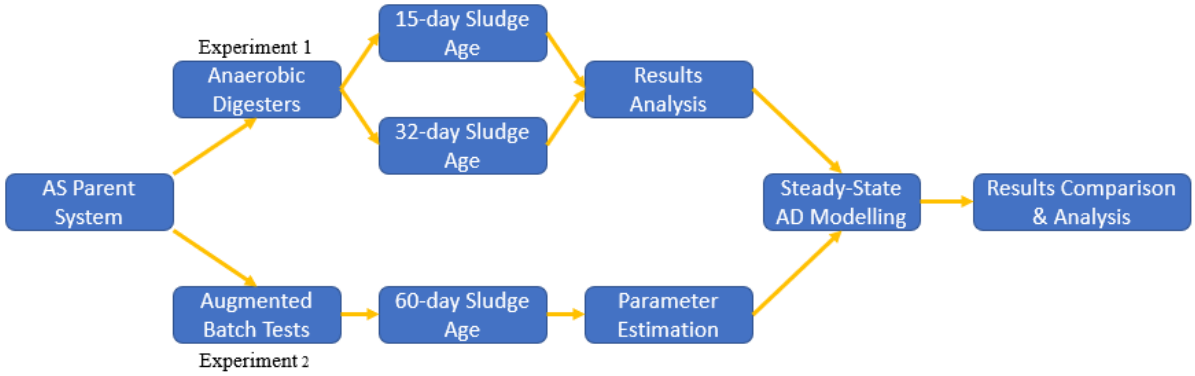

Figure 3-1: Overview of experimental layout

As can be seen from **Figure 3-1** above, the experimental setup for experiment 1 and 2 is explained in this chapter, **Chapter 3**, while the data generated from experiment 1 is analysed in **Chapter 4**. The data generated from experiment 2 is used in a PE, whereby the characteristics and kinetics are determined with the method explained in **Chapter 5**. The extended SS AD model is also discussed in **Chapter 5**. In **Chapter 6**, the results from experiment 1 is compared and analysed against the results obtained from the extended SS model, which utilises the parameters determined from the PE.

3.1.1 The Full scale NDBEPR AS System

The parent system (i.e., the full-scale NDBEPR AS system with an MBR-UCT configuration, used as the source for WAS) is as illustrated in **Figure 3-2**. The system was designed to treat domestic WW with a capacity of 18 Ml/day. The biological reactor consists of 3 zones, anaerobic (2771 m^3), anoxic (2771 m^3) and aerobic zone (4200 m^3), providing a total volume of 9742 m^3.

The MLSS from the bioreactor is filtered by the membranes with a surface area of 41 712 m^2 providing an effluent meeting the standards set out by the DWS (Department of Water and Sanitation, 1998). The membrane thickened MLSS is recycled back into the bioreactor (i.e., Return Activated Sludge (RAS)). This RAS is collected from the full-scale dynamic AS system and used as feed for the ADrs, as shown in the section below, however, the feed (RAS) will be referred to as WAS in the research thesis from here on.

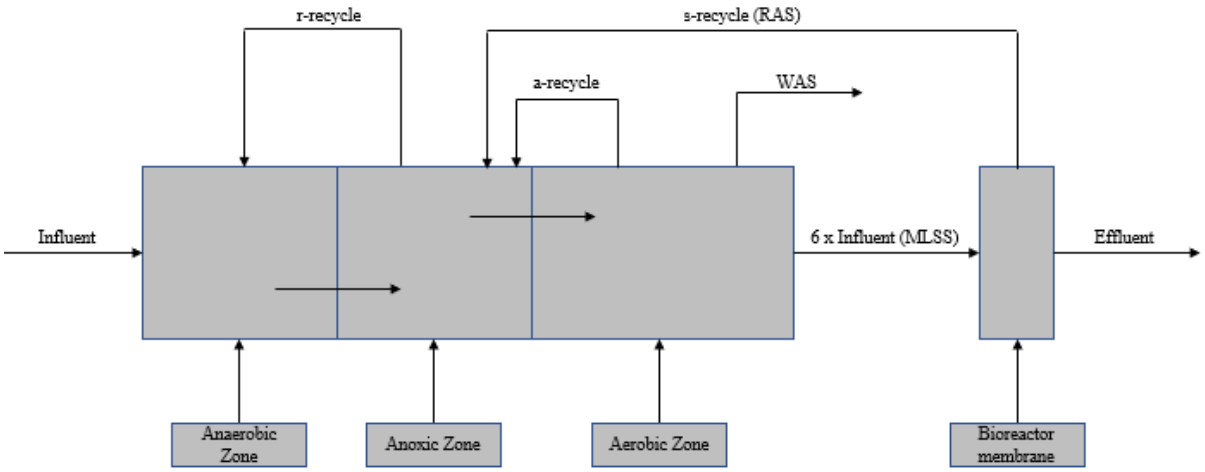

Figure 3-2: MBR UCT configuration of the dynamic plant

To determine the characteristics of the feed WAS to the AD systems, the data obtained from the full-scale AS system required a data reconciliation process shown by Brouckaert, Ikumi & Ekama, (2010). There were some complexities involved with this process due to (i) the system being at a dynamic steady state, the influent concentrations of the material components (i.e., P, N) and metals (i.e., Ca, Mg, and K) varied over time due to flow rates varying diurnally and seasonally.

(ii) Maintenance and repairs on the membranes began two weeks before sampling and testing of the ND-BEPR AS system and continued for about two months thereafter. The influent to the AS system was thus lowered to ±3 Ml/day. This influenced the system sludge production and characteristics.

(iii) The system has no real sampling points such as taps/valve outlets, however it is an open designed system with a walkway, meaning it is open to the environment. Due to the walkway not covering the central areas of each specific zone in the bioreactor, as well as the height difference between the walkway and the bioreactor liquor, not all samples could be obtained from the deepest, most central parts of each respective zone, (iv) storage of samples (stopping or slowing down any biological and chemical reactions), transporting and preparing of each sample in the lab, required sufficient care to ensure that the samples were the best possible representation of the MBR-UCT AS parent system.

3.1.1.1 Collection & Storage of WAS

The feed was collected from the recycling channel running from the membranes back to the reactor, effectively WAS was used as feed for the ADrs (refer to **section 3.1.1**). It was scooped up by a 5-litre bucket attached to a rope (to ensure the bucket does not fall into the WAS), and poured into 5-litre bottles with screw on caps to ensure no spillage occurs.

The feed was then stored in a 20-litre bucket in a 4.0 °C cold fridge which slows down all biological and chemical processes without damaging the microorganisms. At the bottom of the bucket was an air diffuser connected to air. The air supply was in turn connected to a valve which was managed by a timer. For a 3-hour cycle, 30 minutes of air was supplied, then the valve will close for 2 and a half hours. A short aerobic phase was provided to ensure the PAOs take up the phosphates in the feed and to stop any anaerobic digestion, while a longer 'no-air' phase was implemented. This was successfully implemented due to the lack of VFA in the WAS and the cold temperatures (4.0 °C) that delayed the initiation of a fermentation process by anaerobic biomass. The ADrs were fed at the start of the 'no-air' phase, to allow for investigation on the potential release of PP in the ADrs (the ADrs contain sufficient

quantities of VFAs for this to potentially occur in a similar fashion as would in the anaerobic zone of the AS system). (Ikumi & Ekama, 2019)

3.1.2 Anaerobic Digester

The ADrs used in this experiment was Continuous Stirred Tank Reactors (CSTRs) as illustrated in **Figure 3-3**. The ADrs were run at a temperature of 36 °C at an operating volume of 20-litres with 1-litre headspace (i.e., 21 litre total reactor volume).

The tank was built from Perspex with a rubber seal between the top lid and the cylindrical body to ensure a gas tight seal. The gas would then flow through a pipe to the gas counter. After every 34-ml of gas, the counter would tip over, the magnet would then cause an electrical discharge as it passes an electrical wire, ensuring the clicker to digitally count the amount of times the magnet passes. This would thus provide a total gas produced from the ADr system.

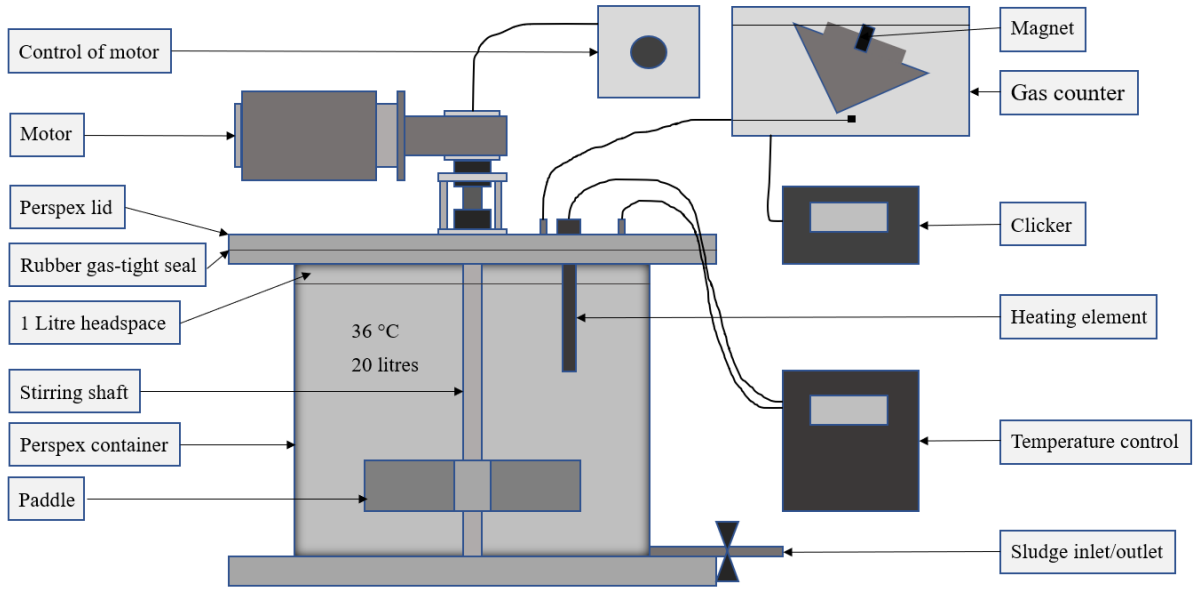

Figure 3-3: CSTR for anaerobic digestion

A stirrer was mounted on top of the lid of the tank, driven by a single-phase motor with a controller, ensuring continuous mixing of the contents at a revolution of 20 Revolutions Per Minute (RPM). The temperature was controlled by a controller, with the heat provided by a heating element. A thermometer was added to measure the in-situ temperature and connected to the controller to ensure continuous automatic management of the temperature of the system.

The two ADrs each had its own respective SRT, which was 15 days and 32 days. This would provide an adequate analysis of the two different mathematical models. When wasting from the system, the gas pipe was disconnected, and waste collected from the sludge outlet as shown in **Figure 3-3**. The systems were fed from the sludge inlet, ensuring no extra air goes into the system. The systems were fed a constant COD of 10 grams-COD/litre daily (24-hour period). As the WAS concentrations varied significantly from the dynamic AS system, it was possible to only feed a constant 10 gCOD/l concentration by diluting the feed accordingly.

Due to the method of wasting and feeding of the ADr, the gas pipe was disconnected for when wasting. This was done to ensure that no H_2O from the gas counter gets sucked into the system. The ingress of

gas was a concern due to the potential for a resultant variation with the operating volume and possibility for acidity addition to the system (the H_2O in the gas counter was very acidic due to continuous carbon dioxide absorption).

A small headspace was introduced, for when opening the system while having a large headspace, the headspace equalises with the atmosphere. After the system is fed and closed, the gas produced first pressurise the headspace before escaping through the gas counter, the potential for this to result in an inaccurate measurement of the total gas produced over a 24-hour period was noted.

Considering that the feed was obtained from a dynamic full-scale AS system, maintaining a consistent feed of 10gCOD/l daily was difficult. However, the feed sludge COD was measured and mixed well in a drum to ensure that the COD is within reasonable range of the 10gCOD/l. This occasional measuring and storage were opted instead of a daily routine of measuring all the metals and material components, during the everyday operation period. The laboratory lacked resources and technology that would allow generation of rapid results prior to feeding.

Initially, it was noted that the Perspex tank of the ADrs let light through, enabling the growth of algae in the system. These algae affect the system as it utilises the nutrients and may possibly generate O_2 as biproduct, effecting the overall performance of the system. To avoid this, the ADrs were wrapped in black plastic bags, and the light of the isolated ADrs room in the laboratory was required to be turned on only when wasting and feeding the ADrs.

3.2 Experimental Testing Methods

To obtain the required results, the following tests were performed:

- Chemical Oxygen Demand (COD)
- Total Kjeldahl Nitrogen (TKN) and Free and Saline Ammonia (FSA)
- Total Phosphate (TP) and Ortho-Phosphate (OP)
- Nitrate (NO_3) and Nitrite (NO_2)
- Magnesium (Mg), Calcium (Ca) and Potassium (K)
- 5-point analysis, pH, and conductivity
- Mixed Liquor Suspended Solids (MLSS) and Volatile Suspended Solids (MLVSS)
- Gas composition analysis

Most of the tests were done in the laboratory of the WRG in the Department of Civil Engineering at the UCT. However, the gas composition was done at Stellenbosch University (SU). The tests mentioned above are described below.

3.2.1 Chemical Oxygen Demand

The COD was measured by using a 10ml sample, refluxing the sample in a strong acidic solution (15ml sulphuric acid) with a known excess of potassium dichromate ($K_2Cr_2O_7$ ~ 5ml at 0.25N). This method is known as the dichromate and sulphuric acid open reflux method. In principle, the organic matter (electron donor) is oxidised by the boiling dichromate (electron acceptor). After boiling, the process is followed by a titration with Ferrous Ammonium Sulphate (FAS) which is an electron donor. The quantity of $K_2Cr_2O_7$ reduced is thus determined, giving the Electron Donating Capacity (EDC) of the oxidised organic matter in terms of oxygen equivalent. (Sawyer, McCarty & Parkin, 1994)

3.2.2 Total Kjeldahl Nitrogen (TKN) & Free and Saline Ammonia (FSA)

The TKN and FSA concentrations were measured using the semi-micro Kjeldahl digestion and distillation method. TKN is a total concentration of organic nitrogen and FSA. For the TKN test, a 10ml sample is digested with sulphuric acid containing potassium sulphate with mercuric sulphate as a catalyst. The digestion converts all the organic nitrogen compounds (i.e., proteins and peptides) to ammonia. Afterwards the sample is steam distilled using micro-distillation apparatus with sodium hydroxide (7ml) and sodium thiosulphate. Due to steam distillation, ammonia gas is stripped from the sample. The ammonia generated from the organically bound N and any other ammonia originally present is condensed and dissolved in boric acid solution (25ml) turning it from purple to green. The solution is then titrated with sulphuric acid (0.001 N) until it is the original purple colour. The volume of acid titrated is proportional to the TKN concentration. For the FSA test, the sample is not digested, only steam distilled. Organic bound nitrogen is the difference between TKN and FSA: Org-N = TKN – FSA.

3.2.3 Total Phosphates (TP) & OP

The TP and OP concentrations were measured using the persulphate digestion and molybdate-vanadate colorimetric method. The OP reacts with molybdates, in the presence of vanadates, to form yellow phosphovandomolybdate solution. The colour intensity is directly proportional to the OP concentration present, which is measured by absorbance using a spectrophotometer. The system obeys Beer's law at a wavelength of 470µm up to a concentration of 300mgP/l. Measuring the total P involves converting the organic and PP to OP through boiling the sample (20ml) with sulphuric acid and potassium persulphate. Through boiling, the organic material P bound in the organics is released into the solution as OP.

3.2.4 Nitrates (NO_3), Nitrites (NO_2) and metals (Ca, K & Mg)

The nitrates, nitrites and metals could only be tested while soluble, for the Gallery Discreet Analyser (GDA) only operates on soluble samples. For the nitrates and nitrites, samples were filtered and then analysed by the GDA.

Total metals were obtained by following the digestion steps from the TKN analysis. The digestion mix used by the TKN analysis is slightly altered by replacing the K_2SO_4 component to Na_2SO_4, as K is one of the counter-ion metals being analysed for in this study. Filtered samples were obtained by filtering the samples which was then tested by the GDA for Ca, K and Mg.

3.2.5 5-point titration, in-situ pH & Conductivity tests

To calculate the VFAs and alkalinity species (i.e., carbonate, phosphate & ammonia) present in the liquor, 5-point titration was done (Moosbrugger *et al*., 1993). A sample is diluted 5 times and is then titrated to 4 predetermined pH points (i.e., 6.7, 5.9, 5.2, 4.3), all done by an auto-titrator with dilute standard hydrochloric acid. The volume of acid added the pH at the key points and the in-situ pH are used to calculate the VFA and alkalinity concentrations. The FSA and OP measurements were also required for the calculation process, as well as the starting pH, conductivity, and in-situ temperature. The 5-point titration method provides insight into an ADr, of which the most important is if there is an acid build up and your system is going to crash (pH below 6.6).

The pH of the system was measured with a pH meter which was calibrated before every measurement made. Care needed to be taken to obtain an accurate pH measurement, for the time since sampling from the ADr to measuring the pH, aqueous CO_2 escapes into the atmosphere as a gas, which increases the pH of the sample, for aqueous CO_2 is acidic and lowers the pH.

3.2.6 Mixed Liquor Suspended Solids (MLSS) & Volatile Suspended Solids (MLVSS)

The MLSS (mg/l) is measured using the Total Suspended Solids (TSS) and Inorganic Suspended Solids (ISS) tests. A 50ml sample is transferred to a clean and dry crucible of known mass and then dried at 105 °C for 24 hours. Afterwards, the crucible is placed in a furnace, incinerating the sample at 600°C for 20min. to obtain the ISS. The difference between TSS and ISS gives the VSS.

3.2.7 Gas Composition Analysis

It was possible to measure the volume of gas produced by the digester by using the gas counter as previously mentioned. The gas meter is based on a batch venting system where the number of fixed batch volumes is counted daily. This gas was captured by using a gas bag of 1.2 litre size. Using a gas chromatograph, the percentage composition of methane, carbon dioxide and other inert gasses of the total gas could be measured. The gas analysis was done by SU in the Engineering Faculty.

3.3 Experimental Test Chart

The following **Table 3-1** provides a summary on all the tests done to each respective experimental setup:

Table 3-1: Summary of test done on experimental setup

	COD		TP	OP	TKN	FSA	Nitrates	Metals		TSS	VSS	ISS	pH
	UF	F	UF	F	UF	F	F	UF	F	UF	UF	UF	UF
ADr	✓	✓	✓	✓	✓	✓	×	✓	✓	✓	✓	✓	✓
ABMP	✓	✓	✓	✓	×	×	×	×	×	×	×	×	✓

AS: WWTW NDEBPR UCT AS system, ADr: Anaerobic digestor; F = 0.45 µm filtered; UF = Unfiltered samples; D = Direct measurement taken. COD (Chemical Oxygen Demand), TKN (Total Kjeldahl Nitrogen), FSA (Free and Saline Ammonia), TP (Total Phosphorus), OP (Ortho-P), TSS (total suspended solids), VSS (volatile suspended solids), ISS (inorganic suspended solids according to (American Public Health Association, 2005). NO3 (Nitrate) and NO2 (Nitrite) by Technicon AutoAnalyser Industrial Method 33.68 and 35.67W; Me+ (metals – Mg, K, Ca) by acid digestion of unfiltered (UF) and filtered (F) samples followed by atomic adsorption (AA) analysis. DSVI (Diluted Sludge Volume Index) according to Ekama and Marais (1984); VFA (volatile fatty acids) and H2CO3 alkalinity with the 5-point titration of (Moosbrugger et al., 1993).

3.4 Augmented Biomethane Potential Tests (ABMP)

The ABMP test is used to measure the potential yield of biogas (i.e., CH_4 and CO_2) from the anaerobic digestion of organic material, including the measurements mentioned in **Section 3.2**. With the assistance of parameter estimation tools applied to AD models, this test can be used to determine the organic composition and biodegradable fraction of an organic waste (Gaszynski, 2020). The ABMP tests were done by Maake & Ikumi, (2021), where the results were used to determine the composition of the biomass, as well as the saturation kinetics which were used in this project.

The ABMP experiment was performed in a similar was as Gaszynski, (2020). A single methanogenic parent ADr was operated (as described in **Section 3.1.2**) in order to provide the required inoculum for the ABMP experiment. The ABMP tests were run in triplicate, which means that identical conditions

were present in 3 of the reactors at the same time. The ADr was fed WAS from the same AS parent system as in this project. The biomass from the ADr was added to the ABMP reactor by a process known as seeding, in which a large sample was drawn from the steady state ADr at the start of the experiment. The substrate is then degraded over a period of 30 to 60 days, with measurements taken daily. The difference between the biogas produced per gram of Volatile Solids (VS) contained in a control sample (ABMP which contain only the inoculum(seed)) and test sample (containing both the substrate and the seed), gives an indication of the potential methane that can be produced through AD from the organics.

The ABMP test (as shown in **Figure 3-4**) uses a glass bottle, with the sample placed inside. The gas escapes through the tubing connected at the top of the bottle. The tubing is filled with H_2O before the test starts, whereby, as gas is produced during testing, the gas displaces the H_2O volume giving a measurement of the gas produced. The test results obtained and used for this project are shown in **Appendix 8.2**.

Figure 3-4: Experimental set-up for an ABMP test (Maake & Ikumi, 2021)

3.5 Closure

All the tests described (except for the gas tests which were done at SU) were done in the Water Quality lab in the New Engineering Building of UCT. The samples for the dynamic AS system were sourced from site, transported, and immediately tested in the lab to reflect the real time parent system as close as possible. The WAS used as feed for the ADrs were sourced from the same full-scale treatment plant and stored in a walk-in-fridge in the Water Quality lab. In doing so, the plant and the lab scale ADrs are linked and can be appropriately modelled.

The data generated from the ADrs are analysed in the following **Chapter 4**, while the data generated from the ABMP reactors are used for parameter estimation in order to determine the characteristics and kinetic rates of the influent and biomass, as described in **Chapter 5**. After which the extended SS AD model results are compared and analysed against the data from **Chapter 4**.

Chapter 4 Experimental Results

4.1 Introduction

This chapter reports the results accumulated from experiment 1 as shown in **Figure 3-1**. As mentioned in **Chapter 3**, two ADrs were operated (i.e., 15- and 32-day SRT), where the short SRT ADr will be referred to as AD-1 and the long SRT ADr as AD-2.

4.2 Measured Data

The averages (mean) of the measured data from the influent (feed) and effluent of both the experimental ADrs are presented in **Table 4-1** and **Table 4-2** respectively. The measured data (after identifying the non-sensical data and leaving it out of any further analysis as seen in **Appendix 8.1**) was further analysed with respect to standard deviation (*s*), after which the % error was determined (mean/*s* = %). All the measured data obtained a % error of less than 20% (meaning the data are within the 80th percentile). The lower value constituents (i.e., FSA, OP, and soluble metals) obtained high % error values, however, this is acceptable as the measured values itself are miniscule.

The data has been further evaluated by performing mass balances over the AD systems for COD, N, P. The relevant output variables (which shall later be used in evaluating the steady state model predictions) include change in COD, VSS, TKN, FSA, TP, and OP. and dissolved counter-ion metal concentrations as well as the inorganic carbon and phosphate alkalinities (H_2CO_3* Alk and H_3PO_4 Alk).

It should be noted however that the two ADrs were not operated in parallel (i.e., not simultaneously). Although the feed came from the same full-scale WWTP, it was collected at different times throughout the year, thus resulting in slight differences in concentrations.

Table 4-1:Influent (feed) concentrations per respective Anaerobic Digester

Steady State	**15-day ADr**			**32-day ADr**		
Description	**Data (Mean)**	**Standard Deviation (*s*)**	**Mean/*s* (%)**	**Data**	**Standard Deviation (*s*)**	**Mean/*s* (%)**
SRT (days)	15	-	-	32	-	-
COD_{Total} (mg/l)	9549	462.1	5	9847	504.6	5
$COD_{Soluble}$ (mg/l)	74	6.4	9	93	8.3	9
TKN (mg/l)	698.8	27.3	4	718	63.4	9
FSA (mg/l)	6.2	1.3	21	3.5	0.9	27
TP (mg/l)	220.8	10.5	5	207.2	12.5	6
OP (mg/l)	3.2	1.1	33	1.2	0.7	57
TSS (mg/l)	8761	59.1	1	8607	582.6	7
VSS (mg/l)	6821	85.4	1	7018	479.1	7
ISS (mg/l)	1941	107.7	6	1527	115.4	8
H_2CO_3* Alk (mg as $CaCO_3$/l)	101.5	3.7	4	109.9	12.6	12
pH	7.0	0.0	0	7.0	0.1	1
Mg_{Total} (mg/l)	27.6	1.9	7	17.3	1.9	11
$Mg_{Soluble}$ (mg/l)	5.4	0.9	16	4.3	1.2	28
Ca_{Total} (mg/l)	125.1	7.5	6	124.3	8.6	7
$Ca_{Soluble}$ (mg/l)	43.7	1.6	4	38.3	5.5	14
K_{Total} (mg/l)	790.9	13.3	2	747.3	57.4	8
$K_{Soluble}$ (mg/l)	15.7	1.8	11	14.0	1.5	11
CH_4 (%)	-	-	-	-	-	-

Table 4-2:Effluent (waste) concentrations per respective Anaerobic Digester

Steady State	15-day ADr			32-day ADr		
Description	**Data**	**Standard Deviation (*s*)**	**Mean/*s* (%)**	**Data**	**Standard Deviation (*s*)**	**Mean/*s* (%)**
SRT (days)	15	-	-	32	-	-
COD_{Total} (mg/l)	7224	267.0	4	5838	323.5	6
$COD_{Soluble}$ (mg/l)	178	11.6	7	190	15.7	8
TKN (mg/l)	675.5	20.6	3	647.3	43.1	7
FSA (mg/l)	257.5	10.4	4	287.4	23.0	8
TP (mg/l)	206.1	9.2	4	180.2	7.2	4
OP (mg/l)	108.9	4.7	4	114.7	4.2	4
TSS (mg/l)	6304	155.8	2	4913	193.0	4
VSS (mg/l)	4770	195.7	4	3768	87.5	2
ISS (mg/l)	1511	150.9	10	1113	94.9	9
H_2CO_3* Alk (mg as $CaCO_3$/l)	1059.8	43.6	4	1177.1	52.1	4
pH	6.7	0.0	0	6.7	0.0	0
Mg_{Total} (mg/l)	25.3	1.3	5	24.3	1.9	8
$Mg_{Soluble}$ (mg/l)	21.0	0.7	3	20.5	2.3	11
Ca_{Total} (mg/l)	124.0	6.6	5	103.5	12.7	12
$Ca_{Soluble}$ (mg/l)	45.4	1.1	2	45.2	3.5	8
K_{Total} (mg/l)	809.2	14.1	2	811.4	52.1	6
$K_{Soluble}$ (mg/l)	401.6	20	5	587.1	29.1	5
CH_4 (%)	43.0	-	-	34.0	-	-

4.2.1 COD Removal in an ADr

In **Table 4-3**, the average COD in the influent and effluent per respective ADr is presented, with the COD influent and effluent also illustrated in **Figure 4-1**. As can be seen from the **Table 4-3**, AD-2 achieved a higher COD removal than that achieved by the AD-1. This is due to the biomass having more time to degrade the feed sludge. Note that the data points marked with crosses are outliers or nonsensical data, and thus was not used in any further analysis.

Table 4-3: Average COD Removal

Component	Unit	15-day ADr	32-day ADr
$COD_{Influent}$	mg/l	9549	9847
$COD_{Effluent}$	mg/l	7224	5838
$COD_{Removed}$	mg/l	2325	4009
$COD_{Removed}$	%	24.3	40.7

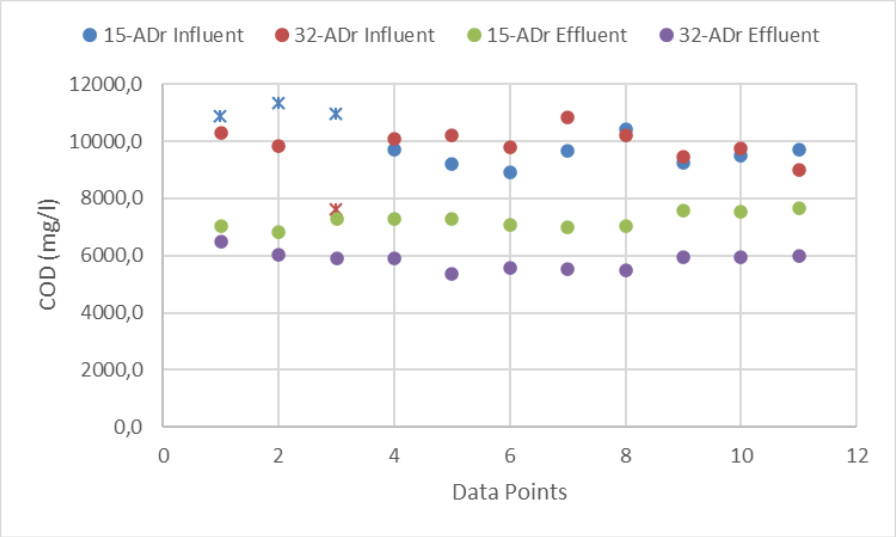

Figure 4-1: Influent vs Effluent COD

4.2.2 FSA Release

In an ADr, organically bound nitrogen in the BPO is released as the organics are degraded. Hence, as is the case with COD removal, the higher the SRT, the higher the amount of FSA released into the ADr liquor. The nitrogen is released in its non-ionic form, NH_3, which is a non-reference species for the ammonia weak acid/base system (Brouckaert, Ikumi & Ekama, 2010). The released NH_3 takes up a proton to form NH_4^+, which results in increased system alkalinity (see **Section 4.2.5**).

In **Figure 4-2**, the influent TKN is compared to the effluent FSA within the two ADrs. On average, the % influent TKN released as FSA from AD-1 and AD-2 was 36.04% and 42.10% respectively. Indicating a higher release of influent TKN as FSA within the longer SRT ADr.

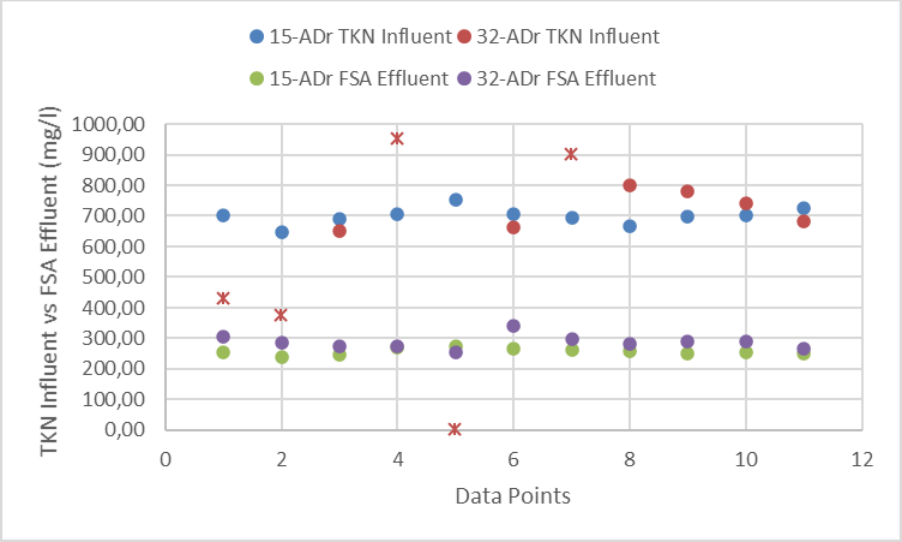

Figure 4-2: Influent TKN vs Effluent FSA

4.2.3 OP Release

In **Figure 4-3**, the influent TP is compared to the effluent OP for AD-1 and AD-2. It is evident from the graph that AD-2 achieved a higher P release than AD-1. AD-1 achieved an average OP release of 47.68% and AD-2 a 55.59% release. The reason for AD-2 to have slightly higher OP release depends

on PP ($Mg_cK_dCa_ePO_3$), where c, d and e were around 0.3, 0.31 and 0.05 respectively (Ikumi *et al.*, 2015). This is because PP release occurs much faster than the organics hydrolysis rate (Harding, Ikumi & Ekama, 2011). This is within the OP release range of 45% - 62% (Ikumi *et al.*, 2015) for SS AD of ND-BEPR sludge.

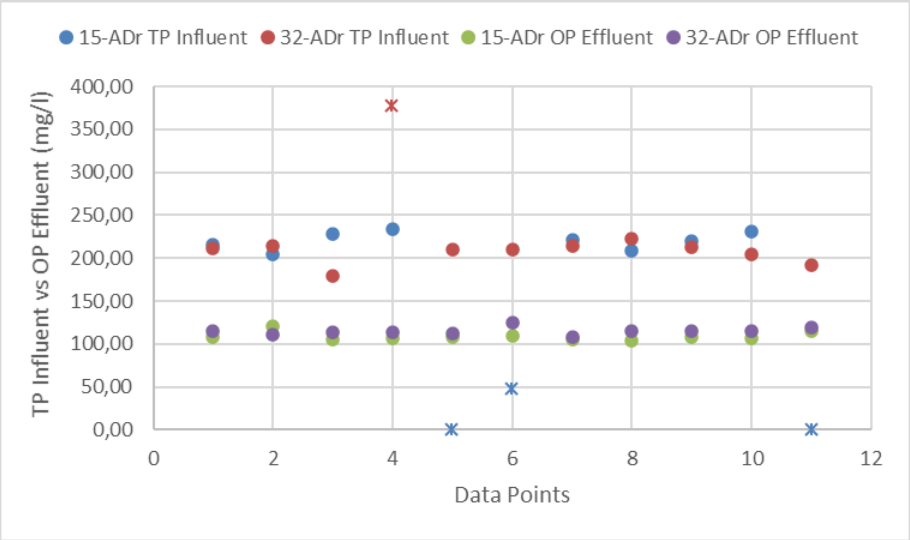

Figure 4-3: Influent TP vs Effluent OP

It is expected that at SS AD operation, all the stored PP within the PAOs are released within a few days (<10 days). This is because when the PAOs are wasted from the aerobic zone, they are full of stored PP. This PP gets released in an anaerobic zone more quickly than the organically bound P in the PAOs and OHOs biomass (Harding, 2009). The evaluation on this result in comparison to what is expected if all the released OP was from the quantity of P bound in biodegradable organics (and not PP) is shown in **Chapter 6**.

4.2.4 Gas Production

Throughout the experimental period, both AD systems were stable and methanogenic. **Table 4-4** presents the volume, together with composition of CO_2 and CH_4, of biogas produced per day, (presented as litres generated per litre influent feed volume/d), for each ADr (i.e., the 15-day and 32-day operated AD systems).

Table 4-4: Average Gas Composition

Description	15-Day ADr	32-Day ADr
Influent COD (mgCOD/l)	9549	9847
Gas Production (litres)	1.41	1.47
CO_2 fraction of total gas	0.40	0.42
CH_4 fraction of total gas	0.42	0.34
COD of CH_4 (mgCOD/l)	1152.60	2035.47

Although proved by Izzett, (1992) and confirmed with stoichiometry by Ikumi *et al.*, (2015) that AD gas composition is in fact independent of SRT, a lower CH_4 fraction was found in AD-2 as compared to AD-1. This is possible due to potential variability of influent characteristics between the two AD systems. On average however, the COD removed as CH_4 was higher in AD-2 as compared to that found in AD-1.

4.2.5 Alkalinity and pH

The alkalinity was measured with the five-point titration method of Moosbrugger *et al.*, (1993) and the effluent alkalinity results are illustrated in **Figure 4-5**, with the pH effluent results in **Figure 4-4**. The total alkalinity is a function of the N content of the BPO (i.e., in this case the WAS biomass) and the PP concentration of the WAS (Ikumi & Ekama, 2019). Both ADrs operated at a pH of 6.7, even though AD-2 had a higher total alkalinity of 1177.1 (±52.1) mg$CaCO_3$/l as compared to 1059.8 (±43.6) mg$CaCO_3$/l of AD-1. Both systems, AD-1, and AD-2, measured an average effluent Alk Volatile Fatty Acids (VFA) of 1.5 (±2.8) and 1.3 (±3.1) mgAcetate(Ac)/l respectively, indicating both systems had negligible concentrations of VFAs, hence they were very stable at the time of testing. The influent Alk VFA on average was higher for AD-2 as compared to AD-1, with 7.6 (±7.3) mgAc/l and 2.3 (±3.2) mgAc/l respectively, which is of a very low concentration, thus negligible.

As previously mentioned, part of the alkalinity generated in the system is influenced by N released during sludge AD breakdown. The NH_3 released picks up a proton (H^+) from the dissolved CO_2 ($H_2CO_3^*$) of the Inorganic Carbon (IC) system, forming HCO_3^-. This contributes part of the $H_2CO_3^*$ alkalinity generated in the ADr, which is crucial in maintaining a steady pH within the system.

The P released from the PP gets released in the form $H_2PO_4^-$, which are not a reference species for the $H_3PO_4^-$ Alkalinity weak acid/base system, thus add alkalinity to the AD system. Since the phosphate weak acid/base sub-system for $H_2PO_4^-/HPO_4^{2-}$ speciation has a pK_{p2} value at 7.13, some of the $H_2PO_4^-$ consumes $H_2CO_3^*$ Alkalinity, forming HPO_4^{2-} , H_2O and CO_2. This means that although the total alkalinity in the system does not change, the partial pressure of CO_2 (p_{CO2}) in the gas changes. The pH of the AD system is thus mostly determined by the IC and the OP systems. (Ikumi & Ekama, 2019)

Usually, a low pH and high effluent VFA would be an indication of impeding digester failure, this was not the case for AD-2. A low effluent VFA concentration indicated that methanogenesis was functional, gas production and pH was constant with respect to COD removed and the effluent alkalinity was high resulting in a stable ADr.

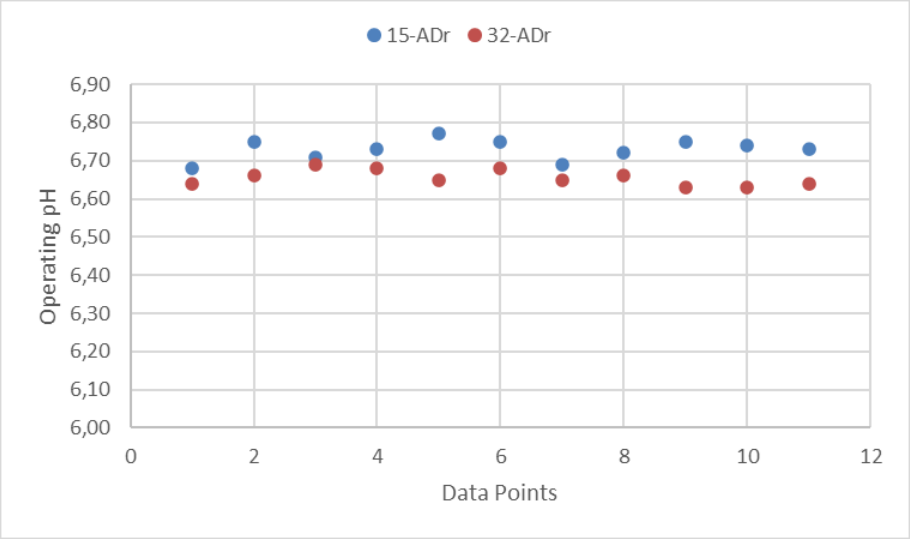

Figure 4-4: pH Comparison of the ADrs

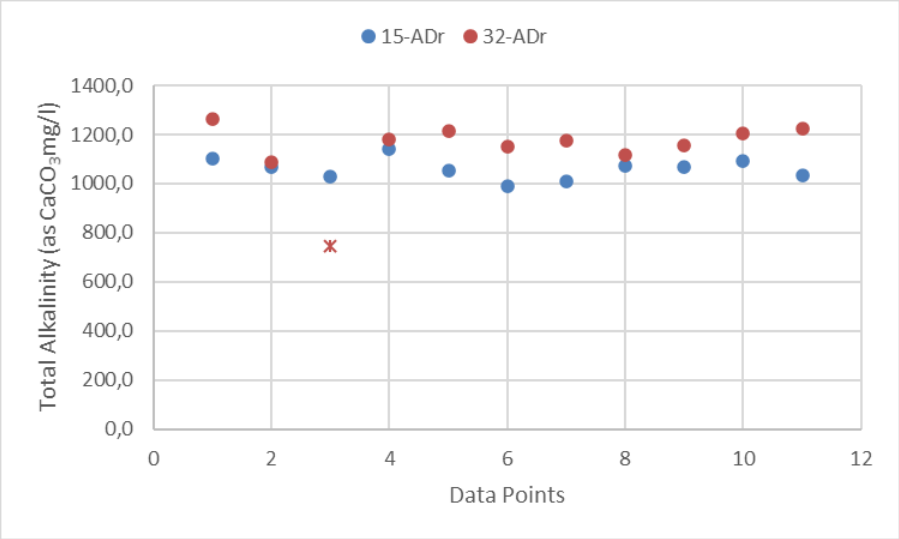

Figure 4-5: Effluent Alkalinity Comparison

4.2.6 Counter-ion Metals

Within the composition of PP, counter metal ions such as Mg, K, and Ca are found to counterbalance the negative charge and balance the PP chain. In an aerobic environment, these metal ions are taken up by PAOs together with phosphorus. When this WAS is then fed to an AD system, the PP is released into the AD liquor, and degraded, releasing the metal ions. The metal ions were measured in the influent and effluent filtered and unfiltered samples in order to determine whether any precipitation (mainly struvite) occurred within the ADrs. **Table 4-5** shows the average measurements obtained from experimental tests done on the ADrs.

Table 4-5: Metal Ion Measurements

Description	15-Day ADr	32-Day ADr
Influent		
Total Mg (mg/l)	27.6	17.3
Soluble Mg (mg/l)	5.4	4.3
Total K (mg/l)	790.9	747.3
Soluble K (mg/l)	15.7	14.0
Total Ca (mg/l)	125.1	124.3
Soluble Ca (mg/l)	43.7	38.8
Effluent		
Total Mg (mg/l)	25.3	24.3
Soluble Mg (mg/l)	21.0	20.5
Total K (mg/l)	809.2	811.4
Soluble K (mg/l)	401.6	587.1
Total Ca (mg/l)	124.0	103.5
Soluble Ca (mg/l)	45.4	45.2

As can be seen from **Table 4-5**, the effluent soluble Mg concentrations for both ADrs are higher as compared to the influent measurements. The effluent and influent soluble concentrations for the Ca in both systems however are very similar. A very high total concentration of K was measured in the influent and effluent, with the soluble K having a low concentration value in the feed but very high concentration in the effluent. There is potential for the particulate metal concentrations to be a part of PP or mineral precipitates. The intricacies of this system require that this be evaluated further, using the scientifically sound reasoning provided in **Chapter 5**. However, this abnormally high K concentration did not seem to decrease the effectiveness of the AD system. A filtered effluent Mg concentration that

is close to the total influent Mg concentration was measured for AD-2, suggesting no precipitation of struvite may have occurred, while a slight difference was observed for AD-1.

4.2.7 Mass Balances

Material mass balance calculations are a good way of verifying the reliability and the accuracy of the experimental results. These calculations are based on the principle that at SS, the flux of the material entering the system, is equal to the flux of the material exiting the system. Therefore, mass balance checks were done on COD, N, P, and counter-metal ions, immediately after completing a SS test period. The following mass balance ranges will be defined as follow:

- 90% - 110%: Indicative of accurate and reliable experimental measurements;
- 80% - 120%: Acceptable if the reasons for it can be determined;
- <80% - >120%: Some of the measured parameters may be incorrect, resulting in careful interpretation;

Table 4-6 presents the results of the mass balances performed over the two ADrs. The mass balances reported below are the values obtained after careful evaluation of the data and removal of visually outlying and inconsistent data, which would otherwise alter the level of accuracy in the results. The mass balances for COD, TKN, TP and counter-ion metals such as Mg, Ca and K are presented in **Table 4-6**.

In anaerobic digesters, the anaerobic biomass has a very low yield. This means that the only a very small portion of the COD feed is converted to new organism mass, while most of the biodegradable organics are converted to CH_4, which is insoluble and escapes the system as a gas. This means COD escapes the system as methane gas. In order thus to achieve a COD mass balance over a methanogenic ADr, the difference between the COD influent and COD effluent should equal the COD that escaped as methane gas.

In order to obtain a 100% mass balance for N, P, Mg, K and Ca, the total unfiltered TKN, TP, Mg, K and Ca in the influent should equal the total unfiltered TKN, TP, Mg, K and Ca in the effluent.

Table 4-6:Mass Balances of the two ADrs

Components	Unit	15-day ADr	32-day ADr
COD	%	87.7	80.0
N	%	96.7	90.2
P	%	93.3	86.9
Mg	%	91.9	140.2
K	%	102.3	108.6
Ca	%	99.1	83.2

As can be noted from **Table 4-6**, the COD balance for AD-1 and AD-2 is 87.7% and 80.0% respectively, which is acceptable. The reason the COD balance is not 100% can be explained by how the gas produced was either sampled from the ADrs or prepared for testing. However, achieving a COD balance of greater than 80% over two lab scale ADrs is deemed acceptable to meet the required objectives of this research. The N balance for AD-1 and AD-2 is 96.7% and 90.2% respectively, while the obtained P balance is 93.3% and 86.9% respectively.

Overall, the metals achieved a good balance, however, the balance for Mg of AD-2 is quite high (140.2%). From **Annexure 8.1**, it can be seen that the effluent results for Mg are constantly higher than the influent. The effluent measured results for Mg of AD-2 is, however, very constant with the values measured for AD-1, and thus, considering the feed was sourced from the same parent system, going

forward, the measured effluent Mg results for AD-2 will be used in the SS AD model in **Chapter 5** & **Chapter 6**.

4.3 Closure

In this chapter, data and results were obtained from two experimental lab-scale ADrs at steady state and presented. An assessment of the results was performed and the two ADrs were compared in relation to their performances. The COD removed, FSA released, OP released, pH, $H_2CO_3^*$ alkalinity, gas composition and counter metal-ions measured were assessed.

It was noted that AD-2 with a longer SRT obtained a higher COD removal %, FSA released and OP released as compared to AD-1. This was expected for the higher the SRT of a system, the more time available for sludge degradation by the AD biomass. The P release was observed to be between 45 % - 56% for both systems, indicating some PP release from PAOs. However, in relation to the soluble effluent counter metal ions, it would seem a low amount of P release originated form the PAOs as PP, suggesting a low population of PAOs within the feed sludge. The results indicate that there was hardly any precipitation that occurred within any of the systems.

Although AD-2 had a low pH as compared to observed by AD-1, both ADrs had stable pH values of greater than 6.5. Relating pH, gas production and effluent alkalinity, both systems were tested while at steady state and were not at any risk of failure. Good material mas balances were obtained over both ADrs during the testing periods.

The results have shown to be sufficiently reliable to meet the research objectives. The data will be further analysed in a SS AD model (Ikumi *et al*., 2015) in **Chapter 6**. The SS model which will be used for the analysis is described in **Chapter 5**. The results will then be compared to the predicted results of the SS AD model and analysed further.

Chapter 5 Extended Steady State Anaerobic Digestion Model

The extended AD SS model by Ikumi *et al*., (2015) which will be the core aspect of the thesis, using the experimental data in **Chapter Chapter 4**, is described in this chapter. The three-phase model, as discussed in **Section 2.4**, will include PP release and degradation as well as the release of organically bound biomass P and mineral precipitation. The AD SS model is described here according to its three main component sections:

i. The sludge characterisation (detail provided on the determination of ND-BEPR WAS characteristics using the method of Harding, (2009)) and using a novel approach of parameter estimation on a SS AD model virtually replicated ABMP test at a long SRT, as described in **Section 3.4**;
ii. The kinetics of sludge degradation (which includes WAS BPO hydrolysis and PP breakdown kinetics) and the findings of a parallel project by Maake & Ikumi, (2021);
iii. The mass balanced bioprocess stoichiometry and weak acid/base chemistry: The mass balanced stoichiometry includes the conversion of biodegradable organics to AD products as shown by Sötemann *et al*., (2005) and Harding, (2009), and the disintegration of PP as explained by Ikumi & Ekama, (2019). The weak acid/base chemistry includes prediction of struvite precipitation and prediction of system pH, which includes predictions made for infinite solubility of precipitates followed by the recalculation of the mineral precipitation potential and the adjustment to system alkalinity (the reason for this recalculation is shown in the section below).

The data obtained from the laboratory set up shall be checked against the predictions of the developed SS AD model to confirm whether the new characterisation method (see **Section 5.1.2**) works well towards generation of reliable influent WAS comprehensive characteristics (which are used as input to the developed SS AD model).

5.1 Influent Characterisation

Two methods were used towards determining the characteristics of WAS that was digested in the AD to obtain the required form of the input variables to the stoichiometric part of the extended AD SS model;

i. The characterisation procedure developed by Harding, (2009) that requires application of the SS AS model of Wentzel *et al*., (1990);
ii. The new method that involves utilisation of results from the operation and testing of ABMP reactors at a long SRT and the application of the SS AD model in a parameter estimation procedure. In principle, although the ABMP reactor is more of a dynamic system, at the long solids retention time, all the bioprocesses have been completed, hence if a SS AD system is virtually operated for a long SRT, it could replicate the outputs at the end of the ABMP reactor operated for a long period.

5.1.1 Fractionation of WAS by application of the AS SS model

The method developed by Harding, (2009) consists of two main steps;

i. The fractionation of ND-BEPR WAS TSS (which comprises of VSS; organics, and ISS);
ii. The determination of elemental compositions for the various WAS components that were determined from the first step. This involves the calculation of each component's molar fractions for C, H, O, N, P and Counter-ion Metals (Me) (i.e., Mg, Ca, and K) using the methods described in **Section 2.2.3**.

The AS model of Wentzel *et al*., (1990) is used towards fractionating the particulate WAS into its organic (VSS) components that include (i) active biomass (OHOs; X_{BH}) and (PAOs; X_{BG}), (ii) ER mass (for both OHOs (X_{EH}) and PAOs (X_{EG})) and (iii) reactor-accumulated influent inert (unbiodegradable) organic mass content (X_I). The inorganic particulate WAS (ISS) is fractionated using the ISS model of Ekama & Wentzel, (2004), into (i) the reactor accumulated influent ISS (X_{IO}), (ii) the ISS from inorganic dissolved solids taken up by biomass that precipitates as ISS during the drying step of the TSS test (X_{IOH}) and (iii) PP accumulated by PAO biomass (X_{PP})). The soluble organics are mainly the unbiodegradable soluble organics and measured inorganic solubles of the AS system effluent (mainly FSA and OP).

$$X_{BH} = \left(\frac{Q_i S_{ti}}{V_p}\right)(1 - f_{upi} - f_{usi})\left[\left(1 - \frac{\%}{100} f_{Sb's}\right)\frac{Y_H R_s}{1 + b_{HT} R_s}\right] \quad (5.1)$$

$$X_{BG} = \left(\frac{Q_i S_{ti}}{V_p}\right)(1 - f_{upi} - f_{usi})\left[\left(\frac{\%}{100} f_{Sb's}\right)\frac{Y_G R_s}{1 + b_{GT} R_s}\right] \quad (5.2)$$

$$X_{EH} = \left(\frac{Q_i S_{ti}}{V_p}\right)(1 - f_{upi} - f_{usi})\left[\left(1 - \frac{\%}{100} f_{Sb's}\right)(f_{EH} b_H R_s X_{BH})\right] \quad (5.3)$$

$$X_{EG} = \left(\frac{Q_i S_{ti}}{V_p}\right)(1 - f_{upi} - f_{usi})\left[\left(\frac{\%}{100} f_{Sb's}\right)(f_{EG} b_G R_s X_{BG})\right] \quad (5.4)$$

$$X_I = \left(\frac{Q_i S_{ti}}{V_p}\right)\frac{f_{upi}}{f_{cv}} R_s \quad (5.5)$$

Where:

- Q_i is the influent flow rate;
- S_{ti} the influent Chemical Oxygen Demand (COD);
- V_p is the volume of the reactor;
- R_S is the SRT in days;
- f_{usi} is the unbiodegradable soluble COD fraction;

- f_{upi} is the unbiodegradable particulate COD fraction;
- X_{BH} the active OHOs; X_{EH} the endogenous OHOs;
- X_{BG} the active PAOs; X_{EG} the endogenous PAOs;
- X_I the UPO inert mass from the influent in the reactor;
- % is the % of readily biodegradable COD (RBCOD) utilised by the PAOs;
- f_{EG} = 0.08, the unbiodegradable residue for PAOs;
- b_H = 0.62/d, the endogenous respiration for OHOs;
- b_G = 0.04/d, the endogenous respiration for PAOs;
- f_{EH} = 0.08, the unbiodegradable residue for OHOs.

5.1.2 Utilisation of a parameter estimation using the AD SS model

In order to identify the composition of the biomass, the bio-process stoichiometry for AD can be used (Ekama, 2009). From **Section 3.4**, the control ABMP test contains only the sludge seed (inoculum from the effluent of the SS ADrs), therefore the C, N and P in the digested inoculum sludge seed becomes part of both the gaseous and aqueous products. Then by measuring the difference in the various concentrations (refer to **Table 5-2**) before the start of the test and the end of the test, the digested COD, VSS, C, N and P of the inoculum sludge can be determined. By using the elemental mass ratios mentioned in **Section 2.2.3**, the composition of the organic material can be identified:

- The carbon content (f_c) of the inoculum sludge:

  With the 5-point titration method (**Section 3.2.5**) and mixed weak acid/base chemistry, the H_2CO_3 alkalinity can be tracked and identified throughout the system. With the change in concentration in CO_2, CH_4 and H_2CO_3 alkalinity before and after the test, the C can be tracked;

- The nitrogen and phosphorus content of the inoculum sludge:

  The N and P content of the inoculum sludge is measured in a similar approach as mentioned above, with the change in concentrations of FSA and OP between the start and end of the test;

- The COD of the inoculum sludge:

  The difference between the COD before and after the test determines the COD lost in the inoculum sludge;

- The VSS content of the biomass:

  The difference of the VSS concentrations before and after the test determines the VSS of the inoculum sludge lost.

With the COD, C, N, P, and VSS known, the mass fractions (i.e., f_c, f_{cv}, f_N, and f_p) required to determine the elemental composition of the sludge can now be determined. This procedure is also applied to the batch test which contains inoculum sludge and a known concentration of substrate organics. The results obtained indicate the concentrations of the various elements transferred to the aqueous and gas phases for both the inoculum sludge and the substrate biodegradable organics. The difference between the test (containing both substrate organics and inoculum sludge) and the control (containing only the inoculum sludge) batch results in various concentrations of the substrate organics.

Three main assumptions were made for the fractionation:

- The Fermentable Biodegradable Soluble Organics (FBSO) in the effluent is zero as the FBSO is completely utilised in the ADr within a 24-hour period. This means that the filtered effluent consists mainly of Unbiodegradable Soluble Organics (USO) and a low concentration of VFA.

- The effluent UPO COD (S_{upe}) is equal to the influent UPO COD (S_{upi}). The ER accumulating due to the decay of microorganisms within the ADr is negligible.
- The total PO COD (S_{pe}) in the SS ADr effluent comprises of UPO, acidogenic biomass (Z_{AD}) and residual biodegradable organics (S_{bp}).

From the components determined, the next step is to determine the BPO and UPO components of the ND-BEPR WAS. The biodegradable organic component of the particulate WAS is defined by the unbiodegradable fraction of the biomass (i.e., f_{EH} and f_{EG}) which according to the death regeneration model used in the AD model is equal to 0.08 (Sötemann *et al*., 2005), whereby [(1-f_{EG}) x X_{BG}] is the biodegradable portion from the PAOs and [(1-f_{EH}) x X_{BH}] is the biodegradable portion from the OHOs. Hence, as influent to the AD, the sum of the biodegradable portions of X_{BH} and X_{BG} form the BPO and the sum of X_{EG}, X_{EH}, X_I and the unbiodegradable constituent of the active OHOs and PAOs (i.e., f_{EH} x X_{BH} + f_{EG} x X_{BG}) determines the UPO (see **equation (5. 6)**). The equation used in fractionating the WAS according to Wentzel *et al*., (1990) are shown below:

$$S_{up\ (AS)} = [X_{inert} + (X_{EH} + X_{EG}) + 0.08(X_{BG} + X_{BH})]f_{cv} \qquad (5.\ 6)$$

With the UPO concentration determined, the difference between the PO determined from the above equations and the UPO will determine the BPO of the WAS .

To determine the characteristics of WAS using the Wentzel *et al*., (1990) SS model, requires that the parent system be at a SS and mass balances are achieved over the AS system. Due to difficulties in achieving this for the full-scale AS system from which the feed was sourced, the second SS AD model parameter estimation-based method was selected as the reliable procedure, in this case, to determine the comprehensive characteristics of the WAS fed to the AD. This includes the BPO, UPO and the PP concentrations, together with the hydrolysis and elemental composition of the BPO (see **Section 3.4** for the description of the ABMP procedure and **Appendix 8.2** for the results obtained). An overview of the parameter estimation process is shown below (Botha, 2015):

PE is a process that adjusts the input parameters of a model by using collected experimental data as an objective for the simulated data. This occurs via the identification of the closest match between the model predicted variable components and experimentally measured variables. Therefore, in order to find a substrate (in this case WAS) composition that better fits the observed ABMP experimental data, PE was conducted on a virtual AD experimental reactor that was replicated using the SS AD model of Ikumi *et al*., (2015). In this case, the parameters that were used as the unknowns were the H, O, N and P molar fractions of the WAS BPO (i.e., x, y, z, a, and b values of $C_xH_yO_zN_aP_b$, the parameters used to define the elemental composition of the PAO biomass) in the WAS. Five observed or known variables were set as the output objectives: total COD, FSA, OP, VSS concentrations and the system pH. The SS AD model was able to replicate the ABMP system (which is usually known to be dynamic) only at the point where all the AD reactions were known to be complete (i.e., at the end of the operations of the ABMP reactor after a long SRT, where no more biogas is generated). This end point of the ABMP test was virtually representable by a SS AD model that was given the same design parameters and waste input but run at SS for a long SRT that similarly allows for completion of all AD bioprocesses. Also, after this long SRT, the remaining organics are all deemed to be unbiodegradable. To initiate the process, the biodegradable and unbiodegradable components of the sludge were calculated from the ABMP experiments as shown in **Table 5-1** below.

Table 5-1: Calculation of Control and Test Masses for Experiment (Maake & Ikumi, 2021)

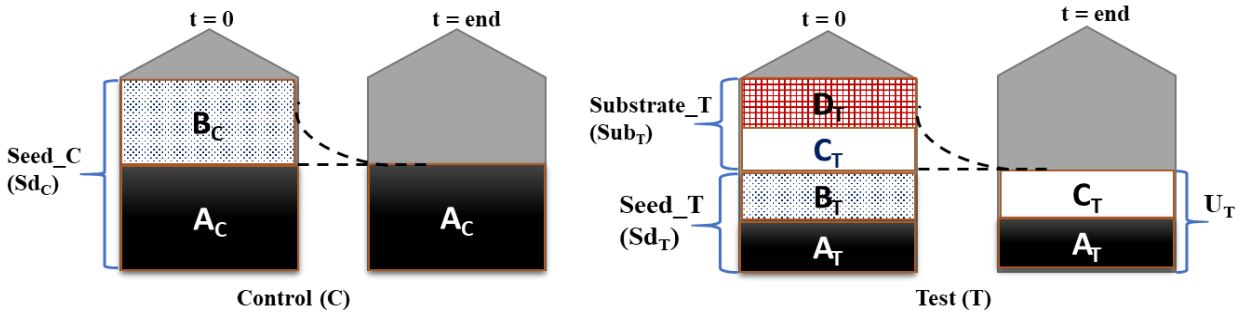

Sd_C: Total mass of inoculum seed sludge added as contents of the control AD batch reactor at t = 0.
Sd_T: Total mass of inoculum seed sludge added to the test AD batch reactor at t = 0.
Sub_T: Total mass of substrate sludge added to the test AD batch reactor at t = 0.
T_T: Total mass of contents added to test AD batch reactor at t = 0, i.e., $Sub_T + Sd_T$.
U_T: Baseline mass containing unbiodegradable material (UPO) obtained at the end of the test AD batch experiment.
A_C: Baseline mass containing unbiodegradable material (UPO) obtained at the end of the control AD batch experiment.
B_C: Mass of BPO (including AD biomass) that gets used up by the end of control AD batch experiment. Hence $B_C = Sd_C - A_C$.
A_T: Equivalent mass of UPO from inoculum seed sludge added to test AD batch reactor. Hence $A_T = A_C/Sd_C * Sd_T$.
B_T: Equivalent mass of BPO from inoculum seed sludge added to test AD batch reactor. Hence $B_T = B_C/Sd_C * Sd_T$.
C_T: Mass of UPO in substrate sludge determined from: $C_T = U_T - A_T$.
D_T: Mass of BPO in substrate sludge determined from: $D_T = T_T - U_T - B_T$.
For all components in the AD batch reactor (i.e., A_C and B_C for the control and A_T, B_T, C_T, D_T for the test), the concentrations are equal to the determined masses divided by the total reactor volume.

Samples	Unbiodegradable Particulates		Biodegradable Particulates		Total Organics	
	Concentration (mgCOD/l)	Mass (mgCOD)	Concentration (mgCOD/l)	Mass (mgCOD)	Concentration (mgCOD/l)	Mass (mgCOD)
Seed_C	3.7	18.5 (A_C)	1.8	9.2 (B_C)	5.5	27.7 (Sd_C)
Test (total)	5.6	27.8 (U_T)	4.5	22.3	10.0	50.0 (T_T)
Seed_T	1.9	9.3 (A_T)	0.9	4.6 (B_T)	2.8	13.8 (Sd_T)
Substrate_T	3.7	18.5 (C_T)	3.5	17.7 (D_T)	7.2	36.2 (Sub_T)

For the given ABMP tests, the 5-litre control reactor comprised 2 litres of seed sludge, sourced from the steady state AD system (which was at about 10gCOD/l), and 3 litres of H_2O; The 5-litre test reactor fed UCT MBR WAS comprised 2.5 litres WAS (at about 4gCOD/l), 1 litre seed sludge and 1.5 litre of H_2O.

The following PE procedure was applied:

i. Setting the initial values in the 5-litre ABMP system. The table below shows the start and the end values of the ABMP reactors that were used to form the initial reactor mass (t=0) components, used as input to the virtual (model replicated) ABMP, and the target values (i.e., the model prediction objectives) for the PE procedure, when calculating the virtual AD reactor outputs.

Table 5-2: ABMP reactor initial and end point concentrations for selected variables

ABMP Reactor set up		period	Variables								
			COD	FSA	OP	VSS	ISS	Ca	Mg	K	pH
Control ABMP values	Control 1	t = 0	4849.7	120.4	92.8	3276.8	440.0	97.8	26.6	280.0	6.7
		t = end	3054.0	213.8	99.0	1940.0	616.0	39.6	31.0	535.0	7.1
	Control 2	t = 0	5531.0	121.0	82.1	3000.0	816.0	79.0	30.4	300.0	6.7
		t = end	3909.1	209.2	99.8	2432.0	732.0	30.2	34.0	609.0	7.2
Measured Test ABMP Values	Test1	t = 0	8096.2	54.0	66.4	5236.0	1132.0	196.4	18.4	280.0	6.6
		t = end	4560.6	238.0	95.2	3564.0	984.0	36.5	31.8	485.0	7.0
	Test2	t = 0	7294.6	62.0	65.3	4152.0	1092.0	102.4	32.2	280.0	6.6
		t = end	4438.5	220.0	83.6	3444.0	1124.0	39.8	31.0	466.0	7.0

ii. The control ABMP reactor is virtually replicated first in order for the information generated during the PE (i.e., the characteristics of the inoculum seed) is added prior to modelling of the test ABMP reactor, which is virtually replicated afterwards. Hence, in the virtually replicated control ABMP reactor, the PE and measured output variables are used to determine the elemental composition of biomass in the inoculum seed sludge. This process involves:

   a. Estimating the biomass concentration at the beginning (t=0) of the ABMP control reactor: since the inoculum seed is sourced from the SS AD system, the SS AD equations of Sötemann *et al*., (2005) are used, with a combined AD organism yield (Y_{AD}) value of 0.113, to estimate the biomass concentration. This biomass concentration is keyed into the SS AD model as the initial total AD biomass concentration for the ABMP reactor to be simulated;
   b. The experimentally measured ABMP output values of variables such as COD, VSS, FSA, OP, pH, and alkalinity are added as target outputs to the SS AD model, where after the model calculations are performed backwards (i.e., the AD products, which are usually AD model outputs, are entered as target values and the biomass composition, which us usually model input, is calculated). This process occurs much simpler and faster than if a complex dynamic simulation model is used together with PE tools in platforms that would house these complex models. Mainly, the simpler SS AD model is explicit and allows for intuitive PE processes that do not require hundreds of trial simulations to be performed. For this to happen, the required parameters (those that would define the elemental composition of the sludge being digested, i.e., the x, y, z, a and b values of $C_xH_yO_zN_aP_b$) are entered as the SS AD model PE adjustable parameters for the PE iterative solver calculations and given realistic constraints (upper and lower bound values) to adhere to;
   c. The solver functions used as mentioned above work to ensure that the theoretically predicted variables are adjusted towards meeting the experimentally measured data. The solver iterations are progressively carried out until the combination of parameter values allow for the best match between the model predicted and experimentally observed variables.

iii. A SS AD test reactor that virtually replicates the one-run ABMP test run experimentally (i.e., with both inoculum and organics added) is simulated (we could replicate ABMP with SS AD since it was for a long SRT as explained earlier). This ABMP test reactor simulation is subsequent to the ABMP control reactor simulation, with the 'initial parameters' that are associated with the inoculum seed and the AD biomass present, having already been determined from the ABMP control reactor simulation. From the ABMP test reactor simulation, the elemental composition of the substrate (in this case WAS biomass) can now be calculated, using the same PE exercise described above.

The compositions determined using the parameter estimation procedure described above, for the biodegradable particulate organics in the control sample, the WAS biomass and the unbiodegradable organics are shown in **Table 5-3** below.

Table 5-3: Determination of Elemental Composition of WAS

Parameter		Control Seed (Particulate Organics)	WAS Biomass	WAS unbiodegradable organics
Description in UCTSDM3P Model (See below)	.i_C_Org_mol_perC	1.00	-	-
	.i_H_Org_mol_perC	1.61	-	-
	.i_O_Org_mol_perC	0.47	-	-
	.i_N_Org_mol_perC	0.13	-	-
	.i_P_Org_mol_perC	0.01	-	-
Resulting Component mass fractions	COD/VSS (f_{cv})	1.48	1.48	1.48
	C/VSS (f_c)	0.52	0.51	0.52
	H/VSS (f_h)	0.07	-	-
	O/VSS (f_o)	0.33	-	-
	N/VSS (f_n)	0.08	0.08	0.10
	P/VSS (f_p)	0.01	0.02	0.03
Where the i_C_Org_mol_perC, i_H_Org_mol_perC, i_O_Org_mol_perC, i_N_Org_mol_perC, i_P_Org_mol_perC are the parameter names for the mole ratios of carbon (C) to C, hydrogen (H) to C, oxygen (O) to C, nitrogen (N) to C and phosphorus (P) to C ratios for the biomass organics elemental formula (i.e. the respective x, y, z, a and b values of $C_xH_yO_zN_aP_b$ expressed according to the standard notational framework proposed by Corominas *et al*., (2010).				

For the ABMP set-up, it is beneficial to test the ABMPs at both the early days (i.e., samples are taken every second or third day from the day 1 to day 40, when the system is still at a dynamic state of COD removal) and at the end of the ABMP experiment (when there is no more biogas being generated and biological activity is deemed to have come to an end). For samples tested, from the early days of the ABMP, when the ABMP is at a dynamic state of COD removal, are useful to determine the hydrolysis kinetics of the sludge while the samples tested from a very long SRT (i.e., a long SRT at the end of the experiment) is useful in determining the unbiodegradable particulate fraction of the sludge. The material that is unbiodegradable (i.e., endogenous residue and influent UPO) from the parent system (AS system) where the feed sludge is sourced from, is not further degraded in the AD system, even at long SRTs of 60 days. This means that the unbiodegradable material (influent UPO) is conserved throughout the ADr SRT. (Ikumi, Harding & Ekama, 2013)

5.1.3 Kinetics of BPO breakdown

For raw influent WW BPO (i.e., the Primary Sewage Sludge (PSS)) the characteristics of the BPO, including the rate at which it would hydrolyse in AD is likely to be system specific and varies depending on the source of pollutants. However, it is not certain whether the required characteristics of WAS organics (i.e., the kinetics of hydrolysis and elemental composition of the OHO and PAO biomass) would remain consistent regardless of the AS system from which they are sourced. Studies from Ikumi, Harding & Ekama, (2013) and of the ABMP tests from Maake & Ikumi, (2021). The determined kinetics from each study are presented in **Table 5-4**.

Table 5-4: Saturation kinetics obtained from (Maake & Ikumi, 2021) and (Ikumi, Harding & Ekama, 2013)

	(Maake & Ikumi, 2021)	(Ikumi, Harding & Ekama, 2013)
Test	Full-Scale WRRF	Lab-Scale WAS-NDBEPR
k_M	2.51	1.95
k_S	4.04	9.11

The difference between the saturation kinetic constants from Ikumi, Harding & Ekama, (2013) and Maake & Ikumi, (2021), is that the former sourced sludge for the ADrs from a lab-scale AS BEPR parent system whereas the latter sourced from a full-scale WRRF (the same source as for this project).

The saturation kinetics are used in the SS model to formulate the hydrolysis kinetics (i.e., refer to **Section 2.5.2**) because the hydrolysis process is known to be rate limiting for AD system treating particulate sewage sludges (Sötemann *et al*., 2005), the mass balanced stoichiometric processes following hydrolysis is assumed to reach instantaneous completion in the SS model to generate the AD products (prior to calculations of the weak acid speciation and mineral precipitation). The volumetric hydrolysis rate (r_{HYD}) according to saturation kinetics formulation is given by the following equation (Sötemann *et al*., 2005):

$$r_{HYD} = \left(\frac{k_M x \left(\frac{S_{bp}}{Z_{AD}} \right)}{K_S + \left(\frac{S_{bp}}{Z_{AD}} \right)} \right) Z_{AD} \qquad (5.\ 7)$$

Where K_S is the substrate and acidogenic biomass concentration ratio, at which the specific hydrolysis rate is half its upper limit (k_M) at saturation.

In order to determine the kinetic constants, a simplified model is used:

1. Due to FBSO (S_{bsfi}) being a complex organic which also requires hydrolysis resulting in the generation of Z_{AD} (i.e., $S_{bp} = S_{bp} + S_{bsfi}$), it will be coupled to BPO (S_{bp});
2. The Z_{AD} concentration represents the biomass formation of all the AD microorganism groups (not only acidogens, which has much lower yield values as Z_{AD} (i.e., 0.089 mgCOD organism/mgCOD substrate)). However, to account for the growth of Acetoclastic Methanogens (Z_{AM}) and Hydrogenotrophic Methanogens (Z_{HM}) biomass (i.e., 0.04 and 0.01 yield coefficients respectively) via improving the predictions on CH_4 and sludge production, Sötemann *et al*., (2005) increased the yield coefficient (Y_{AD}) from 0.089 to 0.113 mgCOD organism/mgCOD substrate.
3. For USO, if it is not accepted as negligible (<100 mgCOD/l in 50 000 mgCOD/l), then it should be subtracted from both the influent and effluent COD concentrations to give the total particulate COD in the influent and effluent.
4. Assume all volatile fatty acids (S_{bsa}) is rapidly utilised.
5. Where the AD SRT is significantly long to allow for utilisation of all biodegradable organics, influent UPO COD can be set equal to the effluent UPO COD ($S_{upi} = S_{upe}$), and the unbiodegradable COD fraction of the sludge ($f_{SL'up}$) can be determined $f_{SL'up} = S_{upi} / S_{ti}$.

To determine the kinetic constants (k_M and K_S) in the hydrolysis rate equations, mass balanced-based principles are first adopted to quantify the Z_{AD} and S_{bp} variables (Ikumi *et al*., 2015; Sötemann *et al*., 2005). Briefly, the system's change in BPO is the quantity increased due to the amount generated with

the death of AD biomass (i.e., Z_{AD}) and the entrance with the AD influent and the BPO decreased due to exit via the effluent and the quantity utilised via hydrolysis as shown below:

$$V\ x\ \partial S_{bp} = Q_i\ x\ \partial t\ x\ S_{bpi} - Q_e\ x\ \partial t\ x\ S_{bpe} - r_{HYD}\ x\ V\ x\ \partial t + (b_{AD}\ x\ Z_{AD})\ x\ V\ x\ \partial t \qquad (5.8)$$

Simplifying the equation to quantify r_{HYD} gives: $r_{HYD} = b_{AD}\ x\ Z_{ADi} + \left(\frac{S_{bpi} - S_{bpt}}{\partial t}\right)$ for batch conditions and: $r_{HYD} = \left(\frac{S_{bpi} - S_{bpe}}{R_s}\right) + (b_{AD}\ x\ Z_{AD})$ for continuous AD systems (Ikumi *et al*., 2015).

Applying a similar mass balance approach to the acidogenic biomass (Z_{AD}) concentration as was done for BPO yields: $\partial Z_{AD} = Y_{AD} \cdot r_{HYD} \cdot \partial t - b_{AD} \cdot Z_{AD_i} \cdot \partial t$. Hence, $Z_{AD} = Z_{AD_i} + \partial Z_{AD} = Z_{AD_i} + \left(Y_{AD} \cdot r_{HYD} - b_{AD} \cdot Z_{AD_i}\right) \cdot \partial t$ for ABMP conditions of Maake & Ikumi, (2021) and $Z_{AD} = \left(S_{bpi} - S_{bpe}\right) \cdot \left(\frac{Y_{AD}}{1 + b_{AD} \cdot R_s \cdot (1 - Y_{AD})}\right)$ for continuous AD conditions (Ikumi *et al*., 2015).

With this established, the biodegradable COD components are simplified (coupled) to a single component (i.e., $S_{bp} = S_{bsf} + S_{bp}$, assuming that the S_{bsa} is used very rapidly, hence dealt with separately. The effluent COD (S_{te}) can then be quantified as $S_{te} = S_{bp} + f_{SL'up}$ x $S_{ti} + Z_{AD}$. Hence, the S_{bp} can be equated to: $S_{bp} = S_t - f_{SL'up} \cdot S_{ti} - Z_{AD} - S_{us}$. The best estimate for $f_{SL'up}$ is selected to ensure that S_{bp} has a value of zero, for the AD system operated for a long retention time, when calibrating the hydrolysis kinetics.

After calculating S_{bp}, rate of hydrolysis (r_{HYD}) and Z_{AD} (with respect to time t) with a corresponding S_t, the hydrolysis rate kinetic constants (k_M and k_S for saturation hydrolysis kinetics) were obtained through non-linear regression methods (i.e., sum of least squares) via the curve fitting software (e.g., the R Studio software) (Maake & Ikumi, 2021; Ikumi *et al*., 2015). The kinetic rate constants that provide the closest predictions are selected for application to the ADr, after which the calibrated hydrolysis rate equation can be applied to calculate the residual biodegradable organics of a given time (S_{bp_t}).

5.1.4 Polyphosphate Breakdown

The observation of PP release by Harding, (2009) and Maake & Ikumi, (2021) in the ABMP reactors confirms that stored PP in PAOs (which forms a large portion of the TP content) is released within 7 days (i.e., a very short time). The rapid release of PP in AD environments would usually be followed by mineral precipitation, hence the kinetics of this process could be useful in dynamic simulation models. However, for the simplified SS model, it is assumed that all the PP is released (i.e., without having to include the kinetics) because the SRTs utilised for beneficially stable AD systems are usually >10 days. Hence a significant aspect consider for the SS AD model is the nature in which the PP is released, the final products generated from this process and its impact on the weak acid/base systems in the aqueous phase. This is all explained in the following section of AD bioprocess stoichiometry.

5.2 Mass Balanced Stoichiometry and Weak acid/base Chemistry

5.2.1 Mass Balanced Stoichiometry of Harding (2009)

As mentioned in **Chapter 2**, Harding, (2009) extended the CHON, COD, and charge mass balance of the SS AD model (Sötemann *et al*., 2005) by adding the biomass P and PP in NDBEPR WAS, which includes P and counter-ion metals such as Mg, Ca, and K, mass balance stoichiometry.

The complications in extending the model with the inclusion of P was due to the different rates (endogenous model vs death rate model of PAOs) of which PP are released, organically bound P are released, the effect of the 2nd dissociation constant (i.e., pK_{p2}~7) of the OP weak acid/base chemistry system and the precipitation of metal phosphates. (Harding, Ikumi & Ekama, 2011)

To include the effect of the 2nd pK_{p2} at a pH of 7.0, Harding, (2009) determined the mass balanced redox half reactions of substrate electron and H^+ donation by dividing the P products from PP and organically bound P into HPO_4^{2-} and $H_2PO_4^-$, since it was noted between the pH range of 5 – 9, the OP species consists almost entirely of the products mentioned. The products released form the PP and biomass (i.e., HPO_4^{2-} and $H_2PO_4^-$) were determined equal to the OP. With the IC system discussed in **Section 2.4** and the OP system, the ADr pH is established via the aqueous phase equilibrium chemistry within the ADr. As noted in the previous section, all the PP inside the PAOs is released within a short AD SRT (>5 days) (Harding, 2009). As shown in **Section 5.1**, there is a fixed ratio (q_{PAO}) between the PAO biomass and the PP, following this, the equations provided below illustrates the general reaction stoichiometry separating the biomass P and PP for any biodegradable organics:

$$\begin{aligned} C_X H_Y O_Z N_A P_B + &\left(2X - Z + A + (2+f)B - E\frac{y_S}{y_B}(2k - m + n + (2+f)p)\right. \\ &\left. - \frac{2y_S}{8}(1-E)\right) H_2O \\ &\leftrightarrow \left(X - A + (2-f)B - E\frac{y_S}{y_B}(k - n + (2-f)p) - \frac{(1-E)y_S}{8}\right) CO_2 \\ &+ \left(\frac{y_S}{8}(1-E)\right) CH_4 + \left(E\frac{y_S}{y_B}\right) C_k H_l O_m N_n P_p + \left(A - nE\frac{y_S}{y_B}\right) {NH_4}^+ \\ &+ f\left(B - pE\frac{y_S}{y_B}\right) {H_2PO_4}^- + (1-f)\left(B - pE\frac{y_S}{y_B}\right) {HPO_4}^{2-} \\ &+ \left(A - (2-f)B - E\frac{y_S}{y_B}(n - (2-f)p)\right) {HCO_3}^- \end{aligned} \qquad (5.\ 9)$$

And for PP:

$$\begin{aligned} q[Mg_c K_d Ca_e PO_3] + fqH_2O + (1-f)q{HCO_3}^- \\ \leftrightarrow (1-f)qCO_2 + fq{H_2PO_4}^- + (1-fq){HPO_4}^{2-} + qcMg^{2+} \\ + qdK^+ + qeCa^{2+} \end{aligned} \qquad (5.\ 10)$$

Where:

- y_S and y_B refer to the Electron Donating Capacity (EDC) of the substrate and biomass respectively:
  - $y_S = 4X + Y - 2Z - 3A + 5B$ (e^-/mol) (5. 11)
  - $y_B = 4k + l - 2m - 3n + 5p$ (e^-/mol) (5. 12)

- E is the fraction of biodegradable COD for the flow through the ADr [no endogenous residue of AD biomass (f_{AD} = 0), COD utilised (S_{bpi} - S_{bpe})] that is converted to biomass (Z_{AD}):

- $E = \frac{Z_{AD}}{S_{bpi}-S_{bpe}} = \frac{Y_{AD}(1+b_{AD}SRT)}{[1+b_{AD}SRT(1-Y_{AD})]}$ *(5. 13)*

- Y_{AD} the yield coefficient (gCOD biomass/gCOD organics hydrolysed);
- b_{AD} the acidogen endogenous respiration rate (/d);
- SRT in days;
- *f* is the fraction of $H_2PO_4^-$ in the total P system (comprising mostly of HPO_4^{2-} and $H_2PO_4^-$).

Due to the release of P and counter-ion metals from hydrolysis of PP in AD, a three-phase (gas-aqueous-solid) weak acid/base stoichiometry as described in **Section 2.4** is required as high concentrations can cause precipitation.

5.2.2 Modelling behaviour of PAOs in the AD system

Due to the characteristics of PAOs in ADrs, the effect and influence that their behaviour has on the weak acid/base chemistry and pH on an ADr system need to be considered in the SS AD model. In a conventional AS BEPR system, the PAOs take up SCFA in the anaerobic zone and convert them to PHA. The PHA is an energy storing compound, which is stored by the PAO biomass for use in the aerobic zone (i.e., due to presence of oxygen that acts as an electron acceptor) to carry out their growth and energy generating metabolism. However, when WAS containing PAOs (with WAS normally taken from the aerobic reactor, the PAOs contain stored PP) is fed to an ADr (which also is known to contain SCFA from the acidogenic fermentation processes), the PAOs would continue to release their PP for SCFA uptake and PHA formation in a similar way as was performed in the anaerobic zone (Ikumi & Ekama, 2019). However, with no alternating aerobic zone present, thus the absence of electron acceptor (oxygen) required for their growth, the PAOs eventually die, releasing any remaining PP and PHA as the rate of death is much faster than the hydrolysis rate of the PAO biomass. The above reasoning validates why it is necessary to model the PP release with PHA formation, P release upon death and the release of organically bound P. (Ikumi & Ekama, 2019)

In the aerobic zone, $NADH_2$ (reducing agent, formed by the uptake of $2e^-$ and $2H^+$) is produced with the uptake of PP and degradation of PHA by PAOs and thus supplied to into the ADr. The PHA is broken down in the ADr with the growth of AD biomass and form CO_2 and CH_4. It can be seen then that PAOs do not compete with AD biomass, however, after an initial rapid uptake of acetate and release of PP by PAOs, the PHA is released with the hydrolysis of the PAO biomass (Ikumi *et al*., 2015). With the inclusion of the P fractionation according to pH by the f value to HPO_4^{2-} and $H_2PO_4^-$ as discussed in the previous section (Harding, 2009), the following equation illustrates the release of PP and is included in the AD model:

$$CH_3COOH + Mg_cK_dC_ePO_3 + \left(\frac{3}{4}+f\right)H_2O + e^- \rightarrow fH_2PO_4^- + (1-f)HPO_4^{2-} + fHCO_3^- + eMg^{2+} + dK^+ + eCa^{2+} + \frac{9}{8}CH_4 + \left(\frac{7}{8}-f\right)CO_2 \quad (5.\ 14)$$

In the case where $NADH_2$ is produced within the ADr as reported by Ikumi & Ekama, (2019), with the breakdown of PHA, producing CO_2 and CH_4, and the breakdown of acetate, producing HCO_3^- and CH_4, which has an equivalent outcome as the PP release occurring with the death of PAOs (Harding, 2009), and the possibility of the process mentioned in **equation (5. 14)**, the generalised stoichiometric model for PP is extended accordingly as illustrated below:

$$\begin{aligned}\emptyset CH_3COOH + [Mg_cK_dCa_ePO_3] + \left(\emptyset\left(\frac{3}{4}+f\right)+(1-\emptyset)f\right)H_2O + \emptyset e^- \\ \rightarrow fH_2PO_4^- + (1-f)HPO_4^{2-} + \left(\emptyset f-(1-\emptyset)(1-f)\right)HCO_3^- \\ + cMg^{2+} + dK^+ + eCa^{2+} + \emptyset\frac{9}{8}CH_4 \\ + \left(\emptyset\left(\frac{7}{8}-f\right)+(1-\emptyset)(1-f)\right)CO_2\end{aligned} \quad (5.\ 15)$$

Essentially, the selection of the reducing agent for PP release results in 2 possible stoichiometry outcomes, which are presented by Ikumi & Ekama, (2019).

5.2.3 Inclusion of Mineral Precipitation and pH Prediction

As discussed in **Section 2.4**, anaerobic digestion of organics result in the production and release of various chemical species with different molar concentrations into the aqueous liquor of the ADr. Some of these products and species belong to the weak acid/base sub-systems which directly affect the pH of an ADr. The SS AD model first assumes infinite solubility, meaning that no precipitation occurs within the ADr, the theory and concepts regarding the weak acid/base sub-systems are discussed in **Section 2.4**. However, with favourable conditions (i.e., high concentrations of dissolved counter-ions, pH > 6.8) mineral precipitates are likely to form (finite solubility) within the ADr liquor (Ikumi *et al*., 2015). With the formation of precipitates, a change in digester pH will be observed due to a change in some of the AD products from an aqueous to solid phase.

The minerals that are most likely to form in the ADr are:

- Calcium phosphate ($Ca_3(PO_4)_2$);
- Calcium carbonate ($CaCO_3$);
- Struvite ($MgNH_4PO_4$).

Although the formation of struvite and the method used to determine the precipitation potential was discussed in **Section 2.4.3.1**, $Ca_3(PO_4)_2$ and $CaCO_3$ are also included into the extended SS AD model. (Ikumi *et al*., 2014)

As is the case with struvite precipitation, total alkalinity decreases with the precipitation of Q mol/l/ of $CaCO_3$. The reason is that 2 x [$CaCO_3$] precipitated as the [CO_3^{2-}] species are $2H^+$ from the $H_2CO_3^*$ reference species, resulting in a change in the inorganic carbon system species concentrations and thus a change in the CO_2 partial pressure (p_{CO2}). This change can be explained as H^+ ions are released when HCO_3^- loses its carbonate mass to calcite, and in order to 'balance' or re-adjust the molar ratios of the carbonate system species according to pH, H^+ ions are taken up by HCO_3^- to form H_2CO_3. This production of more H_2CO_3 result in more CO_2 gas, which increases the p_{CO2}. (Ikumi *et al*., 2015)

With the precipitation of V mol/l of ACP ($Ca_3(PO_4)_2$), Ca and PO_4^{3-} aqueous species are lost to the solid phase. The release of H^+ ions by the phosphate species reduces the HCO_3^- concentration and increases the dissolved CO_2 resulting in a change in the alkalinity, p_{CO2} and system pH. The pH will be determined assuming infinite solubility first, after which finite solubility will be assumed to determine the digester pH after precipitation. For the final determination of the system pH after precipitation, the following stoichiometric equation includes the sum for biomass utilisation and PP release and is provided below:

$$
\begin{aligned}
&\emptyset CH_3COOH + Mg_cK_dCa_ePO_3 + RNH_4{}^+ \\
&\quad + \left(\emptyset\left(\frac{3}{4}+f\right) + (1-\emptyset)f + (5-f)R - Q - 2V(f+1)\right)H_2O + \emptyset e^- \\
&\quad \rightarrow f(1-R-2V)H_2PO_4{}^- + (1-f)(1-R-2V)HPO_4{}^{2-} \\
&\quad + \left(\emptyset f - (1-\emptyset)(1-f) - (1+f)R - 2Q - 2V(f+1)\right)HCO_3{}^- \\
&\quad + (c-R)Mg^{2+} + dK^+ + (e-Q-3V)Ca^{2+} + \emptyset\frac{9}{8}CH_4 \\
&\quad + \left(\emptyset\left(\frac{7}{8}-f\right) + (1-\emptyset)(1-f) + (1+f)R + Q + 2V(f+1)\right)CO_2 \\
&\quad + RMgNH_4PO_46H_2O + QCaCO_3 + VCa_3(PO_4)_2
\end{aligned}
\qquad (5.\ 16)
$$

Due to precipitation, the final inorganic carbon, phosphate, and other species concentrations have changed in the general stoichiometry. The expressions for CO_2 and HCO_3^- in **equation (5. 16)** need to replace the previous (pre-precipitation) stoichiometric expressions in the determination of pH as shown in **Section 2.4**.

5.3 Closure

For the extended SS AD model (Ikumi *et al*., 2015) calibrated in this dissertation, three components were addressed; firstly, determining the sludge characteristics using either the method of Harding, (2009) or a new approach of the PE on a SS AD model, secondly, the kinetics of sludge degradations (Maake & Ikumi, 2021), and lastly the mass balanced bioprocess stoichiometry and weak acid/base chemistry.

In order to determine the characteristics of the WAS using the methods of Harding, (2009) and Wentzel *et al*., (1990), the parent AS system must be at SS with mass balanced achieved for the system. However, due to difficulties in achieving this with a dynamic full-scale AS system from which the feed was sourced, the PE method was selected for determining the WAS characteristics.

Two sets of saturation kinetic constants were used for the calibration of the SS AD model; (1) constants determined from a sludge sourced from a lab-scale AS BEPR system (Ikumi, Harding & Ekama, 2013), and (2) sludge sourced from a full-scale WRRF (Maake & Ikumi, 2021). Calibration of the extended SS AD model will be more accurate by comparing the results obtained from the 2 different sets of kinetic constants (refer to **Section 5.1.3**).

The extended SS AD model include the CHON, COD, and charge mass balance (Sötemann *et al*., 2005), the biomass P, PP and counter-ion metals added by Harding, (2009). However, including organically bound P release and degradation of PP in the model, resulted in a change in the OP weak acid/base system and system total alkalinity as mineral precipitation must also be included in the SS AD model. For the model used, struvite, $Ca_3(PO_4)_2$ and $CaCO_3$ precipitation is included.

In determining the final system pH and p_{CO2}, the pH and effluent products has to be determined prior to any precipitation so as to calculate the precipitation potential within the AD liquor. Precipitation cause a change in some of the AD products from the aqueous to solid phase, influencing the pH and p_{CO2} (Harding, Ikumi & Ekama, 2011)

Chapter 6 Modelling Analysis and Discussions

The results predicted from modelling the extended SS AD model (described in **Chapter 5**) with influent values measured from the experimental tests, are presented, and evaluated in this section. The predicted results will further be compared to the measured results (illustrated in **Chapter 4**) obtained from the experimental setup and procedure (which is described in **Chapter Chapter 3**). The results obtained from the experimental setup of **Chapter 3**, the results obtained from the ABMP tests and the modelled results are presented in **Appendix 8.1, 8.2** and **8.3** respectively.

6.1 Influent Characteristics

In order to determine whether the new characterisation method (refer to **section 5.1.2**) works well, it shall be checked against the predictions of the developed SS AD model. However, in order to ensure the most accurate comparison of the AD predictions, some correlation between Maake & Ikumi, (2021) and Ikumi, Harding & Ekama, (2013) will have to be made regarding the input variables for the extended SS AD model. However, the UPO which are specific to the parent system from which the sludge feed was sourced, can vary depending on this parent system influent characteristics or operational parameters (e.g., SRT) (Ekama, 2017). Hence, because the UPO fraction of the WAS fed to the SS AD systems was determined by Maake & Ikumi, (2021), this value ($f_{S'up}$ = 0.51) was not adjusted (for the values from Ikumi, Harding & Ekama, (2013) could not be applied for these values as they had to be sourced from the actual parent system and not from literature).

The elemental composition mass ratios determined by Maake & Ikumi, (2021) and Ikumi, Harding & Ekama, (2013), and the UPO fraction are presented in **Table 6-1**. The kinetic constants used are presented in **Table 5-4**.

Table 6-1: Mass ratios determined from the ABMP tests (Ikumi, Harding & Ekama, 2013; Maake & Ikumi, 2021)

	Scenario 1 (Maake – 2021)			**Scenario 2 (D. Ikumi – 2013)**
	UPO & ER	WAS BPO Substrate	UPO fraction	WAS BPO Substrate
f_{cv}	1.48	1.48	-	1.43
f_c	0.52	0.52	-	0.51
f_N	0.10	0.08	-	0.14
f_P	0.03	0.01	-	0.04
$f_{S'up}$	-	-	0.51	-

The PP elemental composition ($Mg_{0.23}K_{0.34}Ca_{0.1}PO_3$) was determined by Maake & Ikumi, (2021) using the methods of Ikumi, (2011). Since Maake & (Ikumi, 2021) data is for the WAS that was fed to the SS AD, it will be used as an input in the model. Apart from the characteristics of the WAS feed, the inputs to the SS AD model include parameters such as those for weak acid/base dissociation constants, Henry's Law constant and solubility products for the mineral precipitation. These parameter constants are presented in **Table 6-2**:

Table 6-2: Parameters used in the extended SS AD model (Ikumi et al., 2014)

Description	Component	
Constants	Y_{AD}	0.113
	b_{AD}	0.041
Weak acid/base Dissociation Constants	pK'_{C1}	6.31
	pK'_{C2}	10.25
	pK'_{P2}	7.18
	pK'_{n}	8.95
	pK'_{a}	38.64
Henry's Law Constant	pK_H	1.61
Solubility Products for Mineral Precipitation	Struvite (R)	2.51E-13

Where: Y_{AD} is the yield coefficient (mol/mol) and b_{AD} the endogenous respiration rate (/d); R (mol/l) for struvite

6.2 Evaluation of Results Against Steady State Model Predictions

The results measured in the lab-scale ADrs are compared and analysed against the results modelled in the SS AD model. For the model predictions, two scenarios are presented: **scenario 1** using kinetic rates determined as described in **Section 5.1.3** (Maake & Ikumi, 2021) and input elemental compositions as mentioned in **Table 6-1**, and **scenario 2**, using kinetic rates and elemental compositions determined by Ikumi, Harding & Ekama, (2013).

6.2.1 COD Evaluation

Comparing the effluent COD results between the two different SRT's, 15- and 32-day SRTs, the 32-day sludge ADr resulted in lower COD values, as would be expected, for COD decreases as SRT increases, as the biomass has more time to degrade the biodegradables (Harding, 2009). **Figure 6-1** illustrate the measured effluent COD versus the modelled results of scenario 1 and 2.

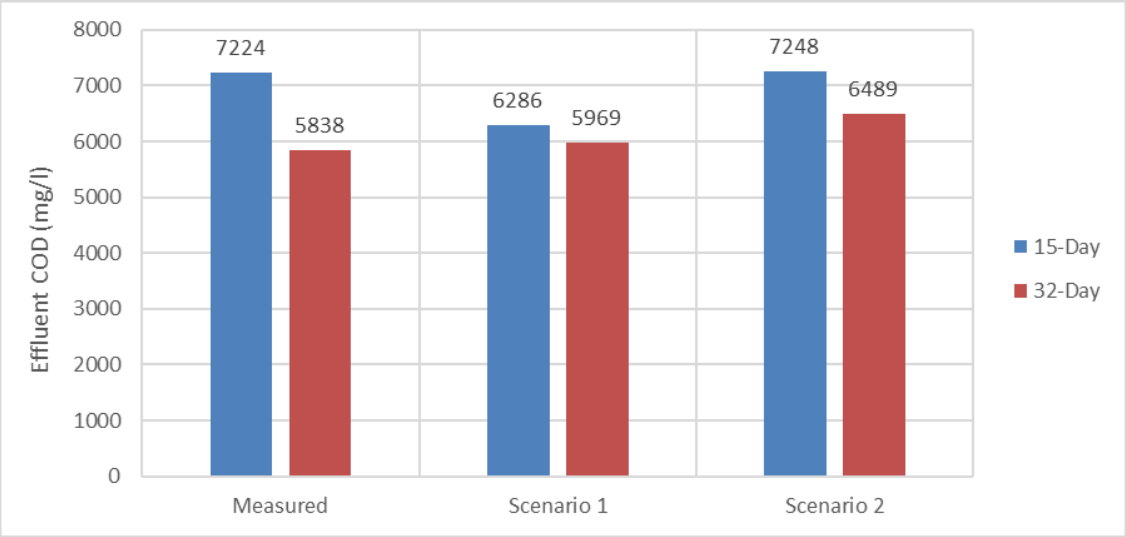

Figure 6-1:Effluent COD comparison

Although variation can be seen between the measured and predicted results of the 15- and 32-day ADrs, the predicted results deviates less than 13% from the measured results, which is acceptable for this parameter. The measured and predicted effluent results matches as they emulate the results of the hydrolysis part of the AD model. The difference between scenario 1 and 2 predicted results can be explained by the difference in the saturation kinetics, as can be seen in **Table 5-4**. The saturation kinetic value of K_S is the substrate and acidogenic biomass concentration ratio, and for scenario 2 it is a lot

larger than scenario 1 (9.11 and 4.04, respectively), resulting in a much higher effluent BPO COD for scenario 2 as compared to scenario 1. The modelled effluent BPO and UPO COD are shown in **Table 6-3**:

Table 6-3: Modelled effluent BPO and UPO comparison

Description	Scenario 1 – 15d	Scenario 2 – 15d	Scenario 1- 32d	Scenario 2 – 32d
BPO (mgCOD/l)	1063.5	2040.0	579.0	1113.2
UPO (mgCOD/l)	5148.5	5134.2	5297.2	5282.5
USO (mgCOD/l)	74.0	74.0	93.0	93.0
Total Effluent COD (mgCOD/l)	6286.0	7248.2	5969.2	6488.7

It should be noted, as mentioned earlier, that CH_4 gas production is associated with the BPO COD removed, and thus can be used to evaluate the COD removal of a system at different SRTs. Comparing the COD removed with the CH_4 gas produced (as mgCOD/*l* influent), can help to determine the reliability of the gas measurement results, and the experimental COD balance.

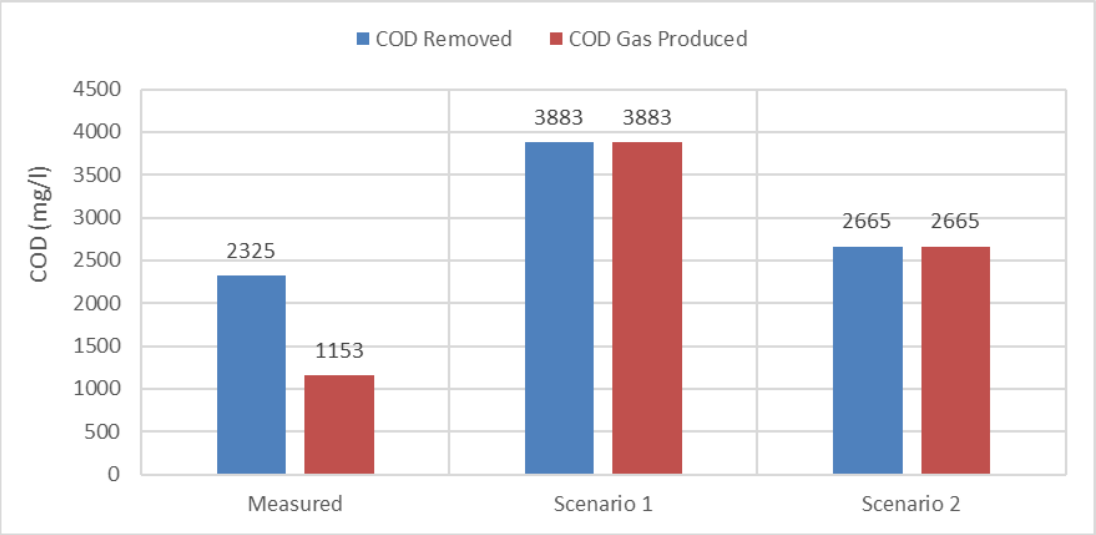

Figure 6-2: 15 -Day COD gas produced versus COD removed

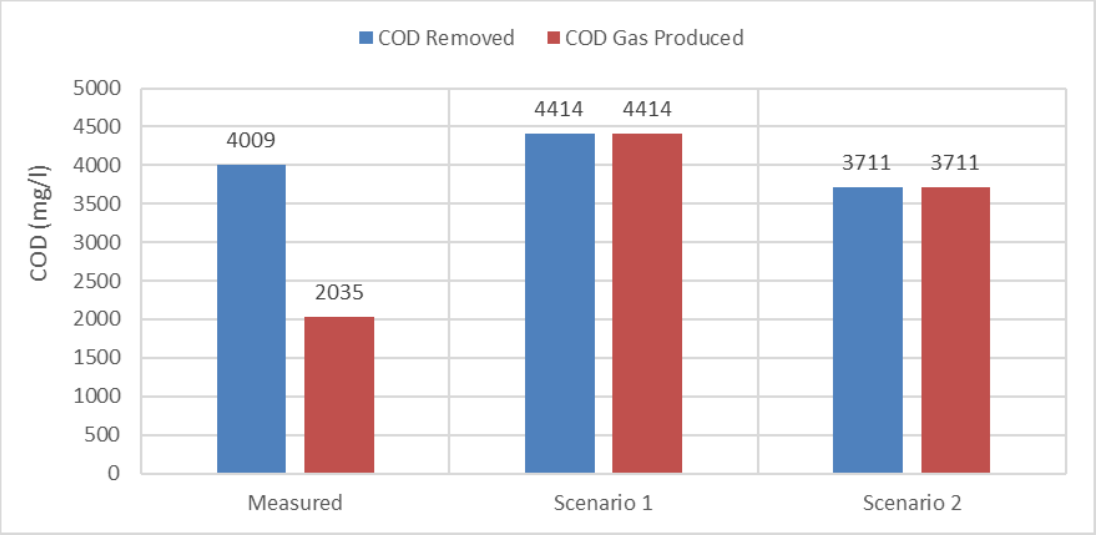

Figure 6-3: 32-Day COD gas produced versus COD removed

In **Figure 6-2** and **Figure 6-3**, the predicted gas produced is higher than the measured data and the measured COD removal does not match the CH_4 COD. However, the predicted CH_4 gas results are based on a 100% COD balance. For the predicted results, scenario 1 obtained a higher predicted COD

gas production compared to scenario 2. More confidence was placed in the COD measurements than the CH_4 data because the sampling and testing procedure (not in situ) resulted in experimental error in determining the CH_4 contribution to COD, as stated above. This seems to be the main reason behind the 12% and 20% COD balance error obtained, as shown in **Table 6-4**. The kinetic constants adapted by Maake & Ikumi, (2021) also seem to have over predicted the COD removal as CH_4, as compared to Ikumi, Harding & Ekama, (2013).

Table 6-4: COD balance comparison

SRT:	Measured COD Balance	Mass Balance Error
15-day	87.7%	12.3%
32-day	80.0%	20.0%

6.2.2 Nitrogen Evaluation

This section presents the evaluation of both predicted FSA and TKN in comparison to the measured values.

6.2.2.1 TKN Evaluation

As shown in **Figure 6-4** and **Figure 6-5** below, good mass balances were achieved for both ADrs systems (96.7% and 90.2% for 15- and 32-day systems respectively), providing confidence in the TKN data obtained from the SS ADrs. It should be noted that the model achieved 100% balances, meaning the influent and effluent TKN values are exactly the same.

For both the 15 and 32-day data sets, the effluent TKN for scenario 1 is underpredicted while scenario 2 is over predicted as compared to the measured effluent TKN. The reason for this is that scenario 1 has a much lower f_N value for both the WAS substrate (0.08), as compared to that for scenario 2 (0.14).

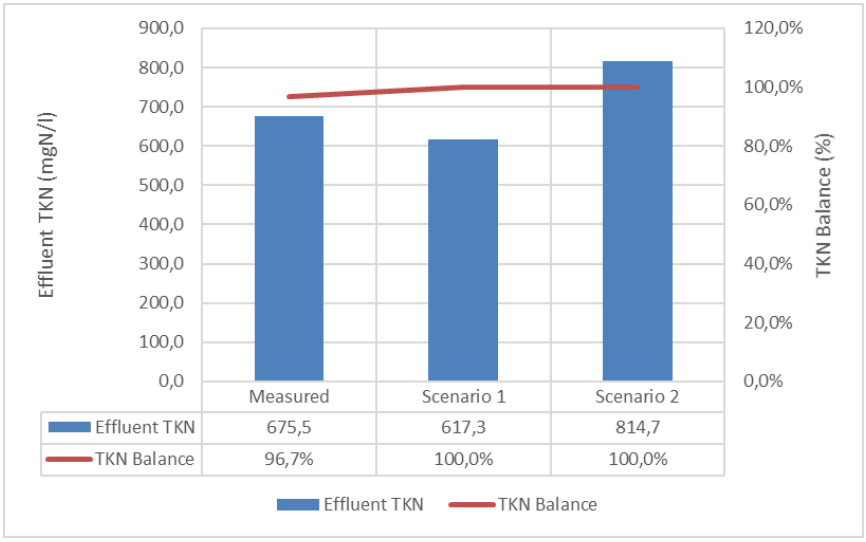

Figure 6-4: 15-day TKN evaluation

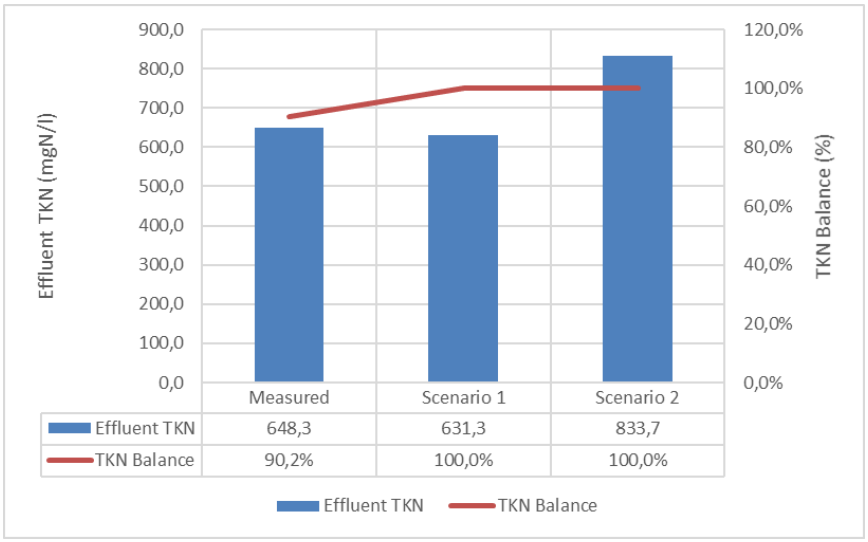

Figure 6-5: 32-day TKN evaluation

6.2.2.2 FSA Evaluation

For ADrs, the longer the SRT, the more substrate is degraded, releasing organically bound N in the non-ionic NH_3 form into the AD Liquor (ADL). Hence, substrate containing N bound BPO, the amount released is dependent on the COD breakdown and amount of N in the bound biodegradable organics of the substrate and the period of degradation thereof. According to the SS model (Ikumi *et al.*, 2015; Harding, 2009; Sötemann *et al.*, 2005), the released NH_3, which is a non-reference species for the NH_4^+ Total Alkalinity, bonds with a H^+ ion that is supplied by the dissolved CO_2 in the ADL, forming HCO_3^-, which is usually the main generation source of alkalinity in an ADr, as shown in **Section 2.4.1.2**.

As can be seen in **Figure 6-6**, a higher concentration of FSA was measured and predicted for the higher SRT, as compared to the lower SRT. Comparing the measured results against the predicted values from scenario 1 and 2, for the 15-day SRT, scenario 2 predicted more accurately than scenario 1, while the reverse occurred for the 32-day SRT, whereby scenario 2 predicted a much higher FSA concentration as compared to the measured and scenario 1 results. The reason for this is due to the nitrogen mass ratio (refer to f_N in **Table 6-1**) and COD removal.

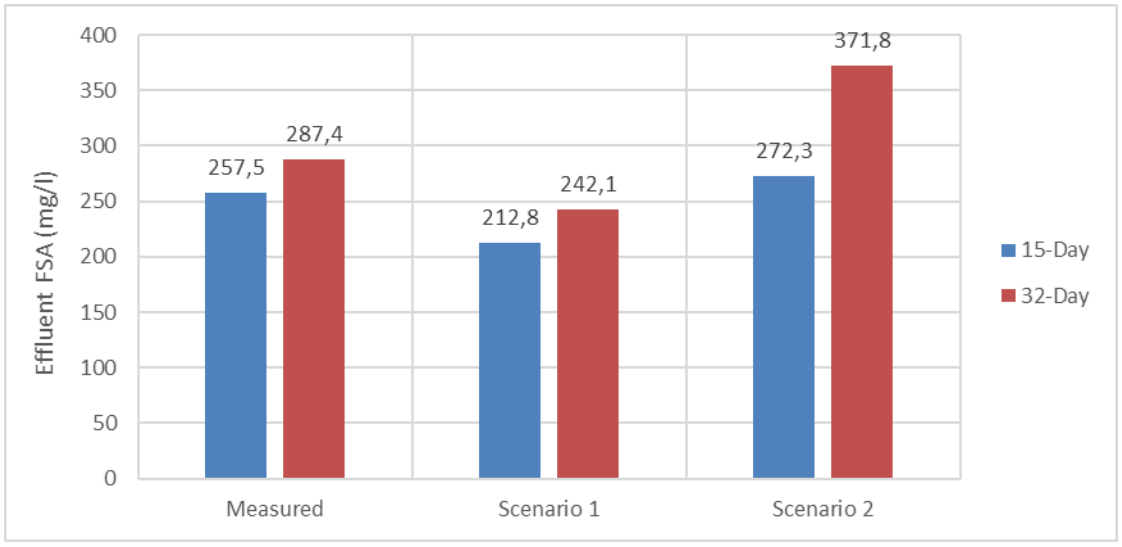

Figure 6-6: Effluent FSA comparison

The N released for scenario 1 is underpredicted despite the overpredicted COD removal, hence the N content of the BPO determined from Maake & Ikumi, (2021) seems to be less than that used to generate the FSA found in the measured SS AD effluent. However, for scenario 2, the COD removal prediction for the 15-day effluent FSA predictions are accurate. The reason for the discrepancies observed in the 32-day predicted effluent are that the BPO substrate f_N is 0.14 for scenario 2, as compared to 0.08 of scenario 1, hence the N content of the BPO determined from Ikumi, Harding & Ekama, (2013) seems to have been slightly overpredicted, as to what was used to generate the FSA in the measured SS AD effluent.

The model predicted that struvite remains undersaturated with respect to the aqueous phase and did not precipitate. If any precipitation had occurred, the FSA and OP would be utilised and thus be even lower in the effluent FSA and OP, increasing the deviation between the measured and predicted effluent FSA and OP (refer to **Section 6.2.3**) values. The deviation error between the measured effluent and predicted FSA results (with respect to the measured results) are shown in **Table 6-5** below. It must be pointed out that for scenario 2, 32-day, although it has such a high FSA effluent, it was not possible for FSA to precipitate (into struvite).

Table 6-5: Effluent FSA deviation error (%)

SRT (days)	Scenario 1	Scenario 2
15	-16.1%	7.3%
32	-15.8%	30.7%

6.2.3 Phosphorus Evaluation

To track the phosphorus throughout the ADrs, both the OP and TP predicted results are evaluated against the measured results. The SS AD model (described in **Chapter 5**) considered the impact of both the PP and organically bound P, where the stoichiometric pathways were used towards this evaluation.

6.2.3.1 TP Evaluation

The effluent TP values for both the measured and predicted data are presented in **Figure 6-7** and **Figure** 6-8, for both ADrs (for 15d and 32d SRT respectively). In these figures the P material mass balances are also shown to indicate a level of confidence in the data.

For both the 15d and 32d SRT data sets, scenario 1 and 2 overpredicted the effluent TP as compared to the measured results. The influent P characterisation involved determining the influent TP from the measured VSS as an input, where after the different constituents of P for the influent are determined (PP content, biomass P, etc., refer to **Section 2.2.5**). The influent results are shown in **Table** 6-6 below.

Table 6-6: Influent TP comparison

SRT (days)	Measured (mgP/l)	Scenario 1 (mgP/l)	Scenario 2 (mgP/l)
15	220.8	220.8	250.0
32	207.2	207.2	244.0

It can be seen from the table above, that for all the scenarios, the influent TP have been accurately determined compared to the measured results, except for scenario 2, where the influent TP determined for the 15- and 32-day SRTs were 250 mgP/l and 244 mgP/l respectively, as compared to the measured 220 mgP/l and 207 mgP/l, respectively. This was due to the fact that the WAS BPO substrate has a higher f_P value for scenario 2 (0.04) as compared to scenario 1 (0.02), as can be seen **Table 6-1**, as the UPO fraction and PP composition are the same.

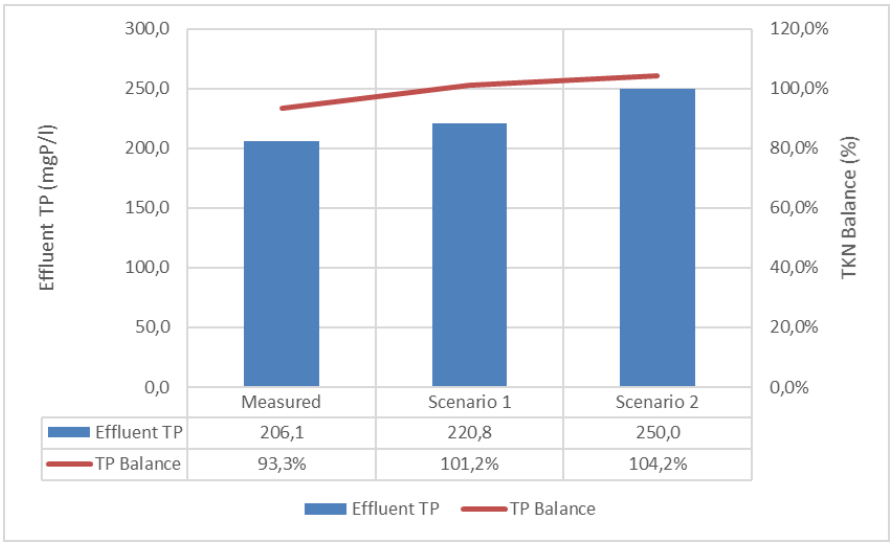

Figure 6-7: 15-day TP evaluation

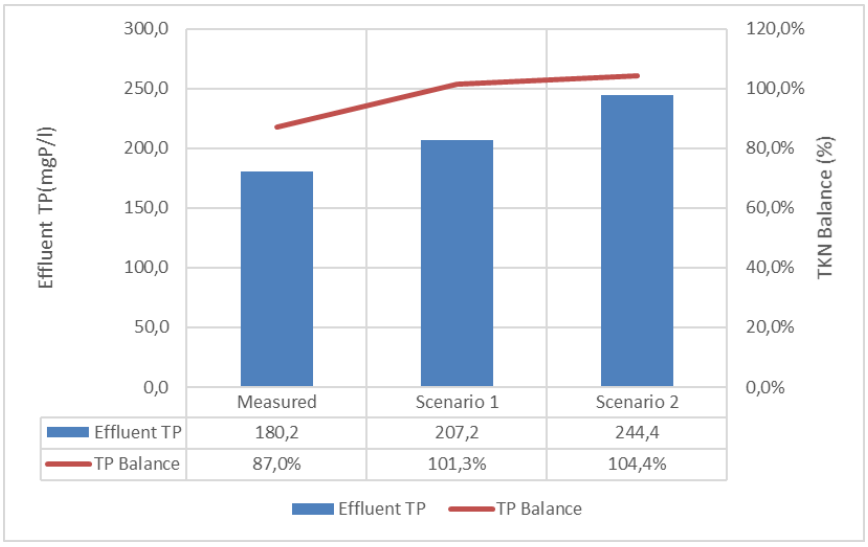

Figure 6-8: 32-day TP evaluation

6.2.3.2 OP Evaluation

As sludge is degraded in ADrs, the biomass P and PP is released into the ADL. The effluent OP is a measurement of the soluble P in the ADL, representing the biomass P and PP that were released due to sludge degradation. As described in **Section 6.2.3**, the effluent OP measured consists of the influent OP, organically bound P released as the substrate is degraded, and P released from the PP found in PAOs. As the ADrs have an operating pH ~ 7, P is released either in the form of HPO_4^{2-} or $H_2PO_4^-$, which is fractionated by an *f* value according to pH in the stoichiometry part of the AD model (Harding, 2009).

For this project, the mass fraction for P of the UPO was assumed to be 0.03, the same as (Harding, 2009). This assumption does not affect the soluble P released generated as mentioned above, however, the P content of the BPO component of the WAS released into the ADL is affected. As stated by Wentzel *et al*., (1990), the P content of the OHOs VSS components (f_P) is accepted to be 0.03 mgP/mgVSS, while for the P content for PAOs (f_{xBGP}) was taken to be 0.38 mgP/mgPAOVSS, of which 0.35 is PP and 0.03 biomass P (Wentzel *et al*., 1989).

From **Figure 6-9** it can be seen that scenario 1 and 2 underpredicted the effluent OP values compared to the measured results. No precipitation (struvite) was modelled, as this would have resulted in a higher error deviation of the predicted effluent OP compared to the measured OP (as mentioned in **Section 6.2.2.2**).

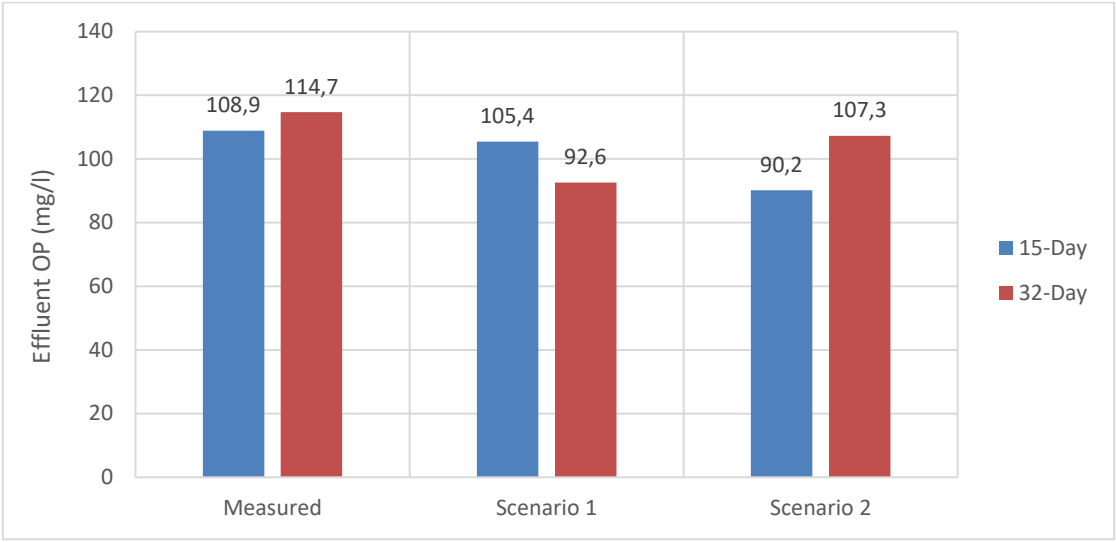

Figure 6-9: Effluent OP comparison

Comparing scenario 1 and 2, for the 15-day SRT, scenario 1 predicted higher effluent OP values as compared to scenario 2 while for the 32-day SRT the opposite was predicted. This would suggest that scenario 1 have either a higher PP content or a higher f_P WAS BPO substrate content for the 15-day SRT. **Table 6-1** show that the substrate f_P (0.01) value for scenario 1 is lower as compared to scenario 2 (f_P = 0.04), which might indicate that scenario 2 have a higher Organically-bound Phosphate (OrgP) and PP content, resulting in a higher predicted effluent OP for longer SRTs, as is the case for the 32-day SRT.

Table 6-7: OP deviation error (%)

SRT (days)	Scenario 1	Scenario 2
15	-3.2%	-17.2%
32	-19.3%	-6.5%

From **Table 6-7** above, the % deviation of the predicted effluent OP values with respect to the measured OP value are given. It can be seen that the predicted results are within the 80th percentile in accuracy to the measured data.

Table 6-8: Predicted OrgP & PP (mgP/l)

SRT (days)	15		32	
Constituents (mgP/l)	Scenario 1	Scenario 2	Scenario 1	Scenario 2
Released OrgP	23,1	76.9	27.4	106.1
PP	79,1	10.1	64.0	0.0
Influent OP	3,2	3.2	1.2	1.2
Total	105.4	90.2	92.6	107.3

In **Table 6-8** the influent OP, OrgP and PP as mgP/l are presented, which in total results in the predicted effluent OP. It can be seen that scenario 2 determined a higher released OrgP into the ADL for both SRTs as compared to scenario 1, while for scenario 1 a higher PP content was predicted. All the P in the PP for both scenarios were released, with the "released OrgP" values representing the P bound BPO released into the ADL as OP due to AD. Although the P in PP was all released, the PP content was too little to promote mineral precipitation. The possible reason for the low characterised PP is the long SRT of the parent AS system, resulting in low active PAO biomass and also the potential release of PP prior

to feeding the WAS into the ADrs. As mentioned in **Chapter 3**, the transport and storage of the WAS was carefully done, however, there is still some PP release that could have occurred during this period. The OP released without prediction of struvite precipitation results in a marginally underpredicted effluent OP. Hence, there thus seems to be a very low chance that struvite precipitated in the ADrs.

It can be assumed that there is a good correlation between the predicted effluent OP and measured OP results. Scenario 2 did not predict as accurately as scenario 1 for a short SRT, this can be attributed to the fact that, scenario 1's influent WAS is the same influent used for the ADrs obtained from a dynamic full-scale plant, as explained in **Chapter 5**, whereas scenario 2's influent WAS originated from literature data. (Ikumi, Harding & Ekama, 2013)

6.2.4 Dissolved Counter-Ion Metals and Precipitates

The effect of mineral precipitation have been discussed in **Section 2.4.3**, where ions (NH_4^+ and PO_4^{3-}) transform from the aqueous phase to the solid phase, affecting the pH and alkalinity of an ADr system. If the ionic product of the aqueous phase is equal to or higher than the solubility product of struvite ($MgNH_4PO_4.6H_2O$), then precipitation would have occurred. It is assumed that no precipitation of the above mentioned occurred in the feed and that no K replacement for NH_4^+ for precipitation of struvite occurred. As seen in **Section 4.2.7**, there is high confidence in the data as all three counter-ion metals have good balances.

In **Table 6-9**, the total and filtered influent (same values measured were used as model input) and effluent filtered counter-ion metals are presented in relation to the measured influent total (unfiltered) counter-ion metals. The inorganic solid influent was divided into the metal contribution to PP (which was characterised according to Harding, (2009)) and inorganic solids that are not contributing to PP (e.g., mineral precipitates in other forms). It can be seen in the table below, that there is no significant difference in the influent and effluent measured and modelled values. This includes the influent and effluent in the aqueous phase. This provides some confidence in model prediction that no precipitation with respect to the respective metal-ion occurred, because if precipitation had occurred, there would have been a mismatch in the values.

Table 6-9: Filtered Metal-ion comparison

		Magnesium (mg/l)		Potassium (mg/l)		Calcium (mg/l)	
	SRT (days)	15	32	15	32	15	32
Measured	Total Influent	27,6	17,3	790,9	747,3	125,1	124,3
	Filt Influent	5,4	4,3	15,7	14,0	43,7	38,8
	Filt Effluent	21,0	20,5	401,6	587,1	45,4	45,2
Scenario 1	Filt Influent	25,4	16,2	714,2	684,6	117,1	117,0
	Filt Effluent	27,6	17,3	790,9	747,3	125,1	124,3
Scenario 2	Filt Influent	27,3	17,3	781,1	747,3	124,1	124,3
	Filt Effluent	27,6	17,3	790,9	747,3	125,1	124,3

Referring to the measured filtered influent vs predicted filtered influent, the predicted results for all the counter-ion metals are higher than those measured. This might indicate precipitation did occur or a precipitant is present in the influent WAS; however, no tests were done to determine what precipitate/s were present in the influent.

The model predicts that all the K that is found in PP is released into the aqueous phase as noted to occur for AD SRTs that are above 10d (Harding, 2009) (refer to assumption above that all the PP is released). However, in order for the model predictions of filtered effluent K to match the measured data, not all the K that was deemed to be in the inorganic solid phase (i.e., the one that did not form part of PP), was released (or redissolved) into the aqueous phase. This suggests the presence of a precipitate form in the

influent that did not completely degrade or dissolve within the ADrs. For scenario 2, this suggests there was no PP present within the influent, which means either the PP was already released by the time of testing or there were no active PAOs with PP stored within them in the WAS feed.

From **Table 6-10** below, it can be seen that for both scenario 1 and 2, all the K was released into the ADL, resulting in no precipitation of K. However, the quantity of measured K that remained in the solid phase (not as PP, as all the PP was released) is quite high, suggesting another form of K precipitate present in the AD systems.

Table 6-10: K comparison

SRT (days)		15	32
Measured	Released K	385,9	573,1
	K in solid phase	389,3	160,2
	Total Influent	790,9	747,3
Scenario 1	Released K	76,7	62,8
	K in solid phase	0,0	0,0
Scenario 2	Released K	9,8	0,0
	K in solid phase	0,0	0,0

For struvite, the components NH_4^+ (FSA), PO_4^{3-} (OP) and the counter-ion metal Mg have to be considered, however, due to only Mg of the 3 measured metals not being present in both ACP and Calcite, it will thus be analysed for potential struvite precipitation. From the measured results, the difference between the total and the filtered effluent provides the amount of magnesium precipitate possibly formed within the ADrs, while the difference between the total and the predicted filtered effluent provides the amount involved in struvite precipitation. **Table 6-11** provides the amount of Mg available for struvite precipitation as described above.

Table 6-11: Potential M that precipitated

	SRT (days)	15	32
Measured	▲ Total - Filt	6,6	-3,2
Scenario 1		0,0	0,0
Scenario 2		0,0	0,0

From **Table 6-11** above, it can be seen that a negligent amount of Mg was available for precipitation for the measured 15-day ADr. However, as no precipitation was modelled for struvite, this suggests that Mg is in a precipitate form which is not modelled. The negative value of -3.20 for the 32-day can be explained by the fact that the measured effluent is higher than the measured influent, suggesting all the Mg was released. Both models (scenario 1 and 2), predicted that all the Mg was released, as can be seen with the filtered effluent values in **Table 6-9**, suggesting that no Mg precipitation to take place.

For Ca, the same procedure was followed as for Mg mentioned above, and the results are shown in **Table 6-12** below. Calcite was not modelled in the SS AD model; however, a check is still done as there is a mismatch between the measured data and the predicted data. In order for calcite to precipitate, the solubility product of the molar species Ca_T (Ca) and C_T (CO_3) must exceed the solubility product of calcite.

Table 6-12: Potential Ca that precipitated

	SRT (days)	15	32
Measured	▲ Total - Filt	79,7	79,1
Scenario 1		0,0	0,0
Scenario 2		0,0	0,0

From **Table 6-12** above, it can be seen that it was not possible for any calcite to precipitate for scenario 1 and 2, as the values are zero. However, the measured results suggest that a Ca precipitate was present

in the system, such as calcite ($CaCO_3$), which is commonly known to precipitate in ADrs. (Musvoto, Wentzel & Ekama, 2000)

6.2.5 pH and Alkalinity

The measured and predicted pH are compared and analysed in this section. In order to include precipitation, the model first assumes infinite solubility, where no precipitation occurs (2-phase model; gas and aqueous), where after, the solid phase is included (3-phase mode; gas, aqueous and solids), and precipitation is modelled. The final effluent pH values will be compared to the measured pH in order to provide insight of the effect of precipitation on an ADr system.

Table 6-13: Effluent pH comparison

Final Effluent pH		
SRT	15	32
Measured	6.7	6.7
Scenario 1	6.7	6.7
Scenario 2	6.8	6.9

From **Table 6-12** above, it can be seen that for the 15-day SRT, the model accurately predicted the pH while for the 32-day SRT, the model only over predicted the pH for scenario 2. The 32-day SRT however, predicted a higher pH in general than the shorter SRT. It can be seen however that the model predicted the pH fairly accurate as compared to the measured pH, for all scenarios.

Generally, at shorter SRTs (10-25 days), the phosphate species is a central factor on the ADr system pH (Harding, 2009). This is due to the disintegration of PP, releasing PO_4^{3-} and Mg into the aqueous phase of the ADr. The hydrolysis of BPO and release of CO_2 is much slower, meaning the release of organic N, which is the primary generation of alkalinity, increases as SRT increases. This alkalinity is generated by the uptake of H^+ from H_2CO_3 (dissolved CO_2) into the form HCO_3^-, resulting in the inorganic carbon system dominating the phosphate system, reducing the effect of struvite precipitation on the ADr system pH.

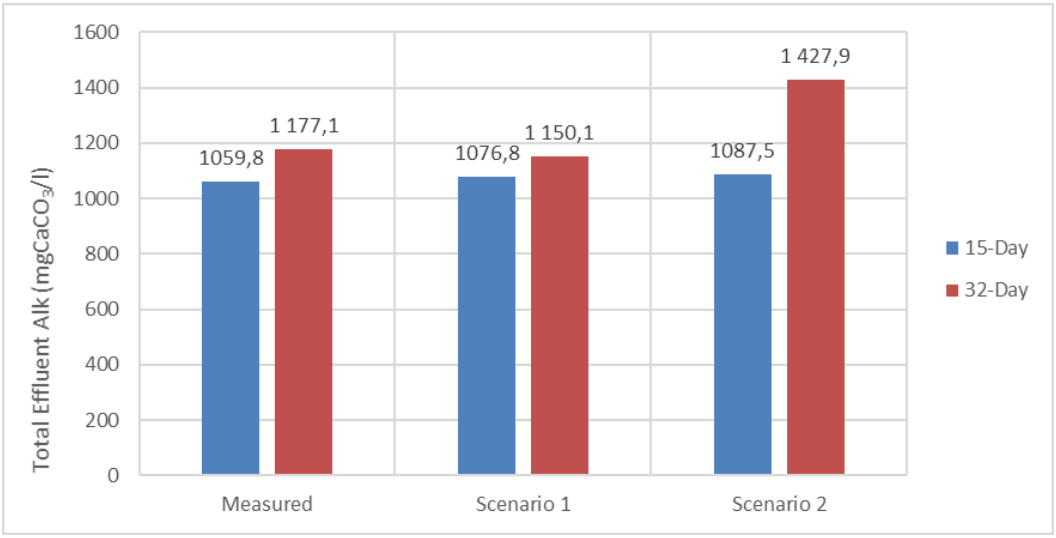

Figure 6-10: Total effluent alkalinity as mgCaCO₃/l comparison

In **Figure 6-10**, the measured 15-day of 1059.8 mg$CaCO_3$/l and 32-day of 1177.1 mg$CaCO_3$/l compared quite well with those predicted for both scenario 1 & 2. As can be seen above, the total alkalinity as $CaCO_3$ mg/l for the 32-day SRT was higher as compared to the 15-day SRT. For scenario 2, the 32-day effluent alkalinity is slightly higher than the data from the measured and scenario 1, which correlates

well with the higher pH (6.9) for scenario 2. The main generation of alkalinity, as briefly described above, results from organically bound N released in the non-ionic NH_3 form. NH_3 is a non-reference species of the NH_4^+ Total Alkalinity weak acid/base system, meaning it increases the N species alkalinity in the system. This NH_3 picks up a H^+ ion supplied by the dissolved CO_2 (H_2CO_3) in the ADr liquor and forms HCO_3^-. This process is shown below:

$$NH_3 + H_2CO_3 \rightarrow NH_4^+ + HCO_3^- \quad (6.\ 1)$$

With an increased SRT, more ammonia is released into the ADr liquor, increasing the molar product (ionic product) of the FSA, OP and Mg species in the system. As can be seen in **Section 6.2.2.2** and **Section 6.2.3.2**, FSA and OP are normally available, it is the availability of Mg that limits struvite precipitation potential.

6.3 Closure

This chapter represented the results predicted in the extended SS AD model (refer to **Annexure 8.3**), then compared it to the results obtained from the experimental setup (refer to **Annexure 8.1**), where after the data was evaluated and discussed. In **Section 6.1**, the influent characteristics used as input variables for the AD model are presented. The UPO are specific to the parent system from which the sludge feed and can vary depending on operational parameters or parent system influent characteristics. The elemental composition for the UPO and UPO fraction ($f_{S',up}$ = 0.51) determined by Maake & Ikumi, (2021) are applied for both Scenario 1 and Scenario 2, with only the WAS BPO substrate elemental composition and the kinetic rates (refer to **Section 5.1.3**) being system specific.

In **Section 6.2**, the predicted results were compared with the results obtained from the measurements taken from the experimental ADrs. The COD removal and the COD released as CH_4 gas were compared, with the COD removal found to be closely the same, however, the COD released as CH_4 gas did match well with the predicted results. More confidence were thus placed in the COD measurements rather than the CH_4 data. The FSA and OP data compared well with the measured data, with both FSA and OP results suggesting that no struvite precipitation occurred. In order for struvite to precipitate, a high PP content is required, so as to over-saturate the ADL with counter-ion metals, OP and FSA., however, the PP content was too little to promote struvite precipitation. A possible reason for the low PP content is the long SRT of the parent system from where the WAS was sourced, resulting in low active PAO biomass. Comparing the measured dissolved counter-ion metals with the predicted results in **Section 6.2.4**, no precipitation occurred within the ADrs, providing confidence in the SS AD model prediction for precipitation. The measured effluent pH and alkalinity also compared well with the predicted data, providing confidence in the overall SS AD model.

Chapter 7 Conclusions & Recommendations

7.1 Conclusions

In this study, a three-phase (aqueous-gas-solid) SS AD model is used to evaluate the performance of AD systems fed with WAS from full-scale BNR AS systems that are operated at long SRT.

To accomplish this study, an experimental investigation that involved feeding laboratory scale SS AD systems with WAS from the BNR AS system of Zandvliet WWTP, in Cape Town, South Africa. The data obtained from the operation and testing was evaluated using material mass balances as a check for consistency in measured variables that can be tracked within the AD system. The quality of the data generated and collected during the experimental stage was found to be consistent for the N, P, and K balances, with the COD, Mg and Ca balances found to be acceptable.

Two methods were looked at in determining the influent characteristics of the WAS that was fed to the AD systems: (1) the characterisation procedure developed by Harding, (2009), which requires the application of the SS AS model of Wentzel *et al.*, (1990), and (2) the novel method that involved the utilisation of results from the operation and testing of ABMP reactors at long SRT (Maake & Ikumi, 2021) and the application of the SS AD model in a PE procedure. It was determined that in order to identify the composition of the biomass, the bio-process stoichiometry for AD could be used Ekama, (2009).

Once the PO, BPO and UPO VSS concentrations of the WAS were known, they were transformed into their elemental compositions in terms of C, N, H, O and P. The following was noted during the WAS characterisation process:

1. The UPO fraction of the WAS determined by Maake & Ikumi, (2021) is 0.51. Comparing this to the $f_{S'up}$ determined by Harding, (2009) of 0.535 (SRT of 10 days), it matches quite well. However, as the parent system for Maake & Ikumi, (2021) had a longer SRT (> 25 days), a lower population of PAOs were present, resulting in less PP (which contains counter-ion metals) within the WAS.
2. The f_{cv} for the UPO was also 1.48 mgCOD/mgVSS, same as the PO above. The f_N was determined to be 0.10 mgN/mgVSS, compared to Harding, (2009) of a range of 0.047 – 0.051 mgN/mgVSS. However, the f_{cv} for Harding, (2009) was set at 1.43 mgCOD/mgVSS, resulting in the lower f_N values. For this study, f_P was accepted at 0.03 mgP/mgVSS (Wentzel *et al.*, 1990), as a very low PP content was determined in the PAOs of the WAS.
3. The f_{cv} for the WAS BPO substrate (determined by Maake & Ikumi, (2021)) was determined to be 1.48 mgCOD/mgVSS, with f_N and f_P mass fractions at 0.08 mgN/mgVSS and 0.01 mgP/mgVSS, respectively. In order to validate the novel method, the WAS BPO substrate elemental composition was compared to that of Ikumi, Harding & Ekama, (2013), with f_{cv}, f_N, and f_P determined as 1.43, 0.14, and 0.04, respectively. Harding, (2009) obtained f_{cv}, f_N and f_P values of 1.44 -1.52 mgCOD/mgVSS, 0.096 – 0.146 mgN/mgVSS and 0.029 – 0.034 mgP/mgVSS, averaging 1.48, 0.12 and 0.03, respectively. This matches closely with what was determined in this study.

Considering the complexity in using the novel method in determining the mass fractions for this study, the results were fairly similar to those found in other studies on ND-BEPR WAS. This study determined with confidence that the novel approach to PO, UPO and BPO components conform well to that of other studies.

The SS mass balanced AD model developed by Sötemann *et al*., (2005), extended by Harding, (2009) and Ikumi, Harding & Ekama, (2013) have been evaluated in this study. As mentioned above, the elemental composition and saturation kinetics were determined by Maake & Ikumi, (2021) (scenario 1) and Ikumi, Harding & Ekama, (2013) (scenario 2), and used as input variables in the SS AD model. It was determined by Maake & Ikumi, (2021), that all the PP was released within 7-days from the PAOs (confirming Harding, (2009) findings), thus it was assumed in the SS AD model that all the PP was released.

1. Comparing the measured and the predicted COD results, the effluent COD matched quite well to model predicted data. However, the COD gas produced was a lot lower than those predicted in the model, resulting in more confidence being placed in the COD measurements. The difference is due to how the gas was sourced from the AD systems, resulting in lower CH_4 gas produced as COD. The effect in the different kinetics can be seen clearly with the difference in predicted CH_4 gas produced, with change in SRT from 15 to 32 days, as the saturation kinetics is essentially the rate of hydrolysis of the BPO during AD.
2. Both TKN and TP predicted acceptable effluent results and mass balances compared to the measured data from the experiment. Referring to both TKN and TP, the characterisation method that utilised data from Maake & Ikumi, (2021) (scenario 1), predicted the most accurate results with respect to the measured data, as compared to the one that utilised literature data from Ikumi, Harding & Ekama, (2013) (scenario 2). This is because the literature data from Ikumi, Harding & Ekama, (2013) have higher WAS BPO values for f_N (0.14) and f_P (0.04) than those determined by Maake & Ikumi, (2021) (f_N (0.08) and f_P (0.01)), resulting in an overprediction of TKN and TP. This provides confidence in the novel approach in determining the WAS characteristics.
3. The FSA for scenario 1 underpredicted for both 15- and 32-day SRT, while scenario 2 slightly overpredicted the 15-day SRT, with the 32-day SRT grossly over predicting. The reason for the underprediction of scenario 1 and over prediction of scenario 2, is due to the determined N content of the BPO, where for scenario 1 the N content (f_N = 0.08) is less than the N used to generate the FSA in the measured effluent, while for scenario 2, the N content (f_N = 0.14) is higher.
4. The OP for scenario 1 and 2 was underpredicted, as compared to the measured results. For scenario 1, the 15-day SRT predicted higher than the 32-day SRT, with the reason being a higher PP content was determined for the shorter SRT as the influent TP for the 15-day SRT is higher. For scenario 2, the 32-day SRT predicted a higher effluent OP than the 15-day SRT. The reason being that scenario 2 have a higher P content for the WAS BPO (f_P = 0.04), as compared to scenario 1 (f_P = 0.01), resulting in the OrgP to have a higher influence in the effluent results. With the parent system for scenario 2 having such a short SRT as compared to the parent system of scenario 1, the PAO population and thus the WAS BPO f_P fraction was higher, resulting in a higher OrgP effluent prediction.
5. The data indicates that all the effluent K and Mg had dissolved within the ADL, and no struvite precipitation occurred during the AD system operation. However, the measured data for K indicate that another precipitate is present within the ADL, which is not included in the SS AD model.
6. As PP release and precipitation occurs in ADrs, it affects the respective alkalinity species, total alkalinity, and pH of the AD system. However, it was noted that the measured and predicted effluent pH values were quite accurate. The same can be said for the total measured and predicted alkalinities. With the measured and predicted pH and alkalinity value, it can be stated with confidence that no precipitation of struvite occurred.

Using the kinetics and WAS characteristics of Maake & Ikumi, (2021) as input values in the SS AD, the COD, N, and P were tracked accurately, with a more accurate final effluent pH and system alkalinity predicted as compared to that predicted by Ikumi, Harding & Ekama, (2013). As the parent system had such a long SRT, a low content of PP was present in the ADrs, resulting in no struvite precipitation taking place. This is of note, as struvite precipitation reduced the total alkalinity in a ADr, lowering the system pH.

7.2 Recommendations

The extended SS AD model have been validated and calibrated in this study. Although the model has been extended to include precipitation during AD, the stoichiometric part of the AD model still requires some further research to eliminate the effect of P and mineral precipitants in the ADrs.

1. As it is not yet certain whether the characteristics of the BPO WAS would remain consistent regardless from where it is sourced, further research would be suggested. Comparing the kinetic rates determined from a full-scale WRRF, lab-scale UCT AS parent system and enhanced-PAO lab-scale UCT AS parent system with a synthetic feed. This would provide more clarity regarding different WAS parent systems and their respective kinetic rates, as well as provide more insight between OHOs and PAOs.

2. It is recommended to feed WAS from a full-scale plant with a higher content of P and a higher population PAOs to lab-scale ADrs. As well as to run a lab-scale UCT system with a 100% synthetic feed, and feeding the WAS produced from the system to lab-scale ADrs. In doing this, a better understanding of the role P and PAOs have on WW treatment will be achieved, resulting in a more accurate SS model. Through this, achieving a higher efficiency in recycling nutrients and H_2O from WRRF is possible.

3. As the SS AD model only predicts whether precipitation occur (struvite, calcite, or ACP) and the effects of precipitation on the AD liquor, pH, and alkalinity, it does not however consider any precipitants in the influent or the type thereof. It is recommended to extend the model regarding precipitation by considering precipitants in the influent and the effects those precipitants have on the system as constituents dissolve back into the AD liquor.

4. It is recommended to source WAS from a lab-scale AS system with a UCT configuration (1 AS system with a short SRT (10 days), 1 with a long SRT (>25 days)), and feed it to lab-scale ADrs, operating at different SRT's. The WAS characteristics will be determined by both methods (Maake & Ikumi, (2021)and Harding, (2009)), and used as input variables in the SS AD models. This will provide insight into AS systems operated at long SRT's, and the effect it has on ADrs, while also accurately comparing the two different methods in determining kinetics and WAS characteristics, as a more controlled environment is provided.

References

American Public Health Association. 2005. Standard methods for the examination of water and wastewater. *Washington, DC, USA: American Public Health Association (APHA).*

Batstone, D.J., Keller, J., Angelidaki, I., Kalyuzhnyi, S.V., Pavalostathis, S.G., Rozzi, A., Sanders, W.T.M., Siegrist, H. *et al*. 2002. The IWA Anaerobic Digestion Model No 1 (ADM1). *Water Science and Technology*. 45(10):65-73. Available: https://www.narcis.nl/publication/RecordID/oai:library.wur.nl:wurpubs%2F319148.

Botha, R.F. 2015. *Characterization of organics for anaerobic digestion by modelling augmented biochemical methane potential test results.* University of Cape Town.

Brouckaert, C.J., Ikumi, D.S. & Ekama, G.A. 2010. A 3-phase anaerobic digestion model. *Proc 12th IWA Anaerobic Digestion Conference.* :1-4.

Butler, J.N. 1964. Ionic Equilibrium: A Mathematical Approach. *Addison-Weatley, Massachusetts, USA Search PubMed.*

Comeau, Y., Hall, K.J., Hancock, R.E.W. & Oldham, W.K. 1986. Biochemical model for enhanced biological phosphorus removal. *Water Research (Oxford).* 20(12):1511-1521. Available: http://dx.doi.org/10.1016/0043-1354(86)90115-6.

Comeau, Y., Rabionwitz, B., Hall, K.J. & Oldham, W.K. 1987. Phosphate Release and Uptake in Enhanced Biological Phosphorus Removal from Wastewater. *Journal - Water Pollution Control Federation.* 59(7):707-715. Available: https://www.jstor.org/stable/25043326.

Corominas, L.L., Rieger, L., Takács, I., Ekama, G., Hauduc, H., Vanrolleghem, P.A., Oehmen, A., Gernaey, K.V. *et al*. 2010. New framework for standardized notation in wastewater treatment modelling. *Water Science and Technology*. 61(4):841-857. Available: https://www.ncbi.nlm.nih.gov/pubmed/20182062.

Department of Water and Sanitation. 1998. *National Water Act Act No 36 of 1998.* Republic of South Africa: .

Ekama, G.A. 2017. Optimizing water and resource recovery facilities (WRRF) for energy generation without compromising effluent quality. *IWA Publishing.*

Ekama, G.A. 2009. Using bioprocess stoichiometry to build a plant-wide mass balance based steady-state WWTP model. *Water Research (Oxford).* 43(8):2101-2120. Available: http://dx.doi.org/10.1016/j.watres.2009.01.036.

Ekama, G.A. & Wentzel, M.C. 2004. A predictive model for the reactor inorganic suspended solids concentration in activated sludge systems. *Water Research (Oxford).* 38(19):4093-4106. Available: http://dx.doi.org/10.1016/j.watres.2004.08.005.

Elser, J.J. 2012. Phosphorus: a limiting nutrient for humanity? *Current Opinion in Biotechnology*. 23(6):833-838. Available: https://www.clinicalkey.es/playcontent/1-s2.0-S0958166912000481.

Filipe, C.D.M., Daigger, G.T. & Grady Jr, C. P. L. 2001. A metabolic model for acetate uptake under anaerobic conditions by glycogen accumulating organisms: Stoichiometry, kinetics, and the effect of pH. *Biotechnology and Bioengineering.* 76(1):17-31. Available: https://api.istex.fr/ark:/67375/WNG-VPZ7VZM7-S/fulltext.pdf.

Gaszynski, C. 2020. *Identification of Wastewater Primary Sludge Composition using Augmented Batch Tests and Mathematical Models.* University of Cape Town.

Harding, T.H. 2009. *A steady state stoichiometric model describing the anaerobic digestion of biological excess phosphorus removal waste activated sludge.* University of Cape Town.

Harding, T.H., Ikumi, D.S. & Ekama, G.A. 2011. Incorporating phosphorus into plant wide wastewater treatment plant modelling–anaerobic digestion. *Proc. 8th IWA Symposium on Systems Analysis and Integrated Assessment (Watermatex2011).* 20.

Henze, M., van Loosdrecht, M. C. M., Ekama, G.A. & Brdjanovic, D. 2008. *Biological wastewater treatment.* IWA publishing. Available: .

Hesselmann, R.P.X., Werlen, C., Hahn, D., van der Meer, J. R. & Zehnder, A.J.B. 1999. Enrichment, phylogenetic analysis and detection of a bacterium that performs enhanced biological phosphate removal in activated sludge. *Systematic and Applied Microbiology.* 22(3):454-465.

Ikumi, D.S. 2011. *The development of a three phase plant-wide mathematical model for sewage treatment.* University of Cape Town.

Ikumi, D.S. & Ekama, G.A. 2019. Plantwide modelling - anaerobic digestion of waste sludge from parent nutrient (N and P) removal systems. *Water S.A.* 45(3):305-316. Available: https://search.informit.org/documentSummary;dn=550628638467655;res=IELENG.

Ikumi, D.S., Harding, T.H., Brouckaert, C.J. & Ekama, G.A. 2014. Plant Wide Integrated Biological, Chemical and Physical Processes Modelling of Wastewater Treatment Plants in Three Phases (Aqueous eGas eSolid). In *Research Report W138, Department of Civil Engineering, University of Cape Town, Rondebosch.*

Ikumi, D.S., Harding, T.H., Brouckaert, C.J. & Ekama, G.A. 2016. Plantwide modelling - anaerobic digestion of waste sludge from parent nutrient (N & P) removal activated sludge systems. (Unpublished).

Ikumi, D.S., Harding, T.H. & Ekama, G.A. 2013. Plant wide wastewater treatment modelling-biodegradability of organics. *Proceeding of the 13th World Congress on Anaerobic Digestion. Santiago De Compostela, Spain.*

Ikumi, D.S., Harding, T.H., Vogts, M., Lakay, M.T., Mafungwa, H.Z., Brouckaert, C.J. & Ekama, G.A. 2015. *Mass balances modelling over wastewater treatment plants III.* (Report No. 18/1/14). Republic of South Africa: WRC Report.

Izzett, H. 1992. *The effect of thermophilic heat treatment on the anaerobic digestibility of primary sludge.* University of Cape Town.

Loewenthal, R.E., Kornmüller, U.R.C. & Van Heerden, E.P. 1994. Modelling struvite precipitation in anaerobic treatment systems. *Water Science and Technology.* 30(12):107.

Loewenthal, R.E., Marais, G.v.R. & Ekama, G.A. 1989. Mixed weak acid/base systems: part 1-mixture characterization. *Water Sa.* 15(1):3.

Loewenthal, R.E., Wentzel, M.C., Ekama, G.A. & Marais, G.v.R. 1991. Mixed weak acid/base systems Part II: Dosing estimation, aqueous phase. *SA Waterbulletin.*

Maake, A. & Ikumi, D.S. 2021. *Calibrating the Anaerobic breakdown of Waste Sludge Containing Enhanced Cultures of Polyphosphate Accumulating Organisms.* University of Cape Town.

Marais, G.V.R. & Ekama, G.A. 1976. The activated sludge process part I-steady state behaviour. *Water Sa.* 2(4):163-200.

McCarty, P.L. & Mosey, F.E. 1991. Modelling of anaerobic digestion processes (a discussion of concepts). *Water Science and Technology.* 24(8):17-33.

Mino, T., Arun, V., Tsuzuki, Y. & Matsuo, T. 1987. Effect of phosphorus accumulation on acetate metabolism in the biological phosphorus removal process. In *Biological phosphate removal from wastewaters.* Elsevier. 27-38.

Moosbrugger, R.E., Wentzel, M.C., Ekama, G.A. & Marais, G.v.R. 1993. A 5 pH point titration method for determining the carbonate and SCFA weak acid/bases in anaerobic systems. *Water Science and Technology.* 28(2):237-245.

Musvoto, E.V., Wentzel, M.C. & Ekama, G.A. 2000. Integrated chemical–physical processes modelling—II. simulating aeration treatment of anaerobic digester supernatants. *Water Research.* 34(6):1868-1880.

Oehmen, A. 2004. Enhanced Biological Phosphorus Removal: Optimization through Process Analysis and Operational Improvements, The Competition Between Polyphosphate Accumulating Organisms and Glycogen Accumulating Organisms in the Enhanced Biological Phosphorous Removal Process, School of Engineering, The University of Queensland. *St.Lucia.*

Pereira, H., Lemos, P.C., Reis, M.A.M., Crespo, J. P. S. G., Carrondo, M.J.T. & Santos, H. 1996. Model for carbon metabolism in biological phosphorus removal processes based on in vivo13C-NMR labelling experiments. *Water Research.* 30(9):2128-2138.

Sawyer, C.N., McCarty, P.L. & Parkin, G.F. 1994. Chemistry for Environmental Engineers.

Siebritz, I.P., Ekama, G.A. & Marais, G.v.R. 1983. A parametric model for biological excess phosphorus removal. *Water Science and Technology.* 15(3-4):127-152.

Smolders, G.J.F., Van der Meij, J., Van Loosdrecht, M. C. M. & Heijnen, J.J. 1994. Model of the anaerobic metabolism of the biological phosphorus removal process: stoichiometry and pH influence. *Biotechnology and Bioengineering.* 43(6):461-470.

Smolders, G.J.F., Van Loosdrecht, M. C. M. & Heijnen, J.J. 1995. A metabolic model for the biological phosphorus removal process. *Water Science and Technology.* 31(2):79-93.

Sötemann, S.W., Ristow, N.E., Wentzel, M.C. & Ekama, G.A. 2005. A steady state model for anaerobic digestion of sewage sludges. *Water SA.* 31(4):511-528.

Sötemann, S.W., Van Rensburg, P., Ristow, N.E., Wentzel, M.C., Loewenthal, R.E. & Ekama, G.A. 2005. Integrated chemical/physical and biological processes modeling Part 2-Anaerobic digestion of sewage sludges. *Water Sa.* 31(4):545-568.

Van Rensburg, P. 2001. *Integrated biological, chemical, and physical processes kinetic model for the anaerobic digestion of primary sewage sludge.* University of Cape Town.

Wentzel, M.C., Dold, P.L., Ekama, G.A. & Marais, G.v.R. 1989. Enhanced polyphosphate organism cultures in activated sludge systems. Part III: kinetic model. *Water SA.* 15(2):89-102.

Wentzel, M.C., Ekama, G.A., Dold, P.L. & Marais, G.v.R. 1990. Biological excess phosphorus removal-Steady state process design. *Water Sa.* 16(1):29-48.

Wentzel, M.C., Ekama, G.A., Loewenthal, R.E., Dold, P.L. & Marais, G.v.R. 1989. Enhanced polyphosphate organism cultures in activated sludge systems. Part II: Experimental behaviour. *Water S. A.* 15(2):71-88.

Wentzel, M.C., Lotter, L.H., Loewenthal, R.E. & Marais, G.v.R. 1986. Metabolic behavior of Acinetobacter spp. in enhanced biological phosphorus removal-a biochemical model. *Water Sa.* 12(4):209-224.

Chapter 8 Appendix

Appendix 8.1: Measured ADr data.

Appendix 8.2: Measured ABMP data.

Appendix 8.3: Modelled AD Results

8.1 Appendix 8.1

Raw data measured from the lab-scale anaerobic digesters as mentioned in **Chapter 3**.

*Nonsensical (Excluded – data points outside of 80th percentile (refer to **Chapter 4**)

*No measurement

Experimental Data														
			Influent		Effluent						Influent		Effluent	
Test	Unit	Data Point	15-ADr	32-ADr	15-ADr	32-ADr		Test	Unit	Data Point	15-ADr	32-ADr	15-ADr	32-ADr
Total COD	mg/l	1	10840	10302	7028	6500		Filtered COD	mg/l	1	95	75	185	196
		2	11325	9840	6807	6020				2	80	80	169	170
		3	10964	7600	7289	5920				3	82	76	165	204
		4	9719	10080	7269	5920				4	77	92	186	176
		5	9197	10200	7269	5360				5	97	92	168	166
		6	8916	9800	7060	5580				6	68	66	163	198
		7	9680	10840	7000	5520				7	69	80	194	210
		8	10440	10200	7020	5500				8	65	110	185	144
		9	9240	9440	7560	5940				9	68	76	193	188
		10	9480	9760	7520	5960				10	99	84	167	200
		11	9720	9000	7640	6000				11	94	188	179	226
Average (mean)			9549	9847	7224	5838		Average (mean)			74	93	178	190
Standard Deviation (s)			462,1	504,6	267,0	323,5		Standard Deviation (s)			6,4	8,3	11,6	15,7
Mean/s (%)			5%	5%	4%	6%		Mean/s (%)			9%	9%	7%	8%
TKN	mg/l	1	702,5	428,4	673,1	565,5		FSA	mg/l	1	4,0	49,0	256,1	306,4
		2	645,8	372,4	644,0	644,0				2	3,1	31,2	240,7	284,2
		3	689,1	649,6	656,1	884,8				3	7,1	15,5	246,6	273,0
		4	705,6	952,0	703,8	-				4	5,8	76,3	271,2	275,8
		5	751,4	-	718,6	627,2				5	6,2	4,2	273,1	254,8
		6	704,2	660,8	672,0	680,4				6	6,7	3,6	268,0	340,2
		7	695,1	901,6	680,5	669,2				7	4,5	3,4	263,1	299,6
		8	667,1	800,8	664,0	705,6				8	8,4	5,0	258,1	281,4
		9	699,2	778,4	668,3	669,2				9	6,1	2,7	251,1	291,2
		10	701,9	739,2	672,6	604,8				10	9,2	2,5	252,8	289,8
		11	725,1	683,2	676,9	669,2				11	6,6	2,6	251,7	264,6
Average (mean)			698,8	718,7	675,5	648,3		Average (mean)			6,2	3,5	257,5	287,4
Standard Deviation (s)			27,3	63,4	20,6	43,1		Standard Deviation (s)			1,3	0,9	10,4	23,0
Mean/s (%)			4%	9%	3%	7%		Mean/s (%)			21%	27%	4%	8%
TP	mg/l	1	215,6	212,0	201,0	183,6		OP	mg/l	1	4,8	0,6	107,5	114,6
		2	204,9	214,2	206,5	178,2				2	1,6	2,0	120,3	111,3
		3	228,4	180,0	190,7	190,7				3	4,3	0,9	105,7	113,1
		4	234,2	377,2	195,7	174,4				4	1,9	7,1	107,1	113,2
		5	-	209,5	309,3	173,8				5	3,5	1,0	108,6	112,2
		6	46,8	210,4	198,0	178,4				6	2,8	1,0	109,6	124,6
		7	221,6	214,0	211,9	34,3				7	4,5	4,5	104,7	108,7
		8	209,3	223,3	197,6	2,0				8	2,8	2,8	104,6	114,7
		9	220,5	212,4	205,7	172,1				9	2,5	1,0	108,5	114,6
		10	231,6	204,7	223,1	7,6				10	3,4	0,9	106,5	115,7
		11	-	191,9	215,1	190,1				11	2,7	0,9	115,0	119,5
Average (mean)			220,8	207,2	206,1	180,2		Average (mean)			3,2	1,2	108,9	114,7
Standard Deviation (s)			10,5	12,5	9,2	7,2		Standard Deviation (s)			1,1	0,7	4,7	4,2
Mean/s (%)			5%	6%	4%	4%		Mean/s (%)			33%	57%	4%	4%
Total Mg	mg/l	1	23,6	-	24,2	-		Filtered Mg	mg/l	1	2,6	4,6	20,5	22,7
		2	28,7	-	26,5	-				2	4,5	0,9	21,7	22,2
		3	27,5	-	25,8	26,7				3	3,8	2,4	21,0	13,4
		4	30,0	15,9	23,0	22,0				4	6,4	3,0	20,7	17,6
		5	27,3	14,4	24,7	16,5				5	6,1	4,3	21,5	16,4
		6	29,8	26,2	26,2	22,6				6	5,1	2,6	22,1	21,6
		7	25,4	17,6	25,1	24,6				7	-	9,0	-	22,2
		8	26,7	17,4	27,6	13,3				8	4,9	6,6	21,4	18,2
		9	27,5	26,5	25,9	25,8				9	5,7	4,6	20,8	22,7
		10	29,0	18,7	24,6	25,6				10	6,4	4,5	20,2	17,2
		11	28,0	19,8	25,1	22,5				11	5,5	4,1	20,2	20,2
Average (mean)			27,6	17,3	25,3	24,3		Average (mean)			5,4	4,3	21,0	20,5
Standard Deviation (s)			1,9	1,9	1,3	1,9		Standard Deviation (s)			0,9	1,2	0,7	2,3
Mean/s (%)			7%	11%	5%	8%		Mean/s (%)			16%	28%	3%	11%
Total Ca	mg/l	1	111,2	-	118,1	-		Filtered Ca	mg/l	1	40,2	34,0	46,1	50,8
		2	128,6	-	117,5	-				2	42,2	-	44,2	39,1
		3	131,5	-	126,2	96,0				3	44,7	31,3	45,8	41,6
		4	118,0	128,5	131,57,	123,5				4	46,4	44,6	43,7	44,4
		5	132,6	128,8	124,0	144,1				5	43,8	40,4	44,3	50,1
		6	121,0	111,4	129,8	94,3				6	43,7	50,9	45,0	45,3
		7	125,8	157,3	117,6	98,1				7	-	45,0	-	44,5
		8	123,1	132,8	128,3	120,5				8	44,0	43,0	46,2	46,9
		9	131,4	96,1	126,9	96,0				9	44,2	34,9	46,4	47,1
		10	135,3	120,1	116,1	41,5				10	43,6	33,6	45,7	42,1
		11	118,1	73,3	136,1	96,1				11	43,8	29,9	47,0	44,9
Average (mean)			125,1	124,3	124,0	103,5		Average (mean)			43,7	38,3	45,4	45,2
Standard Deviation (s)			7,5	8,6	6,6	12,7		Standard Deviation (s)			1,6	5,5	1,1	3,5
Mean/s (%)			6%	7%	5%	12%		Mean/s (%)			4%	14%	2%	8%
Total K	mg/l	1	768,2	-	798,2	-		Filtered K	mg/l	1	14,0	12,0	359,8	310,0
		2	791,5	-	815,5	-				2	9,5	-	420,1	94,0
		3	805,7	-	823,4	620,0				3	17,2	12,0	384,3	54,0
		4	801,0	1840,0	791,4	1690,0				4	8,0	8,0	391,7	316,0
		5	804,7	660,0	810,9	836,0				5	15,4	1,0	411,8	312,6
		6	779,1	740,0	817,6	730,0				6	13,8	2,1	402,1	586,0
		7	795,8	700,0	804,7	870,0				7	-	15,0	-	597,5
		8	780,4	803,0	813,5	770,0				8	10,4	15,7	431,9	622,0
		9	773,2	780,0	834,1	814,0				9	15,6	15,0	398,7	586,8
		10	800,2	728,0	806,7	870,0				10	18,4	14,6	405,7	596,0
		11	799,8	820,0	785,0	790,0				11	19,9	14,0	409,6	534,0
Average (mean)			790,9	747,3	809,2	811,4		Average (mean)			15,7	14,0	401,6	587,1
Standard Deviation (s)			13,3	57,4	14,1	52,1		Standard Deviation (s)			1,8	1,5	20,0	29,1
Mean/s (%)			2%	8%	2%	6%		Mean/s (%)			11%	11%	5%	5%

			Influent		Effluent	
Test	Unit	Data Point	15-ADr	32-ADr	15-ADr	32-ADr
TSS	mg/l	1	8821	8144	6566	4988
		2	8763	8244	4694	4874
		3	8774	6202	5970	5318
		4	8802	9010	6390	4924
		5	8726	9222	6330	4830
		6	8659	8572	6252	5020
		7	8705	9580	6266	4580
		8	8746	8990	6288	4804
		9	8843	7690	6418	4790
		10	8829	8480	6204	5000
		11	8705	8142	6358	-
Average (mean)			8761	8607	6304	4913
Standard Deviation (s)			59,1	582,6	155,8	193,0
Mean/s (%)			1%	7%	2%	4%
ISS	mg/l	1	1964	1532	1486	1344
		2	1909	1448	1248	1166
		3	1956	1180	1424	1470
		4	2197	1406	1688	1128
		5	1881	1672	1446	990
		6	1840	1678	335	1140
		7	1800	1834	1424	848
		8	1862	1846	1778	1180
		9	2030	1396	1470	970
		10	1938	1614	1618	1214
		11	1970	1466	1524	-
Average (mean)			1941	1527	1511	1113
Standard Deviation (s)			107,7	115,4	150,9	94,9
Mean/s (%)			6%	8%	10%	9%
Total Alkalinity	mg/l as $CaCO_3$	1	105,2	67,5	1102,2	1261,8
		2	102,3	106,4	1067,6	1087,8
		3	98,6	108,6	1028,4	741,3
		4	105,7	-	1140,7	1179,2
		5	93,5	119,4	1055,1	1215,5
		6	103,1	85,4	989,1	1149,6
		7	100,7	123,7	1007,6	1176,9
		8	97,4	133,4	1073,4	1116,2
		9	102,9	73,1	1067,3	1155,9
		10	104,2	91,3	1091,0	1205,9
		11	102,7	73,4	1034,9	1222,7
Average (mean)			101,5	109,9	1059,8	1177,1
Standard Deviation (s)			3,7	12,6	43,6	52,1
Mean/s (%)			4%	12%	4%	4%
Phosphate	mg/l as $CaCO_3$	1	1,2	0,2	129,2	114,7
		2	0,4	1,5	115,4	135,8
		3	2,0	0,3	132,3	36,3
		4	0,8	-	124,9	127,7
		5	1,5	0,3	120,1	138,9
		6	1,0	0,3	140,3	155,2
		7	1,8	3,1	118,4	137,4
		8	1,3	2,5	136,5	139,6
		9	1,4	0,3	126,7	134,1
		10	0,9	0,4	125,0	148,7
		11	1,6	0,6	129,3	142,5
Average (mean)			1,3	1,0	127,1	137,5
Standard Deviation (s)			0,5	1,1	7,6	11,1
Mean/s (%)			37%	112%	6%	8%

			Influent		Effluent	
Test	Unit	Data Point	15-ADr	32-ADr	15-ADr	32-ADr
VSS	mg/l	1	6857	6612	5080	3644
		2	6854	6796	3446	3708
		3	6818	5022	4546	3848
		4	6605	7604	4702	3796
		5	6845	7550	4884	3840
		6	6819	6894	5917	3880
		7	6905	7746	4842	3732
		8	6884	7144	4510	3624
		9	6813	6294	4948	3820
		10	6891	6866	4586	3786
		11	6735	6676	4834	-
Average (mean)			6821	7018	4770	3768
Standard Deviation (s)			85,4	479,1	195,7	87,5
Mean/s (%)			1%	7%	4%	2%
pH		1	7,1	7,2	6,7	6,6
		2	7,1	7,1	6,8	6,7
		3	7,0	7,1	6,7	6,7
		4	7,1	7,0	6,7	6,7
		5	7,0	7,1	6,8	6,7
		6	7,0	7,1	6,8	6,7
		7	7,1	7,0	6,7	6,7
		8	7,0	7,2	6,7	6,7
		9	7,0	6,9	6,8	6,6
		10	7,1	7,0	6,7	6,6
		11	7,1	7,0	6,7	6,6
Average (mean)			7,0	7,0	6,7	6,7
Standard Deviation (s)			0,0	0,1	0,0	0,0
Mean/s (%)			0%	1%	0%	0%
Carbonate	mg/l as $CaCO_3$	1	101,3	96,5	1014,7	1119,8
		2	94,9	78,2	1193,0	890,9
		3	81,6	84,5	1181,4	720,6
		4	89,3	-	952,7	998,7
		5	92,0	111,2	1061,5	1048,8
		6	107,7	63,6	980,5	949,0
		7	104,8	129,3	995,6	991,1
		8	94,1	120,3	814,,97	969,0
		9	112,5	104,7	885,4	983,9
		10	103,4	97,1	1031,9	1008,2
		11	85,4	55,9	764,1	1053,7
Average (mean)			100,0	102,4	988,9	1001,3
Standard Deviation (s)			7,8	12,6	57,6	62,8
Mean/s (%)			8%	12%	6%	6%
VFAs	mg/l as $CaCO_3$	1	11,0	0,0	8,5	0,0
		2	2,0	26,2	0,0	7,4
		3	0,0	23,7	0,0	0,0
		4	4,2	-	11,0	13,2
		5	0,0	7,9	0,0	0,0
		6	8,7	21,5	0,0	0,0
		7	0,0	0,0	0,0	0,0
		8	0,0	10,4	0,0	0,0
		9	0,0	0,0	0,0	0,0
		10	9,6	0,0	3,4	0,0
		11	0,0	16,9	0,0	0,0
Average			3,2	10,7	2,1	1,9
Standard Deviation (s)			4,4	10,2	4,0	4,4
Mean/s (%)			137%	96%	190%	233%
VFAs	mg/l as Ac	1	7,9	0,0	6,1	0,0
		2	1,5	18,7	0,0	5,3
		3	0,0	16,9	0,0	0,0
		4	3,0	-	7,9	9,4
		5	0,0	5,6	0,0	0,0
		6	6,2	15,3	0,0	0,0
		7	0,0	0,0	0,0	0,0
		8	0,0	7,5	0,0	0,0
		9	0,0	0,0	0,0	0,0
		10	6,9	0,0	2,4	0,0
		11	0,0	12,1	0,0	0,0
Average (mean)			2,3	7,6	1,5	1,3
Standard Deviation (s)			3,2	7,3	2,8	3,1
Mean/s (%)			137%	96%	190%	233%

8.2 Appendix 8.2

Raw data measured from the ABMP tests done by Maake & Ikumi, (2021) as mentioned in **Chapter 3**.

ABMP Control Data															
	Day	Gas	COD	FSA	TP	OP	TSS	VSS	ISS	Mg	K	Ca	CO_3 Alk	PO_4 Alk	pH
Control 1	0	5,5	2560,0	3,1	99,1	44,5	2180,8	1687,8	493.0	10.9	99.0	14.2	76.9	99.2	7.0
	2	5,5	1620,0	4,1	92,4	44,9	1567,0	1145,0	422.0	14.0	118.0		79.0	71.5	6.6
	3	5,5	1600,0	4,9	84,8	49,6	1444,0	1058,0	386.0	13.2	95.0	14,0	17.2	78.3	6.6
	5	5,5	1440,0	5,9	71,0	49,8	1221,0	959,0	262.0	15.1	100.5	15,8	89.7	103.2	6.9
	6	6,5	1300,0	3,8	81,0	48,9					108.0	16,1	71.0	64.2	6.5
	7	7,0	1380,0	3,6	81,8	49,4	1300,0	1008,0	292.0	11.6	75.5		87.4	126.2	7.2
	8	7,5	2060,0	3,6	100,7	50,8	1087,0	870,0	217.0	15.5	108.5	14.8	62.1	51.1	6.3
	9	7,5	1320,0	3,8	81,0	56,1	1210,0	948,0	262.0	9.9	88.0	15.9	65.4	66.9	6.4
	11	7,5	1320,0	7,3	67,6	49,2	1212,0	960,0	252.0	3.8	78.5	12.5	49.3	63.7	6.5
	12	7,5	1260,0	11,5	67,4	59,9	1247,0	958,0	289.0	5.8	84.5	12.0	56.7	77.0	6.5
	23	9,0	1440,0		99,7	52,8	1460,0	960,0	500.0		124.5	15.2	120.8	47.3	6.8
	25	9,5	1260,0		78,3	51,9	1201,0	874,0	327.0		143.0	15.4	146.0	77.4	6.9
	27	9,5	1200,0		75,3	53,4	1059,0	786,0	273.0		131.5	16.1	118.7	77.6	6.9
	29	10,0	1720,0		73,5	52,3	1042,0	793,0	249.0		144.0	15.3	150.0	41.5	6.9
	40	9,5	1140,0		72,1	53,0	977,4	728,4	249.0		139.0	14.3			
Control 2	0	0.0	2400.0	3.0	82.2	42.2	1878.7	1579.7	299.0	10.1	101.5	13,8	65.4	86.7	6.9
	2	1.0	1460.0	3.6	78.3	39.4	1406.0	1079.0	327.0	10.4	100.5		88.5	76.5	6.8
	3	1.0	1860.0	5.0	88.0	48.0	1316.0	1038.0	278.0	10.3	103.5	13,3	64.9	85.8	6.8
	5	1.5	1380.0	4.9	71.5	47.6	1307.0	1048.0	259.0	11.5	95.5	15,2	58.5	94.5	6.9
	6	2.0	1400.0	3.6	74.7	44.4	1266.0	1023.0	243.0		112.0	16,1	0.0	0.0	6.7
	7	2.5	1360.0	3.5	78.6	44.6	1346.0	1097.0	249.0	9.3	76.0		93.5	112.3	7.2
	8	2.5	1540.0	3.4	79.1	45.9	1342.0	1093.0	249.0	11.6	87.0	14.7	69.6	62.6	6.5
	9	2.5	1740.0	3.3	91.4	54.1	1264.0	1000.0	264.0	6.4	86.5	14.9	64.9	75.8	6.5
	11	2.5	1540.0	7.1	69.3	51.4	1329.0	1071.0	258.0	3.6	71.0	9.7	16.4	68.2	6.5
	12	2.5	1340.0	11.9	70.6	55.6	1310.0	1061.0	249.0	7.7	91.5	11.9	66.9	75.1	6.5
	23	70.5	1580.0		75.9	50.2	1259.0	954.0	305.0		125.5	16.5	130.1	72.2	6.9
	25	70.5	1340.0		93.6	49.6	1117.0	932.0	185.0		136.0	16.3	115.4	101.8	6.9
	27	70.5	1300.0		72.2	50.4	1071.0	840.0	231.0		125.0	17.0	108.2	102.2	6.9
	29	87.5	1680.0		95.5	49.5	1081.0	847.0	234.0		124.5	16.7	179.2	36.0	6.8
	40	71.0	1140.0		67.2	48.1	958.4	728.4	230.0		130.0	15.0			
Average (Control 1 & 2)	0	2.8	2480.0	3.0	90.6	43.4	2029.8	1633.8	396.0	10.5	100.3	14.0	71.2	92.9	7.0
	2	3.3	1540.0	3.8	85.3	42.1	1486.5	1112.0	374.5	12.2	109.3	0.0	83.8	74.0	6.7
	3	3.3	1730.0	4.9	86.4	48.8	1380.0	1048.0	332.0	11.7	99.3	13.6	41.0	82.0	6.7
	5	3.5	1410.0	5.4	71.2	48.7	1264.0	1003.5	260.5	13.3	98.0	15.5	74.1	98.9	6.9
	6	4.3	1350.0	3.7	77.8	46.6	633.0	1023.0	121.5		110.0	16.1	35.5	32.1	6.6
	7	4.8	1370.0	3.5	80.2	47.0	1323.0	1052.5	270.5	10.5	75.8		90.4	119.2	7.2
	8	5.0	1800.0	3.5	89.9	48.4	1214.5	981.5	233.0	13.5	97.8	14.8	65.8	56.9	6.4
	9	5.0	1630.0	3.5	86.2	55.1	1237.0	974.0	263.0	8.1	87.3	15.4	65.2	71.3	6.5
	11	5.0	1430.0	7.2	68.4	50.3	1270.5	1015.5	255.0	3.7	74.8	11.1	32.9	65.9	6.5
	12	5.0	1300.0	11.7	69.0	57.8	1278.5	1009.5	269.0	6.7	88.0	11.9	61.8	76.0	6.5
	23	39.8	1510.0		87.8	51.5	1359.5	957.0	402.5		125.0	15.8	125.4	59.8	6.9
	25	40.0	1300.0		85.9	50.8	1159.0	903.0	256.0		139.5	15.8	130.7	89.6	6.9
	27	40.0	1250.0		73.7	51.9	1065.0	813.0	252.0		128.3	16.5	113.5	89.9	6.9
	29	48.8	1700.0		84.5	50.9	1061.5	820.0	241.5		134.3	16.0	164.6	38.8	6.9
	40	40.3	1140.0		69.6	50.5	968.4	728.4	240.0		134.5	14.6			

ABMP Control Data with added substrate (NDBEPR WAS froma UCT AS System)															
	Day	Gas	COD	FSA	TP	OP	TSS	VSS	ISS	Mg	K	Ca	CO_3 Alk	PO_4 Alk	pH
Control 1	0	1,0	5280.0	3.0	416.3	181.2	4619.7	3525.7	1094.0	50.2	243.0	42,1		201.8	7.0
	2	7,0	3040.0	3.6	439.3	242.1	3246.0	2388.0	858.0	63.0	276.0			202.3	6.7
	3	26,0	3600.0	5.7	440.9	288.5	2932.0	2170.0	762.0	72.0	285.0	32,6		222.8	6.6
	5	161,0	1240.0	8.3	369.8	273.1	1596.0	1182.0	414.0	64.8	314.0	29,1		239.7	6.7
	6	234,0	1400.0	4.7	430.2	282.5	2026.0	1302.0	724.0		342.0	29,1		206.5	6.6
	7	338,0	2760.0	5.0	468.7	290.6	3118.0	2252.0	866.0	82.5	302.0			333.9	7.0
	8	428,0	1960.0	5.3	496.9	271.6	2560.0	1596.0	964.0	85.1	343.0	28.9		168.0	6.4
	9	518,0	2120.0	6.3	799.0	299.8	2892.0	1384.0	1508.0	72.5	352.0	28.3		175.3	6.4
	11	645,0	1960.0	12.3	649.7	301.8	2516.0	1430.0	1086.0	4.2	320.0	16.0		156.5	6.3
	12	647,0	2160.0	22.9	572.8	326.0	3140.0	1664.0	1476.0	6.3	340.0	19.2		203.0	6.4
	23	843,0	2680.0		442.6	302.7	2986.0	1826.0	1160.0	80.9	450.0	26.1	46.1	182.5	6.8
	25	851,0	2920.0		529.0	305.0	2790.0	1830.0	960.0	83.7	459.0	25.9	39.7	203.3	6.8
	27	853,0	2600.0		526.6	309.7	2520.0	1568.0	952.0		464.0	27.1	35.1	212.0	6.9
	29	866,0	2800.0		466.8	298.6	2514.0	1618.0	896.0		462.0	26.7	191.7	89.5	6.7
	40	858,0	2680.0		639.0	301.3	2663.9	1768.9	895.	83,4	488.0	21.8			
Control 2	0	1.0	5600.0	2.8	476.7	187.1	4921.9	3741.9	1180.0	48.5	247.0	43,0		221.1	7.1
	2	2.0	4440.0	3.6	519.7	282.8	3932.0	2826.0	1106.0	91.0	279.0			268.2	6.8
	3	3.0	4800.0	5.5	673.8	319.2	3914.0	2688.0	1226.0	72.1	320.0	33,1		283.3	6.7
	5	86.0	3680.0	8.1	527.4	290.5	3914.0	2664.0	1250.0	50.2	319.0	27,2		109.8	6.9
	6	116.0	5200.0	4.3	802.8	300.9	4922.0	2664.0	2258.0		330.0	28,2		228.5	6.6
	7	138.0	3960.0	4.3	779.7	310.4	3872.0	2504.0	1368.0	15,8	331.0			370.3	7.1
	8	152.0	3320.0	4.5	849.9	302.0	4618.0	2722.0	1896.0	84,3	336.0	27.0		100.7	6.4
	9	152.0	3600.0	4.9	1034.1	318.6	3830.0	2404.0	1426.0		314.0	27.6		205.2	6.5
	11	203.0	4040.0	11.6	1194.7	372.1	5286.0	2768.0	2518.0	8,2	275.0	23.2		216.8	6.4
	12	225.0	3240.0	22.4	1097.3	347.8	5110.0	2554.0	2556.0	9,0	326.0	20.6		116.1	6.4
	23	614.0	3720.0		632.4	328.3	6240.0	2318.0	3922.0	82,7	498.0	25.6	27.2	189.4	6.8
	25	618.0	2760.0		558.6	322.8	3124.0	2074.0	1050.0	90,6	464.0	25.9	38.3	195.1	6.8
	27	619.0	2520.0		579.0	326.5	3516.0	1954.0	1562.0		489.0	26.7	30.1	217.8	6.8
	29	610.0	3160.0		573.4	320.5	2852.0	1624.0	1228.0		512.0	26.4	157.4	89.2	6.7
	40	621.0	2360.0		487.8	316.2	2777.7	1552.7	1225.0	87,0	499.0	26.9			
Average (Control 1 & 2)	0	1.0	5440.0	2.9	446.5	184.2	4770.8	3633.8	1137.0	49.4	245.0	42.5		211.5	7.0
	2	4.5	3740.0	3.6	479.5	262.4	3589.0	2607.0	982.0	77.0	277.5	0.0		235.2	6.7
	3	14.5	4200.0	5.6	557.4	303.9	3423.0	2429.0	994.0	72.1	302.5	32.8		253.0	6.7
	5	123.5	2460.0	8.2	448.6	281.8	2755.0	1923.0	832.0	57.5	316.5	28.1		174.7	6.8
	6	175.0	3300.0	4.5	616.5	291.7	3474.0	1983.0	1491.0		336.0	28.6		217.5	6.6
	7	238.0	3360.0	4.6	624.2	300.5	3495.0	2378.0	1117.0	49.2	316.5			352.1	7.1
	8	290.0	2640.0	4.9	673.4	286.8	3589.0	2159.0	1430.0	84.7	339.5	27.9		134.4	6.4
	9	335.0	2860.0	5.6	916.5	309.2	3361.0	1894.0	1467.0	72.5	333.0	28.0		190.2	6.4
	11	424.0	3000.0	11.9	922.2	336.9	3901.0	2099.0	1802.0	6.2	297.5	19.6		186.6	6.4
	12	436.0	2700.0	22.7	835.1	336.9	4125.0	2109.0	2016.0	7.7	333.0	19.9		159.5	6.4
	23	728.5	3200.0		537.5	315.5	4613.0	2072.0	2541.0		474.0	25.8	36.6	185.9	6.8
	25	734.5	2840.0		543.8	313.9	2957.0	1952.0	1005.0		461.5	25.9	39.0	199.2	6.8
	27	736.0	2560.0		552.8	318.1	3018.0	1761.0	1257.0		476.5	26.9	32.6	214.9	6.8
	29	738.0	2980.0		520.1	309.5	2683.0	1621.0	1062.0		487.0	26.5	174.5	89.3	6.7
	40	739.5	2520.0		563.4	308.7	2720.8	1660.8	1060.0		493.5	24.3			

8.3 Appendix 8.3

8.3.1 Modelled results – 15-day ADr (Maake & Ikumi, 2021)

Nutrients (N & P) 15-day (Maake & Ikumi - 2021)

Steady State model Input

Source	Concentration	Flux (kl/d)
Influent flow (l/d)	1,3	
Influent COD (mgCOD/l)	10169,1	13558,8
Influent COD, Susi (mgCOD/l)	74,0	98,7
Influent COD, Sbsfi (mgCOD/l)	0,0	0,0
Influent VFA, Sasi (mgCOD/l)	0,0	0,0
Influent COD, Stsi (mgCOD/l)	74,0	98,7
Influent COD, Sbpi (mgCOD/l)	4946,6	6595,5
Influent COD, Supi (mgCOD/l)	5148,5	6864,7
Influent COD, Stpi (mgCOD/l)	10095,1	13460,1
Influent TKN (mgN/l)	621,5	828,6
Influent filt TKN (mgN/l)	6,2	8,3
Influent FSA (mgN/l)	6,2	8,3
Influent OrgN (mgN/l)	615,3	820,3
Influent TOD(mgO/l)	13009,1	17345,5
Influent TP (mgP/l)	220,8	294,4
Influent filt TP (mgP/l)	3,9	5,2
Influent OP (mgP/l)	3,2	4,3
Influent OrgP (mgP/l)	217,6	290,1
Influent TSS (mg/l)	8762,0	11682,7
Influent VSS (mg/l)	6821,0	9094,7
Influent ISS (mg/l)	1941,0	2588,0
Influent Carbon (mgC/l)	3572,3	4763,1
Influent Hydrogen (mgH/l)	453,7	605,0
Influent Oxygen (mgO/l)	2224,4	2965,8
Influent Magnesium (mg/l)	27,6	36,8
Filt. Influent Magnesium (mg/l)	25,4	33,8
Influent Potassium (mg/l)	790,9	1054,5
Filt. Influent Potassium (mg/l)	714,2	952,3
Influent Calcium (mg/l)	125,1	166,8
Filt. Influent Calcium (mg/l)	117,0	156,1
Influent Alk mg/l as CaCO3	101,5	135,3
Influent pH	7,0	

Gas Production

Gas production (litres)	3,2
Gas prod. (l gas/l influent)	2,4
Gas composition : CH4 fraction	1,6
Gas composition: CO2 fraction	0,8
COD of CH4 (mgCOD/l feed)	3883,1
pCO2 (atm)	0,3

Anaeribic Digestor

COD and nutrient Removal and Mineral ppt

% FSA released	33,8
% OP released a	46,3
%COD removed (mgCOD/l)	78,5
Struvite precipitated	0,0
ACP precipitated	0,0
Calcite precipitated	0,0

Mass Balances

COD balance (%)	100,0
Carbon balance (%)	100,0
Hydrogen balance (%)	100,0
Oxygen balance (%)	100,0
Nitrogen balance (%)	100,0
Phosphorous balance (%)	100,0
Magnesium balance (%)	100,0
Potassium balance (%)	100,0
Calcium balance (%)	100,0

Steady State model Output

Source	Concentration	Flux (kl/d)
Effluent COD, Ste (mgCOD/l)	6286,0	8381,3
Effluent COD, Suse (mgCOD/l)	74,0	98,7
Effluent COD, Sbsfe (mgCOD/l)	0,0	0,0
Effluent VFA, Sase (mgCOD/l)	0,0	0,0
Effluent COD, Stse (mgCOD/l)	74,0	98,7
Effluent COD, Sbpe (mgCOD/l)	1063,5	1418,0
Effluent COD, Supe (mgCOD/l)	5148,5	6864,7
Effluent COD, Stpe (mgCOD/l)	6212,0	8282,6
Effluent TKN (gN/l)	621,5	828,6
Effluent filt TKN (mgN/l)	216,1	288,1
Effluent FSA (mgN/l)	216,1	288,1
Effluent OrgN (mgN/l)	405,3	540,5
Effluent TOD(mgO/l)	9126,0	12168,0
Effluent TP (mgP/l)	220,8	294,4
Effluent filt TP (mgP/l)	106,2	141,5
Effluent OP (mgP/l)	105,4	140,6
Effluent OrgP (mgP/l)	115,4	153,8
Effluent TSS (mg/l)	5849,6	7799,5
Effluent VSS (mg/l)	4197,1	5596,2
Effluent ISS (mg/l)	1652,5	2203,3
Effluent Carbon (mgC/l)	3572,3	4763,1
Effluent Hydrogen (mgH/l)	453,7	605,0
Effluent Oxygen (mgO/l)	2224,4	2965,8
Effluent Magnesium (mg/l)	27,6	36,8
Filt. Effluent Magnesium (mg/l)	27,6	36,8
Effluent Potassium (mg/l)	790,9	1054,5
Filt. Effluent Potassium (mg/l)	790,9	1054,5
Effluent Calcium (mg/l)	125,1	166,8
Filt. Effluent Calcium (mg/l)	125,1	166,8
Effluent Alk mg/l as CaCO3 (no P)	903,6	1204,8
Effluent Total Alk mg/l as CaCO3	1112,7	1483,6
Digester pH	6,7	

8.3.2 Modelled results – 32-day ADr (Maake & Ikumi, 2021)

Nutrients (N & P) 32-day (Maake & Ikumi - 2021)

Steady State model Input

Source	Concentration	Flux (kl/d)
Influent flow (l/d)	0,63	
Influent COD (mgCOD/l)	10382,7	6489,2
Influent COD, Susi (mgCOD/l)	93,0	58,1
Influent COD, Sbsfi (mgCOD/l)	0,0	0,0
Influent VFA, Sasi (mgCOD/l)	0,0	0,0
Influent COD, Stsi (mgCOD/l)	93,0	58,1
Influent COD, Sbpi (mgCOD/l)	4992,5	3120,3
Influent COD, Supi (mgCOD/l)	5297,2	3310,7
Influent COD, Stpi (mgCOD/l)	10289,7	6431,1
Influent TKN (mgN/l)	631,3	394,6
Influent filt TKN (mgN/l)	3,5	2,2
Influent FSA (mgN/l)	3,5	2,2
Influent OrgN (mgN/l)	627,8	392,4
Influent TOD(mgO/l)	13267,7	8292,3
Influent TP (mgP/l)	207,2	129,5
Influent filt TP (mgP/l)	2,1	1,3
Influent OP (mgP/l)	1,2	0,8
Influent OrgP (mgP/l)	206,0	128,8
Influent TSS (mg/l)	8893,5	5558,4
Influent VSS (mg/l)	6952,5	4345,3
Influent ISS (mg/l)	1941,0	1213,1
Influent Carbon (mgC/l)	3647,2	2279,5
Influent Hydrogen (mgH/l)	462,3	288,9
Influent Oxygen (mgO/l)	2241,4	1400,9
Influent Magnesium (mg/l)	17,3	10,8
Filt. Influent Magnesium (mg/l)	16,2	10,1
Influent Potassium (mg/l)	747,3	467,1
Filt. Influent Potassium (mg/l)	684,5	427,8
Influent Calcium (mg/l)	124,3	77,7
Filt. Influent Calcium (mg/l)	117,0	73,1
Influent Alk mg/l as CaCO3	109,9	68,7
Influent pH	7,0	

Gas Production

Gas production (litres)	1,7
Gas prod. (l gas/l influent)	2,8
Gas composition : CH4 fraction	1,8
Gas composition: CO2 fraction	0,9
COD of CH4 (mgCOD/l feed)	4413,5
pCO2 (atm)	0,3

Anaeribic Digestor

COD and nutrient Removal and Mineral ppt

% FSA released	37,8
% OP released a	44,1
%COD removed (mgCOD/l)	88,4
Struvite precipitated	0,0
ACP precipitated	0,0
Calcite precipitated	0,0

Mass Balances

COD balance (%)	100,0
Carbon balance (%)	100,0
Hydrogen balance (%)	100,0
Oxygen balance (%)	100,0
Nitrogen balance (%)	100,0
Phosphorous balance (%)	100,0
Magnesium balance (%)	100,0
Potassium balance (%)	100,0
Calcium balance (%)	100,0

Steady State model Output

Source	Concentration	Flux (kl/d)
Effluent COD, Ste (mgCOD/l)	5969,2	3730,8
Effluent COD, Suse (mgCOD/l)	93,0	58,1
Effluent COD, Sbsfe (mgCOD/l)	0,0	0,0
Effluent VFA, Sase (mgCOD/l)	0,0	0,0
Effluent COD, Stse (mgCOD/l)	93,0	58,1
Effluent COD, Sbpe (mgCOD/l)	579,0	361,9
Effluent COD, Supe (mgCOD/l)	5297,2	3310,7
Effluent COD, Stpe (mgCOD/l)	5876,2	3672,6
Effluent TKN (gN/l)	631,3	394,6
Effluent filt TKN (mgN/l)	242,1	151,3
Effluent FSA (mgN/l)	242,1	151,3
Effluent OrgN (mgN/l)	389,2	243,3
Effluent TOD(mgO/l)	8854,2	5533,9
Effluent TP (mgP/l)	207,2	129,5
Effluent filt TP (mgP/l)	93,5	58,4
Effluent OP (mgP/l)	92,6	57,8
Effluent OrgP (mgP/l)	114,6	71,7
Effluent TSS (mg/l)	5677,1	3548,2
Effluent VSS (mg/l)	3970,3	2481,4
Effluent ISS (mg/l)	1706,8	1066,8
Effluent Carbon (mgC/l)	3647,2	2279,5
Effluent Hydrogen (mgH/l)	462,3	288,9
Effluent Oxygen (mgO/l)	2241,4	1400,9
Effluent Magnesium (mg/l)	17,3	10,8
Filt. Effluent Magnesium (mg/l)	17,3	10,8
Effluent Potassium (mg/l)	747,3	467,1
Filt. Effluent Potassium (mg/l)	747,3	467,1
Effluent Calcium (mg/l)	124,3	77,7
Filt. Effluent Calcium (mg/l)	124,3	77,7
Effluent Alk mg/l as CaCO3 (no P)	983,2	614,5
Effluent Total Alk mg/l as CaCO3	1170,8	731,8
Digester pH	6,7	

8.3.3 Modelled results – 15-day ADr (Ikumi, Harding & Ekama, 2013)

Nutrients (N & P) 15-day (Ikumi, Harding & Ekama - 2013)

Steady State model Input

Source	Concentration	Flux (kl/d)
Influent flow (l/d)	1,33	
Influent COD (mgCOD/l)	9913,1	13217,5
Influent COD, Susi (mgCOD/l)	74,0	98,7
Influent COD, Sbsfi (mgCOD/l)	0,0	0,0
Influent VFA, Sasi (mgCOD/l)	0,0	0,0
Influent COD, Stsi (mgCOD/l)	74,0	98,7
Influent COD, Sbpi (mgCOD/l)	4705,0	6273,3
Influent COD, Supi (mgCOD/l)	5134,2	6845,6
Influent COD, Stpi (mgCOD/l)	9839,1	13118,9
Influent TKN (mgN/l)	814,7	1086,3
Influent filt TKN (mgN/l)	6,2	8,3
Influent FSA (mgN/l)	6,2	8,3
Influent OrgN (mgN/l)	808,5	1078,0
Influent TOD(mgO/l)	13636,3	18181,7
Influent TP (mgP/l)	250,0	333,3
Influent filt TP (mgP/l)	3,9	5,2
Influent OP (mgP/l)	3,2	4,3
Influent OrgP (mgP/l)	246,8	329,1
Influent TSS (mg/l)	8709,9	11613,2
Influent VSS (mg/l)	6768,9	9025,2
Influent ISS (mg/l)	1941,0	2588,0
Influent Carbon (mgC/l)	3512,3	4683,1
Influent Hydrogen (mgH/l)	435,9	581,2
Influent Oxygen (mgO/l)	1851,9	2469,2
Influent Magnesium (mg/l)	27,6	36,8
Filt. Influent Magnesium (mg/l)	27,3	36,4
Influent Potassium (mg/l)	790,9	1054,5
Filt. Influent Potassium (mg/l)	781,1	1041,4
Influent Calcium (mg/l)	125,1	166,8
Filt. Influent Calcium (mg/l)	124,1	165,4
Influent Alk mg/l as CaCO3	101,5	135,3
Influent pH	7,0	

Gas Production

Gas production (litres)	2,1
Gas prod. (l gas/l influent)	1,5
Gas composition : CH4 fraction	1,1
Gas composition: CO2 fraction	0,4
COD of CH4 (mgCOD/l feed)	2664,9
pCO2 (atm)	0,3

Anaeribic Digestor

COD and nutrient Removal and Mineral ppt

% FSA released	33,2
% OP released a	34,8
%COD removed (mgCOD/l)	56,6
Struvite precipitated	0,0
ACP precipitated	0,0
Calcite precipitated	0,0

Mass Balances

COD balance (%)	100,0
Carbon balance (%)	100,0
Hydrogen balance (%)	100,0
Oxygen balance (%)	100,0
Nitrogen balance (%)	100,0
Phosphorous balance (%)	100,0
Magnesium balance (%)	100,0
Potassium balance (%)	100,0
Calcium balance (%)	100,0

Steady State model Output

Source	Concentration	Flux (kl/d)
Effluent COD, Ste (mgCOD/l)	7248,2	9664,3
Effluent COD, Suse (mgCOD/l)	74,0	98,7
Effluent COD, Sbsfe (mgCOD/l)	0,0	0,0
Effluent VFA, Sase (mgCOD/l)	0,0	0,0
Effluent COD, Stse (mgCOD/l)	74,0	98,7
Effluent COD, Sbpe (mgCOD/l)	2040,0	2720,0
Effluent COD, Supe (mgCOD/l)	5134,2	6845,6
Effluent COD, Stpe (mgCOD/l)	7174,2	9565,6
Effluent TKN (gN/l)	814,7	1086,3
Effluent filt TKN (mgN/l)	276,3	368,4
Effluent FSA (mgN/l)	276,3	368,4
Effluent OrgN (mgN/l)	538,4	717,8
Effluent TOD(mgO/l)	10971,4	14628,5
Effluent TP (mgP/l)	250,0	333,3
Effluent filt TP (mgP/l)	90,9	121,2
Effluent OP (mgP/l)	90,2	120,3
Effluent OrgP (mgP/l)	159,8	213,1
Effluent TSS (mg/l)	6804,3	9072,5
Effluent VSS (mg/l)	4900,2	6533,7
Effluent ISS (mg/l)	1904,1	2538,8
Effluent Carbon (mgC/l)	3512,3	4683,1
Effluent Hydrogen (mgH/l)	435,9	581,2
Effluent Oxygen (mgO/l)	1851,9	2469,2
Effluent Magnesium (mg/l)	27,6	36,8
Filt. Effluent Magnesium (mg/l)	27,6	36,8
Effluent Potassium (mg/l)	790,9	1054,5
Filt. Effluent Potassium (mg/l)	790,9	1054,5
Effluent Calcium (mg/l)	125,1	166,8
Filt. Effluent Calcium (mg/l)	125,1	166,8
Effluent Alk mg/l as CaCO3 (no P)	918,3	1224,4
Effluent Total Alk mg/l as CaCO3	1105,5	1474,0
Digester pH	6,8	

8.3.4 Modelled results – 32-day ADr (Ikumi, Harding & Ekama, 2013)

Nutrients (N & P) 32-day (Ikumi, Harding & Ekama - 2013)

Steady State model Input

Source	Concentration	Flux (kl/d)
Influent flow (l/d)	0,63	
Influent COD (mgCOD/l)	10199,4	6374,6
Influent COD, Susi (mgCOD/l)	93,0	58,1
Influent COD, Sbsfi (mgCOD/l)	0,0	0,0
Influent VFA, Sasi (mgCOD/l)	0,0	0,0
Influent COD, Stsi (mgCOD/l)	93,0	58,1
Influent COD, Sbpi (mgCOD/l)	4823,9	3014,9
Influent COD, Supi (mgCOD/l)	5282,5	3301,6
Influent COD, Stpi (mgCOD/l)	10106,4	6316,5
Influent TKN (mgN/l)	833,7	521,1
Influent filt TKN (mgN/l)	3,5	2,2
Influent FSA (mgN/l)	3,5	2,2
Influent OrgN (mgN/l)	830,2	518,9
Influent TOD(mgO/l)	14009,3	8755,8
Influent TP (mgP/l)	244,4	152,8
Influent filt TP (mgP/l)	2,1	1,3
Influent OP (mgP/l)	1,2	0,8
Influent OrgP (mgP/l)	243,2	152,0
Influent TSS (mg/l)	8893,5	5558,4
Influent VSS (mg/l)	6952,5	4345,3
Influent ISS (mg/l)	1941,0	1213,1
Influent Carbon (mgC/l)	3613,5	2258,4
Influent Hydrogen (mgH/l)	447,6	279,7
Influent Oxygen (mgO/l)	1887,1	1179,4
Influent Magnesium (mg/l)	17,3	10,8
Filt. Influent Magnesium (mg/l)	17,3	10,8
Influent Potassium (mg/l)	747,3	467,1
Filt. Influent Potassium (mg/l)	747,3	467,1
Influent Calcium (mg/l)	124,3	77,7
Filt. Influent Calcium (mg/l)	124,3	77,7
Influent Alk mg/l as CaCO3	109,9	68,7
Influent pH	7,0	

Gas Production

Gas production (litres)	1,3
Gas prod. (l gas/l influent)	2,2
Gas composition : CH4 fraction	1,5
Gas composition: CO2 fraction	0,6
COD of CH4 (mgCOD/l feed)	3710,7
pCO2 (atm)	0,3

Anaeribic Digestor

COD and nutrient Removal and Mineral ppt

% FSA released	33,2
% OP released a	34,8
%COD removed (mgCOD/l)	56,6
Struvite precipitated	0,0
ACP precipitated	0,0
Calcite precipitated	0,0

Mass Balances

COD balance (%)	100,0
Carbon balance (%)	100,0
Hydrogen balance (%)	100,0
Oxygen balance (%)	100,0
Nitrogen balance (%)	100,0
Phosphorous balance (%)	100,0
Magnesium balance (%)	100,0
Potassium balance (%)	100,0
Calcium balance (%)	100,0

Steady State model Output

Source	Concentration	Flux (kl/d)
Effluent COD, Ste (mgCOD/l)	6488,7	4055,4
Effluent COD, Suse (mgCOD/l)	93,0	58,1
Effluent COD, Sbsfe (mgCOD/l)	0,0	0,0
Effluent VFA, Sase (mgCOD/l)	0,0	0,0
Effluent COD, Stse (mgCOD/l)	93,0	58,1
Effluent COD, Sbpe (mgCOD/l)	1113,2	695,7
Effluent COD, Supe (mgCOD/l)	5282,5	3301,6
Effluent COD, Stpe (mgCOD/l)	6395,7	3997,3
Effluent TKN (gN/l)	833,7	521,1
Effluent filt TKN (mgN/l)	375,8	234,8
Effluent FSA (mgN/l)	375,8	234,8
Effluent OrgN (mgN/l)	457,9	286,2
Effluent TOD(mgO/l)	10298,6	6436,6
Effluent TP (mgP/l)	244,4	152,8
Effluent filt TP (mgP/l)	108,2	67,6
Effluent OP (mgP/l)	107,3	67,0
Effluent OrgP (mgP/l)	137,1	85,7
Effluent TSS (mg/l)	6293,8	3933,6
Effluent VSS (mg/l)	4352,7	2720,4
Effluent ISS (mg/l)	1941,1	1213,2
Effluent Carbon (mgC/l)	3613,5	2258,4
Effluent Hydrogen (mgH/l)	447,6	279,7
Effluent Oxygen (mgO/l)	1887,1	1179,4
Effluent Magnesium (mg/l)	17,3	10,8
Filt. Effluent Magnesium (mg/l)	17,3	10,8
Effluent Potassium (mg/l)	747,3	467,1
Filt. Effluent Potassium (mg/l)	747,3	467,1
Effluent Calcium (mg/l)	124,3	77,7
Filt. Effluent Calcium (mg/l)	124,3	77,7
Effluent Alk mg/l as CaCO3 (no P)	1212,0	757,5
Effluent Total Alk mg/l as CaCO3	1442,0	901,2
Digester pH	6,9	